A Groundwater Modelling Investigation of Greywater Disposal: South Tarawa, Kiribati

Amir Jazayeri, S. Cristina Solórzano-Rivas, Peter Sinclair, Andreas Antoniou, Dylan J. Irvine, and Adrian D. Werner

WORLD BANK GROUP

JUNE 2019

A Groundwater Modelling Investigation of Greywater Disposal: South Tarawa, Kiribati

Amir Jazayeri[1]
S. Cristina Solórzano-Rivas[1]
Peter Sinclair[2]
Andreas Antoniou[2]
Dylan J. Irvine[1]
Adrian D. Werner[1]

[1]Flinders University
[2]Secretariat of the Pacific Community (SPC)

JUNE 2019

WORLD BANK GROUP

1818 H Street NW, Washington, DC 20433
Telephone: 202-473-1000; Internet: www.worldbank.org

This report has been produced to provide information specifically for the Pacific Community's purposes, and due care in interpreting the findings of this study is the responsibility of the reader. The analysis described in this report is based on a substantial volume of information provided by others. No additional field data collected by the authors was used in this analysis. While due diligence was exercised in the use of existing information, in some cases it was not possible to validate data or sources of information. This work does not represent itself as definitive guidance for the purposes of water resource or quality management in the Tarawa Atoll. The authors recommend that the results of the current study be interpreted by suitably trained professionals with expertise in groundwater modelling to ensure that the usual uncertainties inherent in groundwater modelling studies are understood. Neither the University, SPC, nor the author of this report will be accountable for any liability incurred by you, any loss of or damage to property incurred by you, or any loss or expense incurred by you in dealing with any claims arising from the use of this work. This report should be reproduced in full. This disclaimer must be included in any copy of this report. Omission of this disclaimer by any third party that results in loss to any other party will not constitute liability to Flinders University, SPC or to the author of this report for that loss. Pacific Community and Flinders University may not necessarily adopt any views or conclusions expressed in this report, which are rather the opinions of the authors.

Executive Summary

Tarawa atoll is the capital of the Republic of Kiribati, located in the central Pacific Ocean. The atoll comprises numerous low-lying islands and islets connected by causeways. North Tarawa (from Buariki in the north to Buota in the south) is largely rural, while South Tarawa (from Betio in the west to Tanaea in the northeast) is the main urban centre of the country, with a population of approximately 56,300 (KNSO 2015).

South Tarawa consists of elongated islands that collectively stretch more than 30 km, with an average width of less than 250 m. Three islands are wide enough to hold significant volumes of groundwater, namely the urbanised Betio Island, and the sparsely populated Bonriki and Buota Islands. Reticulated water is supplied to South Tarawa by the Public Utilities Board (PUB), which maintains the supply system. Otherwise, freshwater is obtained from private and community wells, through rainwater harvesting, with a residual amount provided from bottled water. The majority of households (67%) have access to PUB reticulated water (KNSO and SPC 2010), which supplies treated water from the Bonriki and Buota groundwater lenses.

Up to 75% of the domestic wastewater produced by households is released in urban settings in the form of greywater, which is defined as the wastewater derived from showers, bathtubs, sinks, kitchens, dishwashers, laundry tubs and washing machines, and excludes toilet water (i.e., blackwater) (Eriksson et al. 2002). Greywater is often considered a high-volume, wastewater of relatively low contaminant concentration that has a high potential for reuse for toilet flushing and in agricultural applications (Oteng-Peprah et al. 2018). The reuse of greywater to supplement existing water sources may alleviate an over-reliance on alternative freshwater resources. Households in South Tarawa already practice greywater reuse to some extent for gardening and/or drinking water for livestock, particularly pigs.

The primary objective of this study is to investigate the feasibility of greywater reuse in South Tarawa and to assess the potential benefits and threats to the underlying groundwater systems.

The initial part of this investigation sought to collect field data to support the development of conceptual hydrogeological models, which were subsequently used to set up numerical groundwater flow models. Field data collected included topography, bathymetry, geological/stratigraphic data, aquifer hydraulic parameters, rainfall, recharge, groundwater abstraction, groundwater extent and characteristics, and greywater discharge. Where data required for modelling were lacking, parameters for Betio, Bairiki and Bikenibeu were obtained from previous field campaigns and/or studies of similar settings, e.g., the groundwater modelling investigation of Bonriki by Bosserelle et al. (2015).

Following a data collection expedition and data compilation exercise, conceptual models were developed in the form of transects across the three islands under investigation. These were set up as follows:

- Transect locations were chosen primarily based on the availability of existing monitoring bores.
- The subsurface was conceptualised as a dual-aquifer system to simplify the geological setting and hydrogeological layers. This is consistent with previous studies, which assume that poorly consolidated Holocene sediments overly Pleistocene limestone reef deposits throughout the Tarawa Atoll.
- Recharge was taken as the rainfall passing through the soil zone to the water table, equal to rainfall infiltration minus evapotranspiration. Recharge was taken as 50% of rainfall, following FTP (2011). The rainfall data were obtained from Betio meteorological station.
- Groundwater abstraction was estimated based on 45 L/pers/day (FTP 2011) and considered populations in 2015 and the projected 2030 populations (i.e., to consider current and future scenarios, respectively). Given the difficulty in locating individual wells, groundwater abstraction was treated as a distributed groundwater output, and was subtracted from recharge such that net recharge (equal to rainfall minus evapotranspiration minus abstraction) was applied to the model. As a consequence, 'negative recharge' occurred during dry periods within the 14-day time steps of transient simulations.
- A steady-state model was developed to provide initial conditions in transient models and for use in model calibration. The recharge applied to the steady-state model was based on the average rate of rainfall for the period 1947 to 2018.
- Greywater discharge was estimated based on 35 L/pers/d greywater production and the 2015 population (considered as the 'current situation'). The modelling scenario of future conditions adopted 70 L/pers/d greywater production and used the projected 2030 population. Greywater discharge was applied to the model at distances representing approximately the space between dwellings (about 50 m on average) for the current situation, and using one centralised point of disposal for the future scenario. Two different future scenarios were tested: one where greywater is discharged to the water table and a second where it is injected into the freshwater-seawater mixing zone (i.e., the base of the freshwater lens).

2D (cross-sectional) numerical models of selected transects of Betio, Bairki and Bikenibeu Islands were developed using the USGS software SEAWAT. SEAWAT simulates density-coupled groundwater flow and solute transport, and allows for the modelling of multiple species (i.e., saltwater and greywater). Models were developed for calibration and validation against existing groundwater salinity measurements, and eight simulations were used to assess greywater transport. Calibration and validation models included:

1. Case 1: Steady-state calibration - Steady-state models of Betio, Bairiki and Bikenibeu were developed and calibrated by adjusting model parameters (hydraulic conductivity and solute dispersivity) to minimize the difference between simulated concentration profiles and that measured in the available monitoring wells.

2. Case 2: Transient validation - Using the steady-state result as initial conditions, a transient simulation was developed for the period 1st May 1947 to 23rd December 2015, using 14-day stress periods and calibrated model parameters obtained from Case 1. The simulation of the freshwater lens was compared to available salinity measurements.

Simulations to explore various scenarios of greywater transport within the subsurface included:

3. Case 3: Steady-state simulation of greywater discharge under current conditions – i.e., identical to Case 1 except greywater disposal was added at intervals representing distances between dwellings and based on the 2015 population.
4. Case 4: Steady-state simulation of greywater disposal at the land surface and under future conditions – i.e., identical to Case 3 except with higher abstraction rates and greywater inputs commensurate with the projected 2030 population. Greywater was added in the form of surface infiltration at a disposal location approximately in the middle of each cross-section.
5. Case 5: Steady-state simulation of greywater disposal through well injection and under future conditions – i.e., identical to Case 4 except that greywater discharge was injected into the base of the freshwater lens (i.e., the freshwater-seawater mixing zone).
6. Case 6: Transient simulation of greywater discharge under current conditions – i.e., identical to Case 2 except with greywater added at intervals representing distances between dwellings and with loads based on the 2015 population.
7. Case 7: Transient simulation of greywater disposal at the land surface and under future conditions – i.e., identical to Case 6 except with higher abstraction rates and greywater inputs commensurate with the projected 2030 population. Greywater was added through surface infiltration at a disposal location in approximately the middle of each cross-section.
8. Case 8: Transient simulation of greywater disposal through well injection and under future conditions – i.e., identical to Case 7 except that greywater discharge was injected into the base of the freshwater lens (i.e., the freshwater-seawater mixing zone).
9. Case 9: Transient simulation of greywater disposal at the land surface and under future conditions except with no abstraction – i.e., identical to Case 7, but without groundwater abstraction (thereby increasing the net recharge). This case was intended to represent a future condition with reduced reliance on local groundwater.
10. Case 10: Transient simulation of greywater disposal through well injection and under future conditions except with no abstraction – i.e., identical to Case 8, but without groundwater abstraction.

Table of Contents

1. Introduction

1.1 Background

The World Bank, in cooperation with the Asian Development Bank (ADB) and Green Climate Fund (GCF), is currently exploring options to expand and improve the supply of freshwater to South Tarawa, Kiribati. This project includes the construction of a solar-powered desalination plant that, when combined with the current source, i.e., the Bonriki and Buota groundwater reserves, is planned to provide 50 L/pers/d to the population of South Tarawa by 2025, and 100 L/pers/d by 2030. The current freshwater lenses of Bonriki and Buota provide approximately 22 L/pers/d to the population of South Tarawa (Galvis-Rodriguez et al. 2017). The project also includes the expansion and refurbishment of the water supply network to reach all residents of South Tarawa. Infrastructure improvements are anticipated to deliver an uninterrupted supply of drinkable water.

In 2011, sanitation in South Tarawa was comprised of three, largely non-functioning sewerage systems serving the urban centres of Betio, Bairiki and central Bikenibeu, which were designed to dispose of wastewater (untreated) through ocean outfalls. Elsewhere, human waste was disposed of using septic tanks, pit latrines, compost toilets and open defecation, mainly on beaches. Locally constructed septic tanks discharged to soak pits filled with coral gravel, which subsequently entered local aquifers (GoK 2011).

Even when these improved services are in place, it is expected that urban groundwater will remain, like rainwater, an alternate water resource for the population of South Tarawa. Opportunities exist to harness the increased greywater production, associated with the increased supply of good quality water, by artificially recharging the underlying freshwater lenses of Betio, Bairiki and Bikenibeu islets. This could have beneficial effects in maintaining the thickness of the freshwater lenses during dry periods as well as in improving groundwater quality through natural attenuation processes in the aquifer to eventually make use of the injected and naturally-treated greywater.

The current research is expected to contribute to these broader project aims by delivering advice on the fate of greywater in populated regions of South Tarawa. Specifically, this study aims to evaluate the impact of greywater discharge to island aquifers and the freshwater lenses that are hosted therein.

1.2 Socio-economic overview

Socio-economic information related to living standards, water use and sanitation was sourced from the two latest census reports of 2010 and 2015 (Table 1). This allowed for the identification of trends pointing towards socio-economic changes induced by the rapid population increase.

Table 1. Comparison between November 2010 and 2015 census (Kiribati Government) for selected parameters with respect to households for South Tarawa and Betio.

Parameter	South Tarawa			Betio			Observation
	2010	2015	% change	2010	2015	% change	
Households	4728	5584	18	1977	2293	16	1
Population	34427	39058	13	15755	17330	10	
	% of households		% change	% of households		% change	
Refrigeration	42	42	1	49	46	-3	2
Kerosene stoves	87	86	-1	92	88	-4	
Electric gas stove	25	22	-3	30	29	-1	
Mobile phones	60	56	-4	67	59	-8	
Number of washing machines	NA	19		NA	23		
Cooking fuel type GAS	5	8	4	7	12	5	3
Cooking fuel type Electricity	0	1	0	0	1	1	
Cooking fuel type Kerosene	54	73	20	74	78	4	
Cooking fuel type Wood/other	42	17	-24	19	8	-10	
Drinking water source: PUB	61	30	-31	82	55	-28	4
Drinking water source: Well	30	16	-14	6	3	-3	
Drinking water source: Rainwater	9	53	44	11	42	30	
Drinking water source: Other	0	1	1	0	1	1	
Washing water source: PUB	20	12	-9	25	20	-5	5
Washing water source: Well	78	84	6	73	76	2	
Washing water source: Rainwater	2	3	2	2	3	1	
Washing water source: Other	0	1	1	0	1	1	
Sanitation: PUB reticulated flush	16	8	-7	52	24	-27	6
Sanitation: other flush	47	20	-27	18	24	5	
Sanitation: latrine	7	43	36	19	37	18	
Open defecation	28	22	-5	9	8	-1	
Other	2	6	4	2	7	5	

It is important to note that the 2010 census was undertaken in November 2010 during an extended dry period impacting South Tarawa. The 2015 census was undertaken during a period in which above average rainfall was experienced. The following interesting observations can be made:

1. Household numbers increased between 2010 and 2015 by 18 % and 16 % in South Tarawa and Betio, respectively, while total population increased by 13 % and 10 %, respectively over the 5-year period. The average number of persons per household was 7 – 8 with a

slight reduction between 2010 and 2015 (0.3 – 0.4 persons per household reduction). This indicates the continued urbanisation of South Tarawa with an average annual population growth rate of 2.7 % per year between 2010 and 2015 compared with total annual population growth rate for Kiribati of 0.6 % for the same period.

Figure 1. Household handwashing, Betio May 2019.

2. A comparison of the percentage of households that have access to refrigeration, stoves (gas electric and kerosene), and mobile phones between 2010 and 2015 in Betio and South Tarawa provides some indication of the households access to disposable income for "luxury white goods". It is suggested that the number of households that have access to white goods is a relative indicator of the standard of living and accessibility to other improvements such as washing machines and indoor showers, electric pumps, etc. In lieu of metered water volumes for households it is suggested that any increased access to items such as washing machines is an indicator of likely increased water consumption. This has implications for understanding the water supply needs of households. The census data indicates a decrease in the access to consumable white goods found in households, indicating that households are unlikely to be able to afford goods such as washing machines suggesting that the increase in water use is not significantly rising, and the trend is that households are not increasing their access to disposable income, which would seem counter to what could be expected. Further attempts to crosscheck this trend with washing machine import figures over the last 5 years through the Government of Kiribati were unsuccessful. In 2015 only 19 % of households had access to washing machines (Census 2015) across South Tarawa suggesting that the majority of households (~80 %) rely upon hand washing, which is expected to use less water than a washing machine. Refer to Figure 1.

3. It is interesting to note that while the number of households that have a stove (gas, electric, kerosene) decreased in 2015, the use of kerosene in households in 2015, compared with 2010 census, shows a significant increase, with a corresponding decrease in the reliance on combustibles such as wood and coconut shells and use of open fires for cooking. This may suggest that there is some increased communal use of kerosene stoves in South Tarawa by

those households that do not have a kerosene stove. This however does not seem to be the case for Betio, where the change in the use of kerosene for cooking is not as pronounced.

4. The reliance on PUB water for potable water supply in South Tarawa during November 2010, an extended dry period, was 61 % of all households, while in 2015, a period of above average rainfall, the reliance on PUB for drinking water was only 30 % of all households for South Tarawa, with a proportional increase in the use of rainwater for potable water supply. Similar trends in the use of well water for drinking water were also observed (30 % reliance in 2010 reduced to 16 % reliance in 2015) with about only half of those households using well water for drinking during periods of adequate rainfall. Betio demonstrates similar trends. This would suggest that there is a perception amongst households that rainwater is a superior water source when compared to PUB supplied water and/or well water, when it is available. Reliance on PUB and well water for drinking purposes seems to double during dry times when rainwater is not available. It is suggested that the driver for this is most likely water quality, either taste aesthetics and/or health aspects, possibly coupled with the level of service and accessibility to PUB water. During 2010 and 2015, PUB did not have metered usage charges to households suggesting that it is not a function of cost of PUB delivered water causing this observed trend (Fraser Thomas, 2011).

5. Well water is the preferred water source for washing purposes (84 % of all households for South Tarawa and 76 % of Betio households, 2015). This reliance on well water could be cultural or due to accessibility of the volumes of water needed for washing from PUB water sources. It is interesting to note that during the 2010 extended dry period there was an increased reliance on PUB water for washing purposes. This reliance on PUB water for washing purposes during the dry period of 2010 may be in response to the perceived or actual water quality (increased salinity) of the shallow well water during this period. As PUB water is not metered at the household, costs based on usage would not seem to be a major factor in the household reliance on well water, although accessibility to PUB water may be a contributor (Fraser Thomas, 2011).

It is observed that from 2010 to 2015 there is a decrease in the reliance by households on PUB reticulated sewage systems and other flush systems (pour flush), and an apparent increase in the reliance of latrine style sanitation systems. This outlier could be an artefact of the census questionnaire, whereby some confusion on waste water disposal options was introduced into the census questionnaire, or more probable is an indication of the general decline in the access to reticulated and other pour flush septic tank wastewater disposal options by households in 2015 compared with 2010.

1.3 Introduction to greywater reuse

Greywater is defined as wastewater without any contributions from toilet water (Oteng-Peprah et al 2018), constitutes 50 – 80 % of household wastewater and has high reuse potential. Reusing greywater may soften water shortages for non-potable purposes and lead at the same time to significant savings in water expenditures. Non-potable reuse applications include industrial, irrigation, toilet flushing and laundry washing, depending on the treatment type the

greywater undergoes. Greywater reuse has been accepted as an environmentally sustainable method of protecting freshwater resources and pollution prevention. Public perception plays an important role in determining the acceptance of greywater reuse strategies. According to Oteng-Peprah et al 2018, the highest acceptability of greywater reuse schemes are for non-potable uses. Dolnicar and Schafer (2006) identified reduced levels of acceptance as the recycled water got closer to human contact.

Greywater may also be used in coastal areas to create a buffer zone between a fresh groundwater and underlying brackish/saline water. This way, the volume of precious freshwater lenses can be maintained longer during droughts where freshwater lenses tend to thin out with the upward gradual movement of the brackish transition zone. When greywater is used for such purposes, artificial injection wells are required and water quality aspects become less significant as the water is not going to be directly reused. Simple treatment prior to injection, however, such as grease traps and leaching pits may be required to prevent clogging issues of the injection wells.

The composition of greywater is a reflection of the household activities and its characteristics are strongly dependent on living standards, social and cultural habits, number of household members and the use of household chemicals. Greywater generally contains high concentrations of easily biodegradable organic materials and household-generated constituents including nutrients such as nitrates and phosphorus, xenobiotic organic compounds (Fatta-Kassinos et al. 2011), pathogenic bacteria such as faecal coliforms and salmonella, pharmaceuticals, health and beauty products, aerosols, pigments (Eriksson et al. 2003) and toxic heavy metals such as Pb, Ni Cd, Cu, Hg and Cr (Aonghusa and Gray 2002; Eriksson et al. 2010). According to Oteng-Peprah et al 2018, nitrogen in greywater ranges between 4 and 74 mg/L while phosphates range between 4 and 14 mg/L. Dishwashing and laundry detergents are the main sources of phosphorous in greywater whereas in countries where phosphorous-free detergents are used, these loads are minimal. Kitchen greywater is the main source of nitrogen. Faecal contamination (Escherichia coli and enteric viruses) is largely associated with poor personal hygiene and washing of nappies (O'Toole et al. 2012).

In order for greywater to be reused as a non-potable water source, it has to be collected separately from blackwater, treated and eventually disinfected. The collection of greywater may consist of bucketing or systems that divert the greywater towards centralized collection basins consisting of simple treatment facilities such as grease traps and leaching pits. Additional treatment may be achieved through natural filtration processes of greywater below ground. With respect to subsurface water quality improvements, processes such as filtration, sorption, and biodegradation are responsible for the water "recycling" during its passage through subsurface media. The intentional use of the natural attenuation processes to improve water quality has been referred to as natural aquifer treatment (Maliva and Missimer 2010). NAT is a beneficial side-effect of artificial injection systems; however it could be used as an integral

component of the treatment processes for reclaimed water or surface water. Water quality improvements during soil and aquifer passage may consist of denitrification, biodegradation of organic micropollutants (Pavelic et al. 2005) and pharmaceuticals (Overacre et al. 2006), and removal of pathogens.

Microbial removal rate (λ) is defined as the logarithmic reduction in microbial concentration per transport distance in the porous media. This natural attenuation process consists of a combination of physical straining, adsorption due to surface complexation and die-off of microorganisms (Schijven et al. 2017). Straining is achieved by the physical filtration within adjacent grains in the subsurface media blocking the passage of microbes (Xu et al. 2006) and promoting their necrosis due to lack of nutrients and oxygen (Vanderzalm et al. 2002, Antoniou et al. 2012). Adsorption involves the attachment of microbes to the solid surface of porous media when they have opposite electric charges (Schijven et al., 2017).

Subsurface media have different degrees of microbial removal capacity which depends on the physical and chemical properties of the media, heterogeneity, preferential flow paths and flow mechanisms. At the same time, microbial removal rates also depend on the physical and chemical properties of the microbial contaminants and their source characteristics as well as on the chemical properties of their carrier.

Microbial removal efficiencies of subsurface media have been summarised by Pang (2009) (Table 2). Soils[1] seem to promote the more efficient microbial removal compared to the vadose zone whereas removal rates in aquifers are much more variable and certainly lower due to saturated conditions. The air-water interface interaction plays a major role in enhancing microbial removal in soils as opposed to the unsaturated zone (vadose zone) below soils where biological activity is lower and the effect of the air-water interface is reduced. Pang concludes that the most effective microbial removal takes place in allophanic soils, pumice sand, fine sand, and highly weathered aquifer rocks while the least effective media are clayey soils, coarse gravel aquifers and fractured rocks (Table 2). Removal rates for sands show a clear inverse relationship with pore-water velocity, hydraulic conductivity, hydraulic loading, and infiltration rates. Clays and silts have a reduced microbial removal capacity compared with sands due to the effect of soil structure, (macropores). Soil structure being important in the effectiveness of microbial removal, where cracks and channels my form preferential pathways. Long-term continuous input of effluent especially in fine grain aquifers may also reduce the effectiveness of microbial removal. Pang (2009) also concludes that for the same media, removal rates for viruses and for bacteria are in the same order of magnitude while removal rates for enteroviruses are lower compared to other human viruses.

[1] Soils are the unconsolidated minerals and organic materials on the immediate surface of the earth and serve as a natural medium for the growth of plants.

Table 2. Summary of the magnitude of removal rates for different subsurface media (Pang 2009).

Category	Magnitude of removal rate λ log/m	Conditions
Soil	$>10^{1}$	Allophanic and pumice sand soils
	10^{0}	Most soil types
	10^{-1}	Clayey soil, clay loam and clayey silt loam
Vadose zone	10^{0}	Pumice sand, clay till, occasionally sand
	10^{-1}	Clay and silt, sand, sand-gravels, coarse gravels, fractured chalk and granite
Sand aquifers ($V < 2$ m/d)	10^{0}	Pumice sand aquifers
	10^{-2}–10^{-1}	Sand aquifers
Sand and gravel aquifers ($V < 3$ m/d)	10^{-1}	$x < 17$ m, clean and contaminated, occasionally 10^{-2} log/m and 10^{0} log/m
	10^{-2}–10^{-1}	$x < 177$ m (including river bank filtration)
	10^{-3}	$x = 183$–970 m, contaminated
	10^{-4}	$x = 210$–2930 m, contaminated
Sandy gravel aquifers ($V > 11$ m/d)	10^{-3}–10^{-2}	$x < 163$ m , clean
Coarse gravel aquifers ($V > 50$ m/d)	10^{-2}	Clean
	10^{-3}	Contaminated
Fractured rock aquifers	10^{-1}–10^{0}	Clean fractured clay till and fractured clayed shale saprolite
	10^{-2}–10^{-1}	Clean fractured gneiss
	10^{-2}	Contaminated sandstone
	10^{-3}–10^{-2}	Contaminated fissured chalk
Karst limestone aquifers	10^{-2}–10^{-1}	$x < 85$ m, contaminated
	10^{-3}	$x = 1250$ m, contaminated
	10^{-4}	$x = 5000$ m, contaminated

According to Humphries (2018), little research has been conducted on the ability of coral sands to attenuate microorganisms contained in domestic effluent. Firouzi et al. (2015) conducted column experiments with undisturbed saturated calcareous soils and observed high reduction rates of bacteria which they attributed to the calcium carbonate within the soil which has favourable attachment sites for bacteria. Burbery et al. (2015) conducted column experiments using disturbed saturated coral sands sampled from the top of the Bonriki Reserve in South Tarawa. They concluded that coral sand is relatively effective at filtering E. coli J6-2 bacteria and F-RNA MS2 bacteriophage (MS2 phage) and that is much less effective at virus removal. Crennan (2001) conducted tracer experiments on Lifuka island in the Kingdom of Tonga to establish whether contaminants were likely to move from point sources of pollution to water supply sources, and whether pathogens would survive that rate of movement. Crennan's experiments indicated that diffusion through the water table of disease causing micro-organisms could occur at a minimum rate of 0.4 m per day in all directions. This suggests that certain pathogens could theoretically travel up to 100 m before their die-off.

Humphries (2018) conducted column experiments using unsaturated coral beach sand, obtained from Bikenibeu beach in South Tarawa, and containing 85% magnesium calcite ($CaMg(CO_3)_2$) and 15% aragonite ($CaCO_3$). A solution containing bacterial microbial indicators (Escherichia coli J6-2, Enterococci faecalis and MS2 bacteriophage) and pathogenic viruses (adenovirus, echovirus, norovirus, and rotavirus) was injected through (1) clean and (2) conditioned (with domestic effluent) coral sands to assess the removal capacity of the sands. None of the microorganisms injected through the clean coral sands were detected in the

column drainage suggesting that the microorganisms were likely physically retained in the sand due to unsaturated conditions. E. coli J6-2 and E. faecalis however were detected in the drainage from the conditioned column experiment suggesting a reduction in removal rates compared to the clean coral sands. High levels of E. coli J6-2 and E. faecalis were also mobilized when groundwater and rainwater were injected through the previously tested columns to simulate and assess the potential mobilization of contaminants upon contact with groundwater and rainwater, respectively. These results suggest that the removal is predominantly a physical process (straining).

Humphries (2018) concludes that effluent disposal in coral sands needs to avoid interaction with sources of groundwater and rainwater to minimise the mobilisation of microorganisms into the underlying groundwater. Mounded coral sand effluent disposal fields are recommended to increase the distance between the disposal point and the groundwater table maximising the available treatment thickness of the unsaturated coral sand.

1.4 Description of the study area

The Republic of Kiribati is a sovereign state in Micronesia in the central Pacific Ocean, with a population of more than 110,000. Kiribati comprises 32 atolls and reef islands and one raised coral island, covering a total land area of 811 km^2 that is dispersed over 3.5 million km^2 (GoK 2010). The Tarawa Atoll is the capital of the Republic of Kiribati and comprises the largely rural North Tarawa islands and islets, and the mainly urbanised South Tarawa islands and islets (Figure 2), which are separated by a series of causeways.

South Tarawa has a length of more than 30 km and is on average less than 250 m in width and contains the main urban centres of the country, with a population of 56,307 (KNSO 2015). Only three islands are wide enough to hold fresh groundwater volumes of sufficient storage to support intensive extraction, namely the urbanised Betio Island, and the largely unpopulated Bonriki and Buota Islands. Groundwater from the Bonriki and Buota freshwater lenses is treated and distributed via a reticulation network to the majority of households (67%) in South Tarawa by the Public Utilities Board (PUB) (KNSO and SPC 2010). Otherwise, freshwater is obtained from private and community wells, and through rainwater harvesting, with a residual amount provided from bottled water.

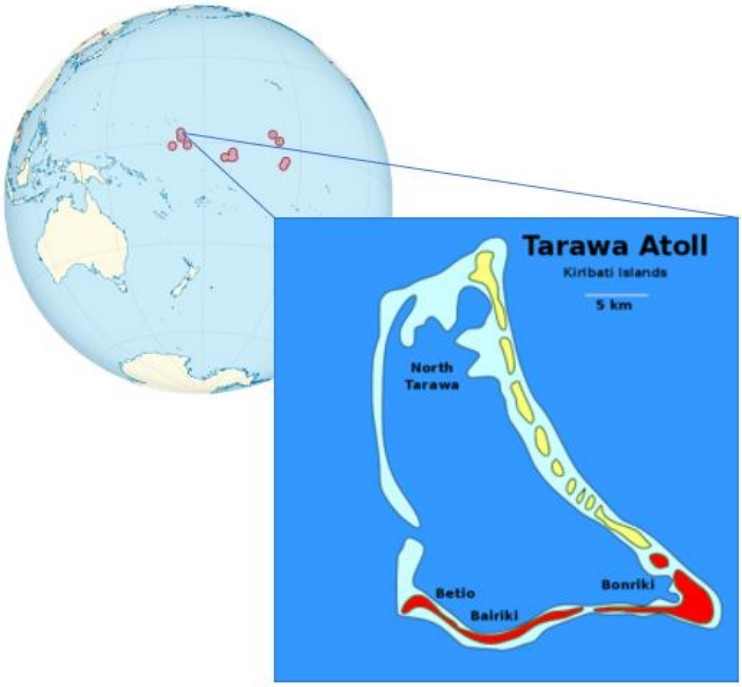

Figure 2. Location of the main islands of the Republic of Kiribati, and the country's capital, Tarawa Atoll (South Tarawa, map within Tarawa Atoll by Дэя-Бøяg (2011).

1.5 Objectives of the study

The primary objective of the current study is to investigate the fate of greywater discharge within typical urban settings of South Tarawa. To achieve this, the study produced calibrated 2D cross-sectional groundwater flow models to investigate the flow and transport processes within the island aquifers of Betio, Bairiki and Bikenibeu. The models were utilised to simulate both the extent of freshwater lenses and the subsurface movement of greywater discharge under two different disposal methods (e.g., surface disposal and well injection) while taking into account climate variability.

2. Data Collection

2.1 Groundwater monitoring

The multi nested monitoring bores at Betio, Bairiki, and Bikenibeu islets, installed in 2011 by GWP Consultants, provide valuable insight into the fresh groundwater lenses accessed by the large communities who live above and rely upon them for their non-potable water needs, washing and gardening. Regular monitoring undertaken by MISE of these South Tarawa monitoring bores and those in Bonriki and Buota water reserves allows for improved understanding of the anthropogenic and climate induced impacts, promoting improved access and sustainability for the population water demands. Maintaining these monitoring bores for future use and reference is critical in addressing the future water security needs of South Tarawa.

The groundwater in the existing monitoring bores was tested for salinity, total coliform and E.coli bacteria and nitrate/nitrite content. Prior to measuring and sampling groundwater, the bores were purged to ensure sampled groundwater was representative of the aquifer. Total depth of the boreholes was also measured to ensure that no boreholes were blocked and thus allowing monitoring at the right depth. Salinity was measured in-situ using a portable conductivity meter. Coliform bacteria contamination was assessed using Compact Dry™ EC plates which allowed obtaining results within 24 hours. Samples for nitrate/nitrite content analysis were preserved frozen and sent to USP lab in Suva, Fiji which carried out the analyses.

2.2 Ground Penetrating Radar surveys

To gain a better appreciation of the shape of the freshwater lens away from the monitoring bores and to assist with the numerical groundwater modelling, geophysics using a ground penetrating radar were employed. Available tracks and roads were used to conduct surveys from south to north (ocean to lagoon) across each islet, close to the line of the monitoring bores to aid in model development.

Ground Penetrating Radar (GPR) is a technique that employs high-frequency radio electromagnetic waves, usually between 10 – 2000 MHz, to acquire subsurface information and to map metallic/non-metallic structures/features buried in the ground. Buried objects or boundaries with an abrupt change in electrical properties create a reflection from the electromagnetic signals. The radio waves are reflected back to the antenna with amplitudes and arrival times that are related to the electrical conductivities (equivalently, dielectric constants) of the material layers. Across the interfaces, part of the energy is reflected and part is absorbed, depending on the dielectric contrast of the materials. The propagation velocity of the radio wave through a subsurface layer is related to the electromagnetic behaviour of the layer:

$v = c / \sqrt{\varepsilon}$
where: ε = dielectric constant of layer and c = speed of light in air = 0.3 m/ns

GPR applications include civil engineering, geotechnical, environmental, archaeology and military. Under the right conditions, GPR can also provide useful information on shallow hydrogeology in coastal zones, including the identification of the depth to the water table, the depth to the freshwater/saltwater interface, and the mapping of hydrostratigraphic units. GPR waves are immediately attenuated once they hit clay layers and saltwater-saturated sediments due to their high electrical conductivity causing the wave to get "scattered" before it can return to the antenna. These high conductivity layers/interfaces can therefore be indirectly identified by the attenuation of the GPR signal.

The rapid change in moisture content upon reaching the water table, produces a distinct GPR reflection, especially where the capillary zone is thin relative to the length of the emitted wave. According to Kruse et al, the water table is not readily apparent at frequencies > 200 MHz. The freshwater/saltwater interface is generally thicker than the radar wavelength and does not cause a reflection. Identification of the extent of a freshwater lens is inferred by the signal attenuation associated with the high conductivity of the underlying seawater-saturated sediments. Signal attenuation should always be interpreted with care as surficial obstacles (e.g. concrete) and shallow geological layers (e.g. mudflats) may impede the radio wave penetration. It is strongly recommended to always calibrate the interpretations for the depths to water table and saltwater/freshwater interface locally through existing shallow wells and monitoring boreholes.

Table 3. Propagation velocities in relevant materials

Material	**Propagation velocity (cm/ns)**
Unsaturated sand	12 – 15
Saturated with freshwater	5.5 – 6.5
Seawater	1

2.3 Elevation survey

Topographical surveys were undertaken using Real-Time Kinematic (RTK) positioning along three transect representing the three modelled cross sections along the three islands. Existing local benchmarks from Kiribati Lands Department provided reference points for the topographical surveys. The elevation data were used to correct the cross-sectional models for elevation changes.

3. Site investigation results

3.1 Groundwater quality in monitoring bores

Table 4 presents the results from the testing and sampling of groundwater in the monitoring bores at the three sites. The estimated thicknesses of the three freshwater lenses at the location of the monitoring bores in Betio, Bairiki and Bikenibeu were 20, 7 and 5 m, respectively, during the time of measurement. These thicknesses are larger compared with the available monitoring data from 2011, possibly a result of the very high rainfall experienced in South Tarawa since January 2019. The substantial thickness of the freshwater lens in Betio indicates its high potential for groundwater exploitation. It also indicates the higher groundwater storage properties of the aquifer implying its high potential for managed aquifer recharge of treated greywater to maintain the lens thickness during dry periods or to promote greywater reuse. The freshwater lenses in Bairiki and Bikenibeu, albeit thinner compared to Betio, also hold some potential for induced greywater recharge.

The bacteriological results from the tested Betio monitoring bores indicate no E. coli contamination and low total coliform counts. The location of the monitoring bore in the Betio sports stadium, located away from the dense housing suggests that the groundwater in the area under the stadium has the potential for potable purposes. Testing of the Bairiki and Bikenibeu monitoring bores indicates similar results with regards to low levels of E. coli contamination and are likely to be more representative of the groundwater. The exception to the low E. coli contamination is the Bikenibeu monitoring bore, which has an E. coli CFU of 21/100 ml. It is noted that this monitoring bore is located in the garden bed of a vegetable farm which undertakes mulching and soil improvement using garden waste and also has a small piggery, whose waste is likely to be included in the farming practices and may impact on the sample results.

Nitrate in groundwater is usually derived from diffuse pollution from agriculture and from sewage sludge disposal to land. Wastewater disposal (on-site systems and leaky sewers) and solid waste disposal (landfills and waste tips) constitute the main non-agricultural sources of nitrogen to groundwater. Nitrogen removal in groundwater occurs by different natural biogeochemical processes often referred to as retention or reduction. Denitrification is a microbially facilitated process where nitrate (NO_3-) is reduced and ultimately produces molecular nitrogen (N_2) through a series of intermediate gaseous nitrogen oxide products, including nitrite (NO_2-). Anaerobic bacteria perform denitrification as a type of respiration that reduces oxidized forms of nitrogen in response to the oxidation of an electron donor such as organic matter.

Nitrate levels exceed the WHO drinking water guideline of 50 mg/l in three of the tested bores whereas the guideline for nitrite of 3 mg/l is not exceeded in any of the bores. Nitrate contamination is clearly decreasing (as observed in the Bairiki monitoring bores) with depth due to advancing denitrification. Nitrite concentration initially increases with depth due to nitrite production by nitrate reduction and then decreases as well as denitrification progresses towards more reduced nitrogen oxide products. The nitrate contamination in Bairiki is probably deriving from leaky sewers whereas the higher contamination in Bikenibeu is probably deriving from agricultural activities conducted at the vegetable farm where the monitoring bore is located.

Table 4. Groundwater quality in monitoring bores.

Monitoring bore	Depth	EC	Total Coliforms		E. coli		NO_3	NO_2
	m	µS/cm	CFU/ml	CFU/100ml	CFU/ml	CFU/100ml	mg/l	mg/l
Betio-1	6	485	0	72	0	0	0.12	<0.01
Betio-2	10	535	0	12	0	0	<0.02	<0.01
Betio-3	14	574	0	10	0	0	<0.02	<0.01
Betio-4	18	583	0	0	0	0	<0.02	<0.01
Betio-5	21	845	0	0	0	0	<0.02	<0.01
Betio-6	24	11470	-	-	-	-	-	-
Bairiki-1	5	621	0	3	0	1	69.2	1.42
Bairiki-2	7	669	0	9	0	2	59.8	1.66
Bairiki-3	9	1997	0	78	0	0	21.9	0.74
Bairiki-4	12	3170	0	1	0	1	8.69	0.13
Bairiki-5	15	8570	0	0	0	0	-	-
Bairiki-6	18	13620	-	-	-	-	-	-
Bikenibeu-1	6	1484	1	63	0	21	114	0.33
Bikenibeu-2	9	10820	-	-	-	-	-	-
Bikenibeu-3	12	21580	-	-	-	-	-	-
Bikenibeu-4	15	27800	-	-	-	-	-	-
Bikenibeu-5	18	41130	-	-	-	-	-	-
Bikenibeu-6	24	46600	-	-	-	-	-	-

3.2 Groundwater quality in shallow wells

Comparing the bacteriological results from the monitoring bores with the ones obtained from the uncovered shallow household wells, located in the densely populated areas of Betio, indicates that groundwater sourced from open wells, which are closer to contamination sources including livestock and septic tanks are, not unexpectedly, contaminated with E. coli making them unsuitable for potable purposes without treatment. It was observed that the shallow wells in Bairiki had higher E. coli CFU/100 ml when compared with the wells from Bikenibeu. The higher density of housing in Bairiki, and the possible leakage of reticulated sewage pipes is likely to be a consideration in this higher contamination observed in Bairiki.

The low E. coli contamination observed in the monitoring wells in all three locations compared with the high E. coli levels in the shallow wells suggests that the migration of pathogens is restricted to the close vicinity of the contamination source, and that the contamination is likely due to ingress to open wells from overland flow during rain events and normal well operation.

Anomalously high salinities were recorded in two shallow wells (W4 and W5) towards the centre of the islet of Bairiki and away from the coast at depths of 0.6 and 0.3 m, respectively, below the water table. This is unusual in that at this depth the groundwater should be fresh given the recent rains, and that the nearby monitoring bore suggests a freshwater lens thickness of 7 m. Government of Kiribati, MISE staff indicated that there is saltwater sewage reticulation in Betio, Bairiki, and Bikenibeu, and recently new HDPE pipelines have been installed which supply saltwater as additional non potable water to households. There is potential that either the reticulated saltwater pipeline or the reticulated saltwater sewage lines may be leaking which could result in the elevated salinities encountered at shallow depths. Consideration to geological factors which could result in the elevated salinity at these locations would

seem unlikely given the location of the wells, their shallow depths and that other wells closer to coast and lagoon indicate fresh groundwater. The location of the saltwater pipelines and the reticulated saltwater sewage lines were obtained from Public Utilities Board (Tom Rautu, pers comm 8/5/2019). Although a limited number of shallow wells were sampled, there is a positive correlation between the elevated salinities in W4 and W5 and the estimated distance to the closest saltwater supply line or the seawater sewage line. While the data is not conclusive it does suggest that further investigation is warranted.

Nitrate levels exceeded the WHO drinking water guideline at three of the tested shallow wells whereas nitrite levels were below the guideline value. In Betio, nitrate contamination is probably due to wastewater and solid waste disposal whereas in Bikenibeu nitrate contamination could be derived from the agricultural activities affecting groundwater quality around the vicinity of the vegetable farm.

Table 5. Groundwater quality in shallow wells

Shallow well	**Depth to water**	**EC at base**	**Total Coliforms**		**E.coli**		**NO_3**	**NO_2**
	m	µS/cm	CFU/ml	CFU/100ml	CFU/ml	CFU/100ml	mg/l	mg/l
W1 (Betio)	1.65	900	TNTC	TNTC	TNTC	TNTC	54.2	0.20
W2 (Betio)	0.94	605	61	TNTC	0	25	12.4	0.13
W3 (Bairiki)	1.16	401	TNTC	TNTC	26	TNTC	3.46	<0.01
W4 (Bairiki)	1.27	2450	TNTC	TNTC	TNTC	TNTC	18.7	1.84
W5 (Bairiki)	1.83	5450	NA	NA	NA	NA	-	-
W6 (Bairiki)	1.94	628	TNTC	TNTC	5	180	3.41	<0.01
W7 (Bikenibeu)	1.32	1122	TNTC	TNTC	3	128	79.5	0.13
W8 (Bikenibeu)	1.99	583	90	TNTC	1	53	7.58	<0.01
W9 (Bikenibeu)	1.58	1017	TNTC	TNTC	2	70	60.2	<0.01
W10 (Bikenibeu)	1.40	828	NA	NA	NA	NA	-	-
W11 (Bikenibeu)	1.57	820	NA	NA	NA	NA	-	-

Nitrate needs to be regulated in drinking water because excess levels can cause methaemoglobinaemia, or "blue baby" disease. Short-term exposure to drinking water with a nitrate level above the health standard is a potential health problem for babies and lactating mothers. Although nitrate levels that affect babies are not dangerous for older children and adults, they do indicate the possible presence of other more serious pollutants, such as bacteria.

While generally groundwater in urban areas is not used for potable purposes it is worth noting that nitrate/nitrite are not removed from water using normal disinfection methods such as boiling.

3.3 Ground Penetrating Radar surveys

GPR surveys were conducted along 3 cross sections in Betio, Bairiki and Bikenibeu respectively, along the existing monitoring boreholes and a number of shallow wells to allow for local calibration of the GPR results. The main objective of these surveys was to approximate the lateral variation of the vertical extent of the freshwater lenses along the width of the three islands. This in turn would also serve as a comparison for the results derived from the numerical groundwater model. The ranges in the lateral variation of the estimated freshwater lens thicknesses are summarized in Table 6. The freshwater lens thicknesses are probably underestimated, especially for Betio, due to the limited penetration depth of

the GPR waves not allowing for the identification of the full extent. The complete GPR profiles can be found in Appendix 3.

Table 6. Estimated thickness of freshwater lenses through GPR.

Site	Depth to salt/freshwater interface (m)	Freshwater lens thickness (m)
Betio	8 – 9.5	6.5 – 8
Bairiki	4.5 – 6	3 – 4.5
Bikenibeu	4 – 6.5	2.7 – 5.2

4. Conceptual Model

4.1 Geometry and location of cross-sections

In this study, transects across the islands of Betio, Bairiki and Bikenibeu were adopted for 2D (cross-sectional) groundwater modelling. Transect locations were chosen to coincide with existing monitoring wells in each island. The cross-sectional models traverse the island width and extend beneath the seafloor and lagoon to minimise boundary effects on the modelling of freshwater lens behaviour. The location of transects are shown in Figure 3, and transect dimensions are summarised in Table 7. Approximate land surface elevations are shown in Figure 4.

Figure 3. The location of RTK (real-time kinematic) survey lines and transects for cross-sectional models.

Table 7. Transect lengths, including offshore distances.

	Betio	Bairiki	Bikenibeu
Transect length (m)	554	442	376
Subsea extent (m)	910	636	493
Lagoon extent (m)	526	265	350
Total length (m)	1990	1343	1219

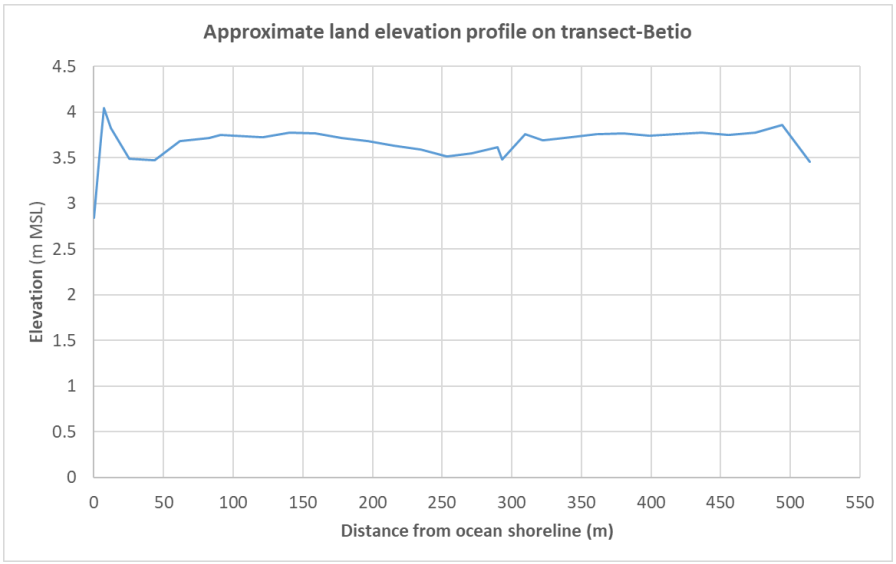

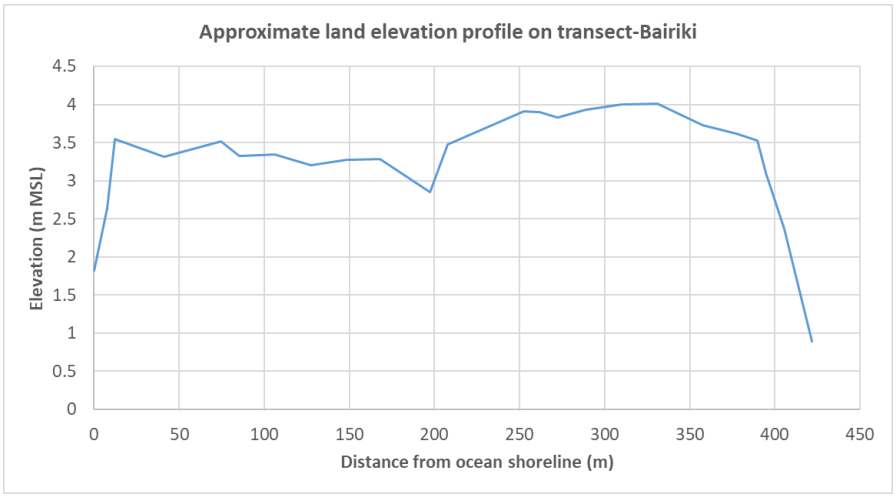

Figure 4. Approximate land elevation profiles for model transects ('m MSL' denotes mean sea level).

The bathymetry of the ocean and lagoon, used to define the top of groundwater models for the offshore components of each transect, was approximated from the shape of the lagoon and sea

floor around Bonriki Island, as obtained from the bathymetric survey by Kumar et al. (2015). It was assumed that the slopes of the lagoon bottom, the reef flat and the sea floor beyond the reef around Bonriki Island are similar to that of Betio, Bairiki and Bikenibeu Islands. However, the offshore lengths of these regions (i.e., lagoon, reef flat, ocean floor) were obtained from the actual field sites. These are shown in Figure 5.

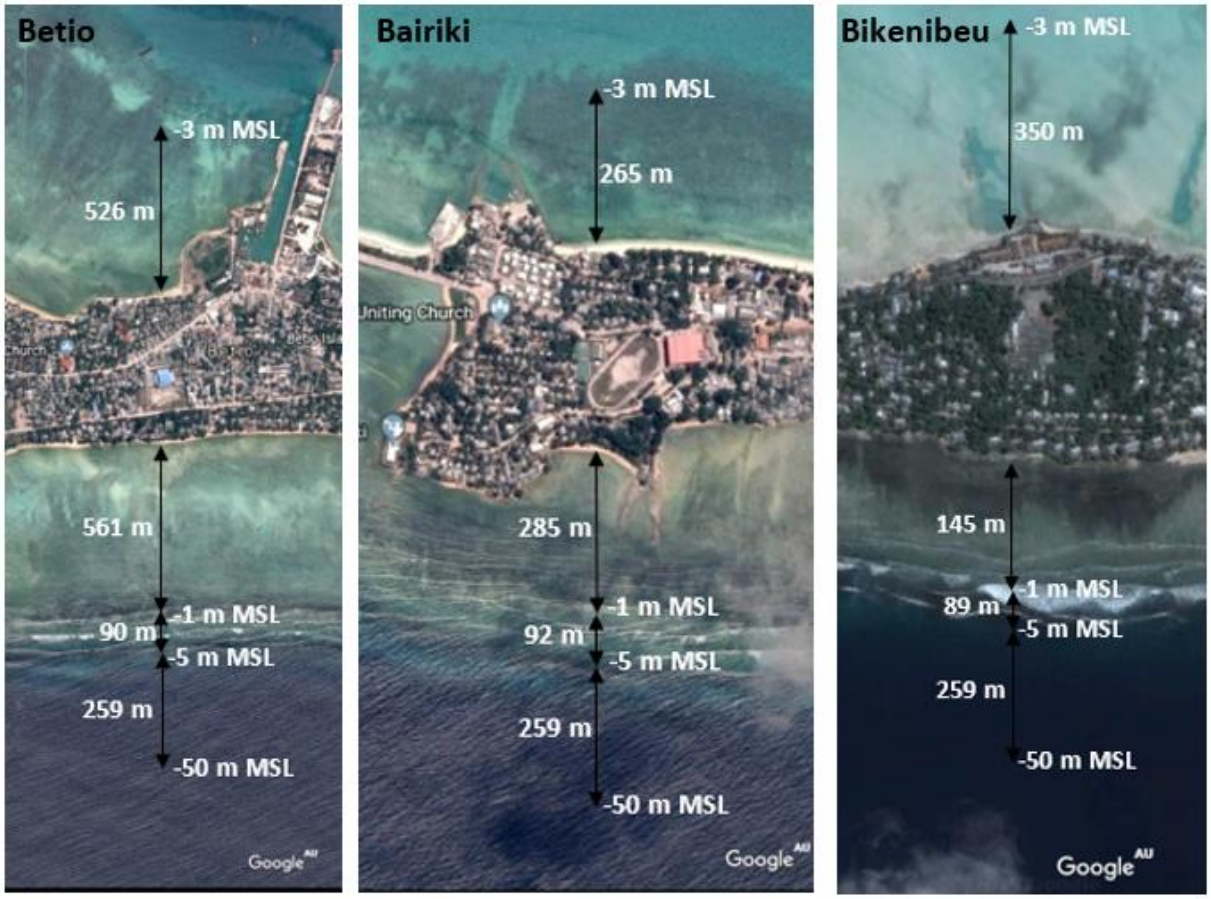

Figure 5. Approximate bathymetry of offshore parts of modelled transects at Betio, Bairiki and Bikenibeu.

A real-time kinematic (RTK) survey was undertaken by SPC to collect topographic data in the vicinity of the investigation transects. The RTK survey lines and groundwater model transects are shown in Figure 3., and topographical variability projected to groundwater model transects is illustrated in Figure 4. Land surface elevations inland of the intertidal zone fall in ranges of 2.84-3.46 m MSL (mean seal level) for Betio, 0.89-1.82 m MSL for Bairiki, and 1.60-4.38 m MSL for Bikenibeu. It should be noted that there are different vertical reference points in Tarawa, including the Sea Level Fine Resolution Acoustic Measuring Equipment (SEAFRAME) tide gauge installed by the Bureau of Meteorology of Australia and Tide Gauge Zero (TGZ) installed by the

University of Hawaii, which is 0.42 m above SEAFRAME (Bosserelle 2015). The SEAFRAME datum is used in this study as the vertical reference datum (i.e., 0 m MSL).

4.2 Geology

The Tarawa Atoll, as with many atoll islands, is composed of poorly consolidated Holocene sediments deposited on Pleistocene limestone reef deposits (Ayers and Vacher 1986; White and Falkland 2010). This stratigraphic sequence was observed during drilling on Betio, Bairiki and Bikenibeu (GWPC 2011), and is also the stratigraphy adopted in groundwater modelling of Bonriki Island by Bosserelle (2015). Following GWPC (2011), the main features of the Holocene-Pleistocene sequences are:

- Holocene: Loose coral sands, gravel and loose rock to a depth of approximately 10-20 m below ground level. The lower portion of this zone typically comprises sands with cemented layers.
- Pleistocene: Typically presents as an older weathered limestone, usually comprised of calcified coral with significant porosity.

The change in geology (i.e., contact between Holocene and Pleistocene sequences), known as the Thurber discontinuity or the Holocene-Pleistocene unconformity (HPU), is a key factor controlling freshwater lens thicknesses in atoll environments (Ayers and Vacher 1986; Anthony 2004; Buddemeier and Oberdorfer 2004). The freshwater zone is typically restricted to the Holocene sediments, which have lower permeability, while the transition zone (i.e., the region of mixing between freshwater and seawater) is usually found predominantly in the higher permeability Pleistocene limestone (Falkland et al. 2003).

The location and depth of boreholes and depths to the HPU are given in Table 8 for the three transects (Betio, Bairiki and Bikenibeu).

Table 8. Borehole locations and depths, and depth to the HPU in Betio, Bairiki and Bikenibeu Islands (GWPC 2011).

Borehole name	Location		Total depth (m BGL*)	HPU depth (m BGL)
	Northing	Easting		
Betio	1°21'20.1"	173°55'41.0"	24.5	21.0
Bairiki	1°19'46.4"	173°58'35.5"	19.0	18.0
Bikenibeu	1°21'48.7"	173°06'38.0"	25.0	16.5

* m BGL = metres below ground level

4.3 Aquifer hydraulic parameters

Falling-head tests were carried out by GWPC (2011) in the three boreholes in each of Betio, Bairiki and Bikenibeu Islands to obtain local estimates of hydraulic conductivity, *K*. A summary of the results is shown in Table 9.

Table 9. Falling-head test results to obtain localised estimates of hydraulic conductivity (*K*) for Betio, Bairiki and Bikenibeu (GWPC 2011).

Borehole name	Test depth (m BGL)	*K*	Test depth (m BGL)	*K*
Betio	9.0	3×10^{-4} m/s (26 m/d)	18	4×10^{-3} m/s (350 m/d)
Bairiki	9.2	1×10^{-3} m/s (86 m/d)	15	1×10^{-3} m/s (86 m/d)
Bikenibeu	9.2	1×10^{-3} m/s (86 m/d)	17	$>1\times10^{-2}$ m/s (>1000 m/d)

Falling-head test results show high *K* values for both sand and limestone, with limestone *K* generally equal to or higher than that of sand, as expected from previous studies (e.g., Oberdorfer and Buddemeier 1983; Peterson 2004; Vacher 2004). Note that the *K* of limestone at Bikenibeu was higher than the limit of the falling-head test methodology, and therefore a value greater than or equal to 1000 m/d is expected, consistent estimates for other atoll islands (Werner et al. 2017).

The range for *K* from in-situ permeability tests in Bonriki and Buariki, undertaken in several previous studies, are shown in Table 10. The values for *K* show spatially heterogenous coral-derived sediments and increasing *K* with depth near the HPU.

Table 10. In-situ hydraulic conductivity values for Buariki and Bonriki.

Location	Target aquifer	*K* (m/d)	Reference
Buariki	Limestone	180	Jacobson and Taylor (1981)
Bonriki	Holocene sediments	3-54	Falkland and Woodroffe (1997)
	Unconformity at top of Pleistocene limestone	6-39	
	Superficial Holocene sediments	1-97	White et al. (2005)

Prior studies of atoll islands similar to those under investigation in this study adopt spatial variability in aquifer hydraulic properties (e.g., Post et al. 2018), because differences in sediment characteristics have been shown to be critical in assessing freshwater lens behaviour (Werner et al. 2017). Although there is insufficient field data to infer spatial variability in the models developed here, we nonetheless adopt a template of *K* zonation that is based on the

study of Bonriki Island by Bosserelle et al. (2015) and Post et al. (2018). The geometry and *K* zonation within the three transects of this study is shown in Figure 6.

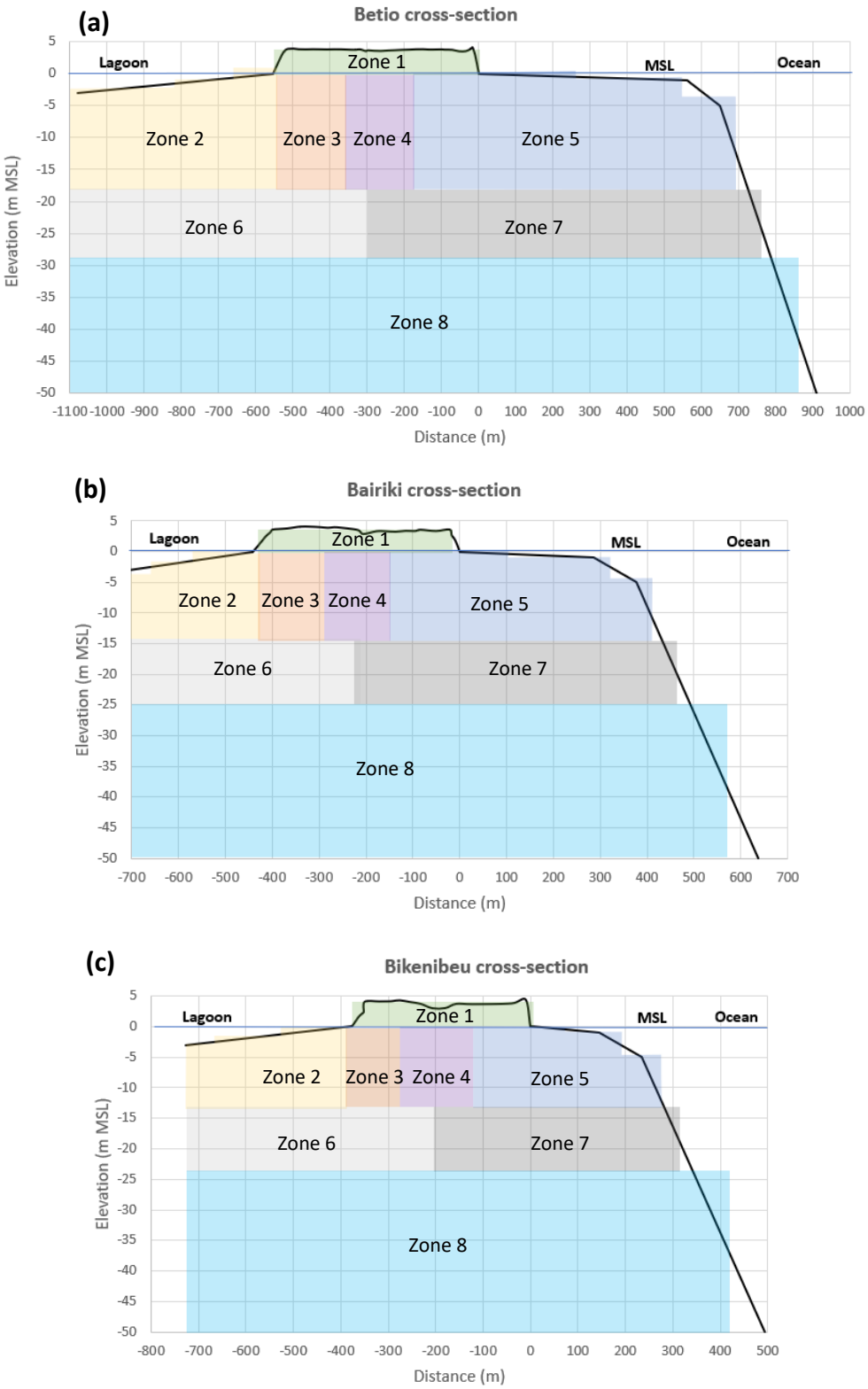

Figure 6. The spatial distribution of hydraulic conductivity for the three representative cross-sections of: (a) Betio, (b) Bairiki, and (c) Bikenibeu. Zones are numbered 1 to 8, where Holocene sand is 1 to 5, and Pleistocene limestone 6 to 8.

The hydraulic parameters required for simulating freshwater lens extent and greywater transport in SEAWAT are horizontal hydraulic conductivity (K_H), vertical hydraulic conductivity (K_V), porosity (n), longitudinal dispersivity (α_L), horizontal transverse dispersivity (α_T) and vertical transverse dispersivity (α_V). Likely parameter ranges and their distribution are needed to constrain the calibration of model parameters to reasonable bounds. Ranges of values adopted in similar settings were obtained from Alam et al. (2002) and Bosserelle et al. (2015) and are summarised in Table 11.

Table 11. Hydraulic parameter values in previous numerical modelling for Bonriki (Alam et al. 2002; Bosserelle et al. 2015).

Parameter	**Zone # (Fig. 5)**	**Value**
Top soil and surficial Holocene sediments, K_H (m/d)	1	5
Top soil and surficial Holocene sediments, K_V (m/d)	1	1
Beach rock Holocene sediments (ocean side), K_H (m/d)	2-3	4
Beach rock Holocene sediments (ocean side), K_V (m/d)	2-3	0.8
Unconsolidated Holocene sediments, K_H (m/d)	4-5	1-30
Unconsolidated Holocene sediments, K_V (m/d)	4-5	0.2-5
Upper Pleistocene, K_H (m/d)	6-7	8-50
Upper Pleistocene, K_V (m/d)	6-7	3.5-10
Lower Pleistocene, K_H (m/d)	8	500-1400
Lower Pleistocene, K_V (m/d)	8	100-200
n	All	0.2
α_L (m)	All	0.05-12
α_T (m)	All	0.05-0.5
α_V (m)	All	0.01

The initial hydraulic parameter values used in the current study were specified for each of the three islands based on the previous investigation of Bonriki Island by Bosserelle et al. (2015). These are presented in Table 12 and Figure 6. Initial values of hydraulic parameters were subsequently modified via model calibration using a simple trial-and-error methodology, consistent with the approach of Post et al. (2018) and considered adequate for the current project scope and resource-constraints.

Table 12. The initial model parameter values for Betio, Bairiki and Bikenibeu. Note colours in this table match those of the Figure 6. Values of n, α_L, α_L, α_V are for all zones.

		Elevation (m MSL)				
		Betio	**Bairiki**	**Bikenibeu**	**K_H (m/d)**	**K_V (m/d)**
Zone 1	Top soil	0 to 3.46	0 to 1.82	0 to 4.38	5	1
Zone 2	Holocene sediment	-17.3 to 0	-14.3 to 0	-12.9 to 0	1	0.2
Zone 3	Holocene sediment	-17.3 to 0	-14.3 to 0	-12.9 to 0	5	1
Zone 4	Holocene sediment	-17.3 to 0	-14.3 to 0	-12.9 to 0	8	1.6
Zone 5	Holocene sediment	-17.3 to 0	-14.3 to 0	-12.9 to 0	12	2.4
Zone 6	Upper Pleistocene	-27.3 to -17.3	-24.3 to -14.3	-22.9 to -12.9	10	2
Zone 7	Upper Pleistocene	-27.3 to -17.3	-24.3 to -14.3	-22.9 to -12.9	16	3.2
Zone 8	Lower Pleistocene	-100 to -27.3	-100 to -24.3	-100 to -22.9	500	100
Depth of unconformity		-17.3	-14.3	-12.9		
n		0.2	0.2	0.2		
α_L (m)		1	1	1		
α_T (m)		0.05	0.05	0.05		
α_V (m)		0.01	0.01	0.01		

4.4 Freshwater lens distribution

The extent of the freshwater lens needs to be determined because the transport of greywater within islands will depend on the density-dependent flow within the lens. Lens extent within each island was assessed using measurements of electrical conductivity (EC) in monitoring wells, combined with surface geophysical surveys. Measured EC profiles from 2010, 2011 and 2019 are presented in Table 13, and the mean EC profiles from these three times are shown in Figure 7. Graphical representations of measured EC profiles in each monitoring well are provided in Appendix 1. Freshwater lens thicknesses in Betio, Bairiki and Bikenibeu were determined by interpolating the depth where the EC is equal to 2500 µS/cm from EC profiles. These are presented in Table 14.

Table 13. Average of EC profiles in monitoring wells in 2010, 2011 and 2019.

	Elevation (m MSL)	EC (µS/cm)					
		Jul-10	Oct-10	Jan-11	Mar-11	May-19	Mean
Betio	1.92	-	-	623	-	-	623
	-0.31	-	-	1411	-	-	1411
	-2.31	559	560	552	586	483	548
	-6.31	1676	524	568	605	535	782
	-10.31	401	631	687	685	574	595
	-14.31	669	840	970	994	581	811
	-17.31	1623	3560	6543	7440	845	4002
	-20.31	-	-	31,300	30,767	11,473	24,513
	Water table (m MSL)	2.31	1.96	1.92	-	2.04	2.06
Bairiki	0.90	-	-	1249	-	-	1249
	-1.12	-	-	4960*	-	-	4960*
	-2.12	2342	4497	6480	4870	621	3762
	-4.12	2627	5493	7293	6207	669	4458
	-6.12	8183	10,137	11,700	11,163	1997	8636
	-9.12	10,827	13,207	14,760	14,123	3167	11,217
	-12.12	17,783	21293	22,597	23,133	8573	18,676
	-15.12	19,777	22,913	25,200	25,800	13,617	21,461
	Water table (m MSL)	0.90	0.90	0.90	-	1.00	0.93
Bikenibeu	1.52	-	-	1270	-	-	1270
	-0.37	-	-	1475	-	-	1475
	-2.37	3613	5270	9373	9807	1484	5909
	-5.37	15,603	21,430	26,800	29,533	10,823	20,838
	-8.37	-	-	37,767	38,333	21,580	32,560
	-11.37	-	-	40,233	41,100	27,800	36,378
	-14.37	-	-	42,633	43,400	41,133	42,389
	-20.37	-	-	47,667	48,433	46,600	47,567
	Water table (m MSL)	1.46	1.38	1.52	-	1.54	1.48

* This is considered as an outlier and was therefore omitted from the dataset hereafter.

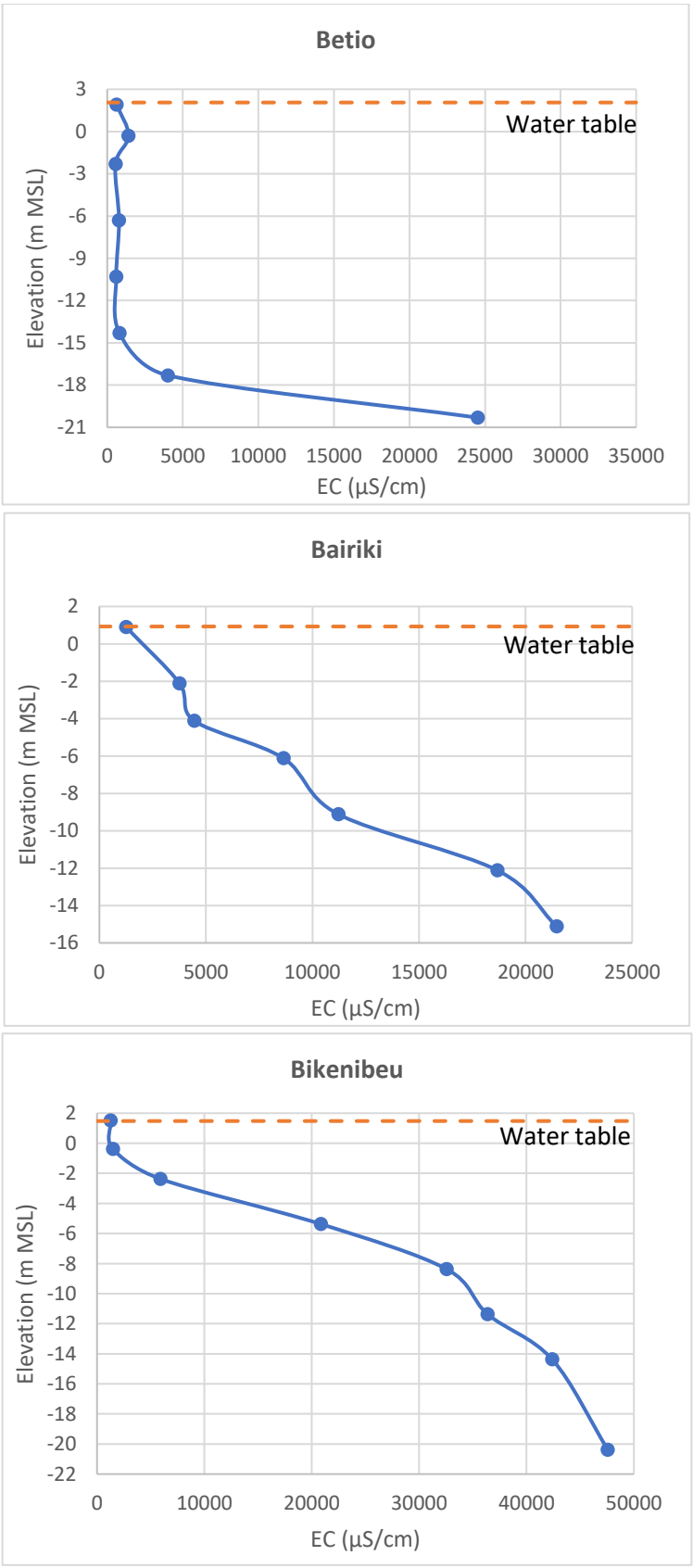

Figure 7. Average of 2010, 2011 and 2019 measured EC profiles in monitoring wells located on the three islands investigated in this study. Data provided in Table 13.

Table 14. Freshwater lens thicknesses based on the interpolated depth (below the water table) to EC = 2500 µS/cm in monitoring wells. Note that groundwater of EC < 2500 µS/cm was not recorded where values are given as upper limits (showing "<").

Island	Lens thickness (m)					
	Jul 2010	Oct 2010	Jan 2011	Mar 2011	May 2019	Average
Betio	19.7	18.1	17.1	17.1	19.8	18.4
Bairiki	5.0	<3.0	0.7	<3.0	8.4	4.7
Bikenibeu	<3.8	<3.8	2.1	<3.8	4.2	3.2

The salinity distribution at the three sites shows differing characteristics, in that the transition from freshwater to saltwater in Bairiki and Bikenibeu is wide relative to the freshwater thickness, whereas the transition (or mixing) zone is relatively narrow in Betio. The larger island width of Betio causes this effect, as described by White and Falkland (2010).

Electromagnetic surveys undertaken in 2011 using an EM34 apparatus assessed the freshwater-saltwater distribution in various locations throughout South Tarawa (FTP 2011). Freshwater lens thickness maps were subsequently created for Betio, Bairiki and Bikenibeu (FTP 2011). For the purposes of the current study, freshwater lens distributions at each transect were extracted from maps developed by FTP (2011). The results are shown in Figure 8. The EM34 results are generally consistent with the observations of freshwater lens thickness from well measurements, whereby Betio has a well-developed lens, whereas Bairiki and Bikenibeu have only thin freshwater lenses.

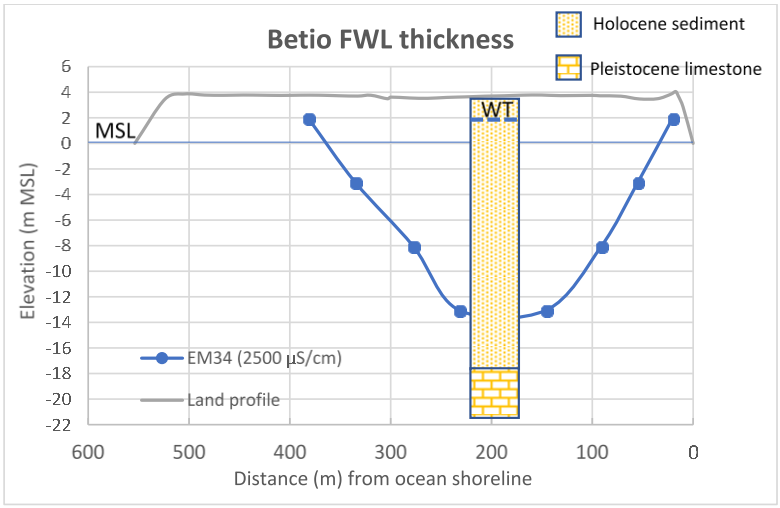

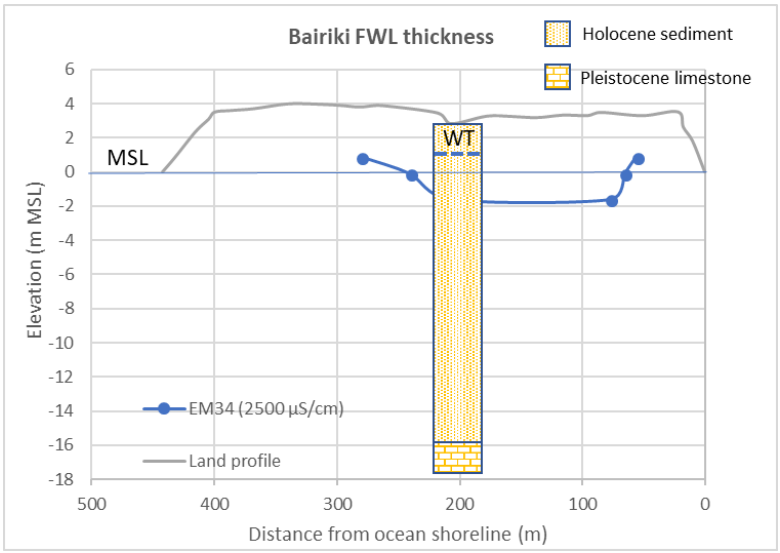

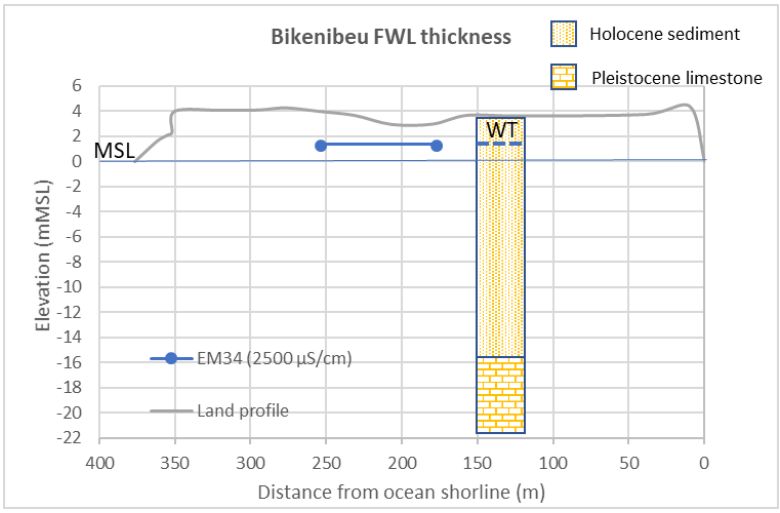

FWL = Freshwater Lens; MSL = Mean Sea Level; WT = Water Table.

Figure 8. Freshwater lens distribution (defined by the interpolated 2500 µS/cm salinity contour) extracted from EM34 data (FTP 2011) from Betio, Bairiki and Bikenibeu. The stratigraphy and water table depth in monitoring wells are also shown.

4.5 Recharge

A key factor in atoll freshwater lens occurrence is the temporal and spatial distribution of recharge, which is primarily a function of rainfall and evapotranspiration. To estimate recharge rates, a water balance analysis can be undertaken on the unsaturated zone (i.e., the region between the land surface and the top of the saturated zone/water table). The basic water balance equation is given by (Alam et al. 2002):

$$R = P - E \pm \Delta V \quad (1)$$

where, R is recharge (mm/d), P is rainfall (mm/d), E is evapotranspiration (mm/d), and ΔV is the change in the storage (per unit land area; mm/d) within the unsaturated zone, which is often neglected for atoll islands due to shallow water tables. Applying equation (1) typically requires climate records and the vegetation cover to estimate the transpiration component of evapotranspiration, including from both soil water and groundwater. The interception of rainfall by tree canopies may also be important (Alam and Falkland 1997; Alam et al. 2002).

This approach was applied in previous studies to model recharge to various atoll islands, including Bonriki Island (Alam et al. 2002; Werner et al. 2017). Alam et al. (2002) estimated the average recharge for Bonriki as 50% of rainfall based on a tree cover of 20%. FTP (2011) assumed that the tree cover percentage is less than 20% in Betio, Bairiki and Bikenibeu based on the urban environments of these islands. Hence, recharge for these three islands may be greater than 50% of the rainfall. Nevertheless, FTP (2011) suggested to use 50% of rainfall as a conservative estimate of recharge for Betio, Bairiki and Bikenibeu in their sustainable yield estimations.

Rainfall inputs to Eq. (1) were available from the meteorological station on Betio (Station No J61000, 01°21'N 172°56'E). These include monthly totals from 1947 to 2018 and daily values from 1947 to 2015, with sporadic records before 1947. Annual rainfall totals for Betio are shown in Figure 9.

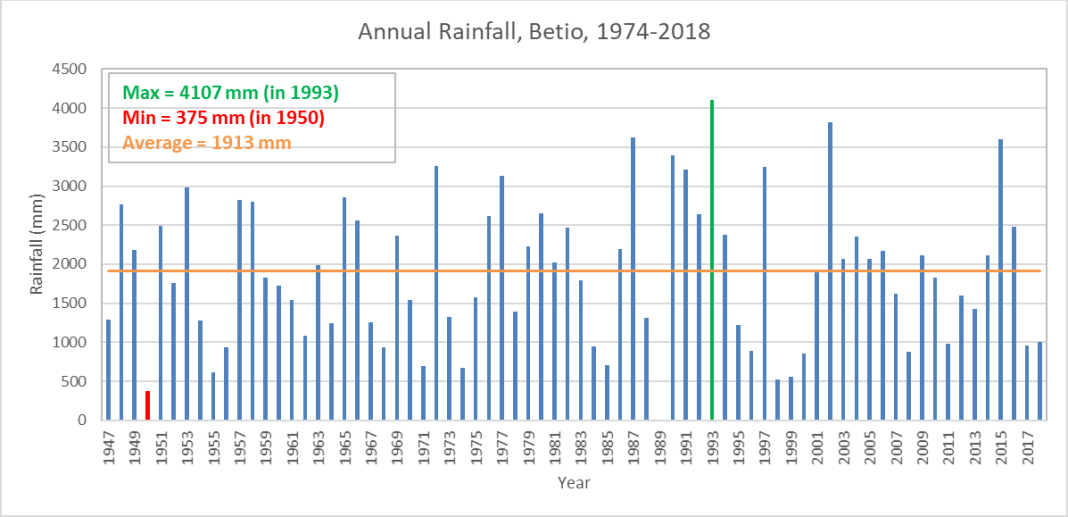

Figure 9. Annual rainfall and statistics for Betio (1974-2018).

In this study, 50% of the average annual rainfall (1913 mm/y) from 1947 to 2018 was used in setting the recharge in steady-state simulations (i.e., equilibrium conditions), whereby R = 0.5×1913 mm/y = 956.5 mm/y. In transient (time-variant) modelling, daily rainfall data were aggregated to time steps (i.e., "stress periods") of 14-days, using the period 1947 to 2015.

4.6 Well abstraction

In South Tarawa, groundwater has been abstracted from shallow wells in Holocene sediments from the 1960s. A survey undertaken in 2011 found more than 174 private wells distributed across Betio, Bairiki and Bikenibeu (FTP 2011). The rate of daily water abstraction from each well was approximated by data collected from household questionnaires (FTP 2011), which indicated that well water use ranged from 18 to 72 L/pers/d. Given the difficulty in locating individual wells, groundwater abstraction was treated as a distributed groundwater output in the models developed in this study. Values of distributed groundwater abstraction were estimated from: (1) the average daily well abstraction, assumed to be 45 L/pers/d (FTP 2011), (2) the number of people in each house, based on the 2015 census (KNSO and SPC 2016) (i.e., for the 'current situation'), and (3) the number of houses in a ~100 m buffer around each model transect (50 m either side of cross-island transects; see Appendix 2). In addition, the rate of abstraction in 2030 (i.e., the 'future scenario') was estimated based on the percentage increase in population from 2015 to 2030 (i.e., increase in number of people per house) assuming the number of houses in a 100 m buffer and the rate of abstraction remain unchanged. The calculations of well abstraction for each cross-section for the current scenario (based on 2015 population) and the future scenario (based on 2030 population) are shown in Table 15.

Table 15. Estimated well abstraction for Betio, Bairiki and Bikenibeu.

	Betio	Bairiki	Bikenibeu
[1] Average volume of well water used (L/pers/d)	45		
[2] Area of a 100 m strip around cross-section line (m^2)	55,382	44,229	37,614
[3] Number of people per house in 2015	8	7	7
[4] Number of houses in a 100 m strip	49	34	22
[5] Number of people in a 100 m strip (= [3]×[4])	392	238	154
[6] Total volume of abstraction in a 100 m strip (L/d) (= [5]×[1])	17,640	10,710	6930
[7] Average total abstraction per cross-section for current situation (mm/y) (= 365.25×[6]/[2])	**116**	**88.4**	**67.3**
[8] Number of people per house in 2030	12	11	9
[9] Number of people in a 100 m strip (= [8]×[4])	588	374	198
[10] Total volume of abstraction in a 100 m strip (L/d) (= [9]×[1])	26,460	16,830	8910
Average total abstraction per cross-section for future scenario (mm/y) (=365.25×[10]/[2])	**175**	**139**	**86.5**

Notes:
[1] based on FTP (2011)
[2] equal to 100 m (the width of buffer around the cross-section line) multiplied by the length of each transect (see Table 7)
[3] based on 2015 census (KNSO and SPC 2016)
[4] see Appendix 2
[8] based on the projected increase in population in 2030 (FTP 2011)

4.7 Greywater discharge

In the Tarawa Water Master Plan developed by White (2010), the amount of water required per capita was assumed to be 50 L/pers/day, increasing to 100 L/pers/d by 2030 due to anticipated increased freshwater availability from additional water supply options (e.g., desalination). Up to 75% of the domestic wastewater produced by households is released in urban settings in the form of greywater, which is defined as the wastewater derived from showers, bathtubs, sinks, kitchens, dishwashers, laundry tubs and washing machines, and excludes toilet water (Eriksson et al. 2002). In this study, it is assumed that 70% of the freshwater provided to households is discharged in the form of greywater, hence 35 and 70 L/pers/d of greywater discharge are adopted for the current situation and future scenarios, respectively.

For the purposes of developing cross-sectional models, the greywater flux entering the model domain was calculated from greywater flux rates per person (see above), the number of households, and the number of people per household in the vicinity of transects, and taking into account the width of the cross-sectional model (i.e., 1 m) versus the width perpendicular to transects (~100 m) over which the number of residents was estimated. This provided numerous points of greywater input to the model, as illustrated in Figure 10. These locations are not true sites of greywater disposal but are meant to approximate the typical spatial frequency of greywater disposal under current conditions. Maps showing transect alignments and assumed

locations of greywater input are given in Appendix 2. The calculation of greywater inputs is also detailed in Appendix 2 for the three transect locations.

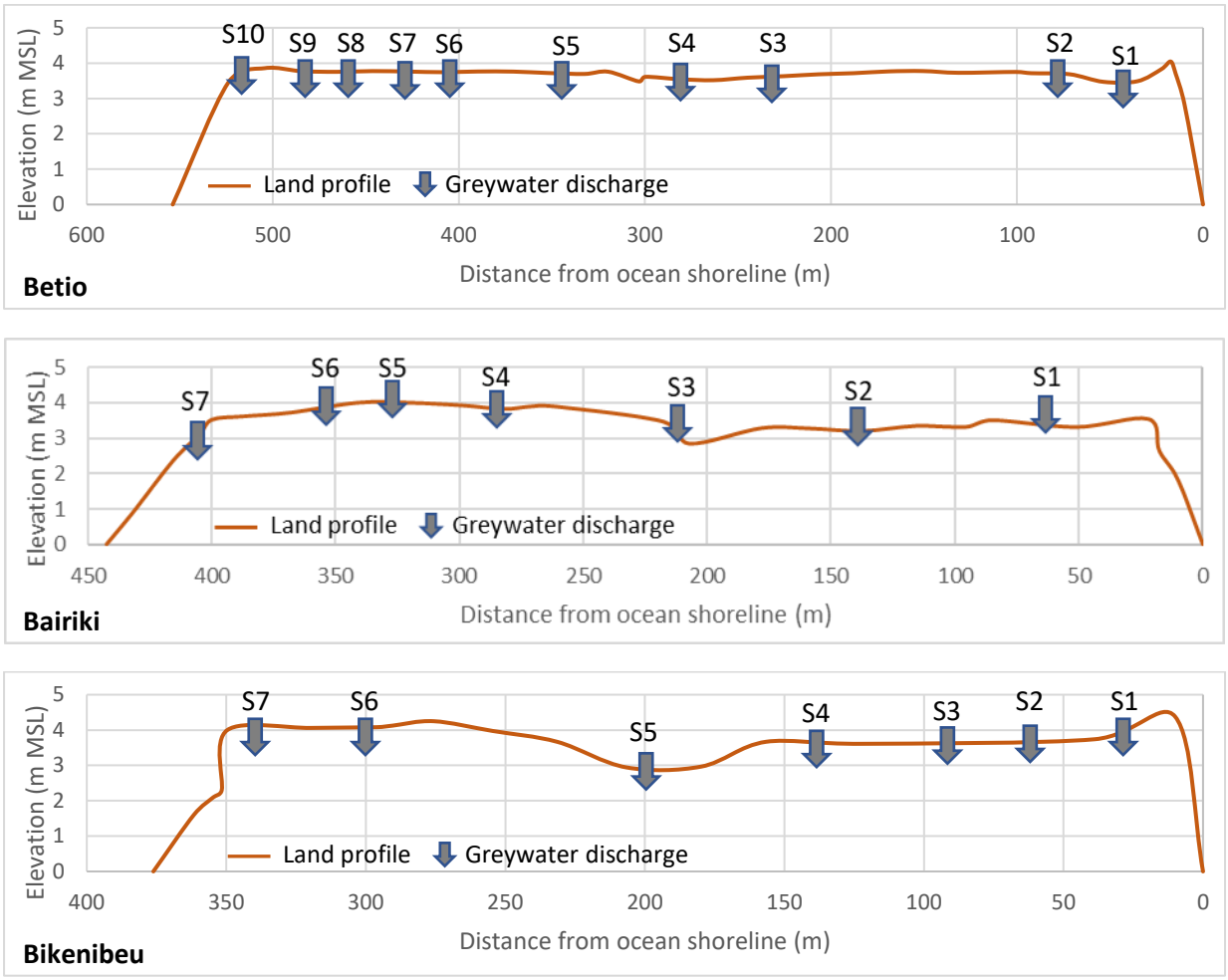

Figure 10. Greywater disposal points, representing the typical spatial resolution of greywater discharge locations. Grey arrows indicate the location of disposal. Greywater fluxes are given in Table 16, in which the arrow labels (S1, S2, S3, etc.) match those given in the diagrams above.

Table 16. Points of greywater disposal (current situation) and flux per unit area.

		S1	S2	S3	S4	S5	S6	S7	S8	S9	S10
Greywater discharge per unit transect width (L/d)	Betio	8.18	8.18	2.80	5.60	16.8	14.0	13.9	23.4	16.7	16.7
	Bairiki	14.7	2.45	2.45	19.6	17.0	12.2	14.6	-	-	-
	Bikenibeu	7.35	9.80	7.35	14.7	2.45	2.45	9.62	-	-	-
Distance from ocean shoreline (m)	Betio	42.1	77.3	233	282	346	407	429	463	483	521
	Bairiki	64.4	139	213	285	326	354	405	-	-	-
	Bikenibeu	31.1	61.8	90.5	137	200	302	339	-	-	-

In the future scenario, greywater is piped from groups of houses and transferred to centralised disposal points (Figure 11). We assume that one disposal point is adopted for each cross-section. Two alternative methods of greywater disposal at a centralised point are considered for future scenarios, namely land surface infiltration or through an injection well into the mixing zone (i.e., the base of the freshwater lens).

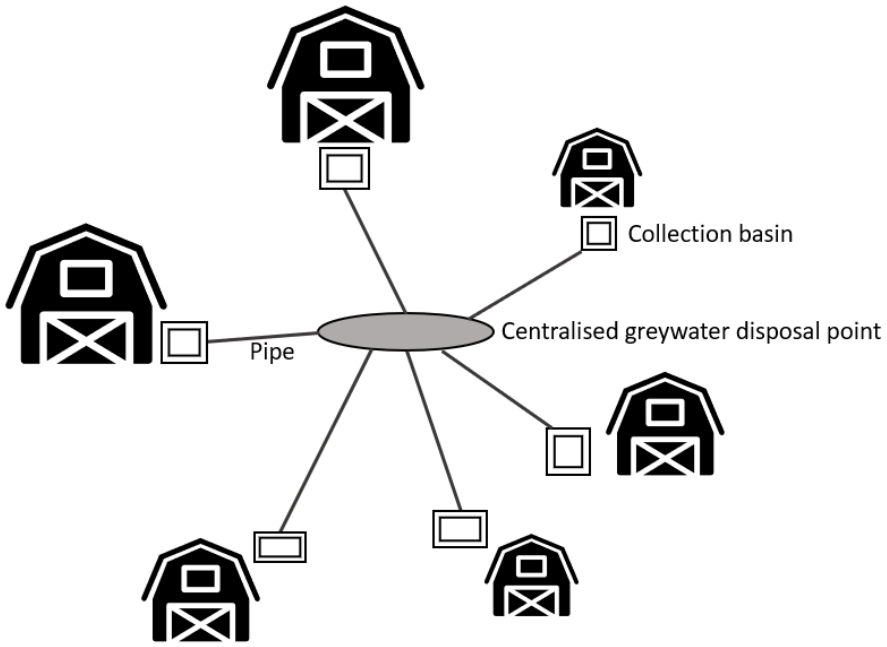

Figure 11. Schematic illustration of future greywater disposal system.

The locations of centralised disposal points depend on the availability of vacant land in the central part of each transect. Disposal points and rates of greywater discharge are shown in Figure 12.

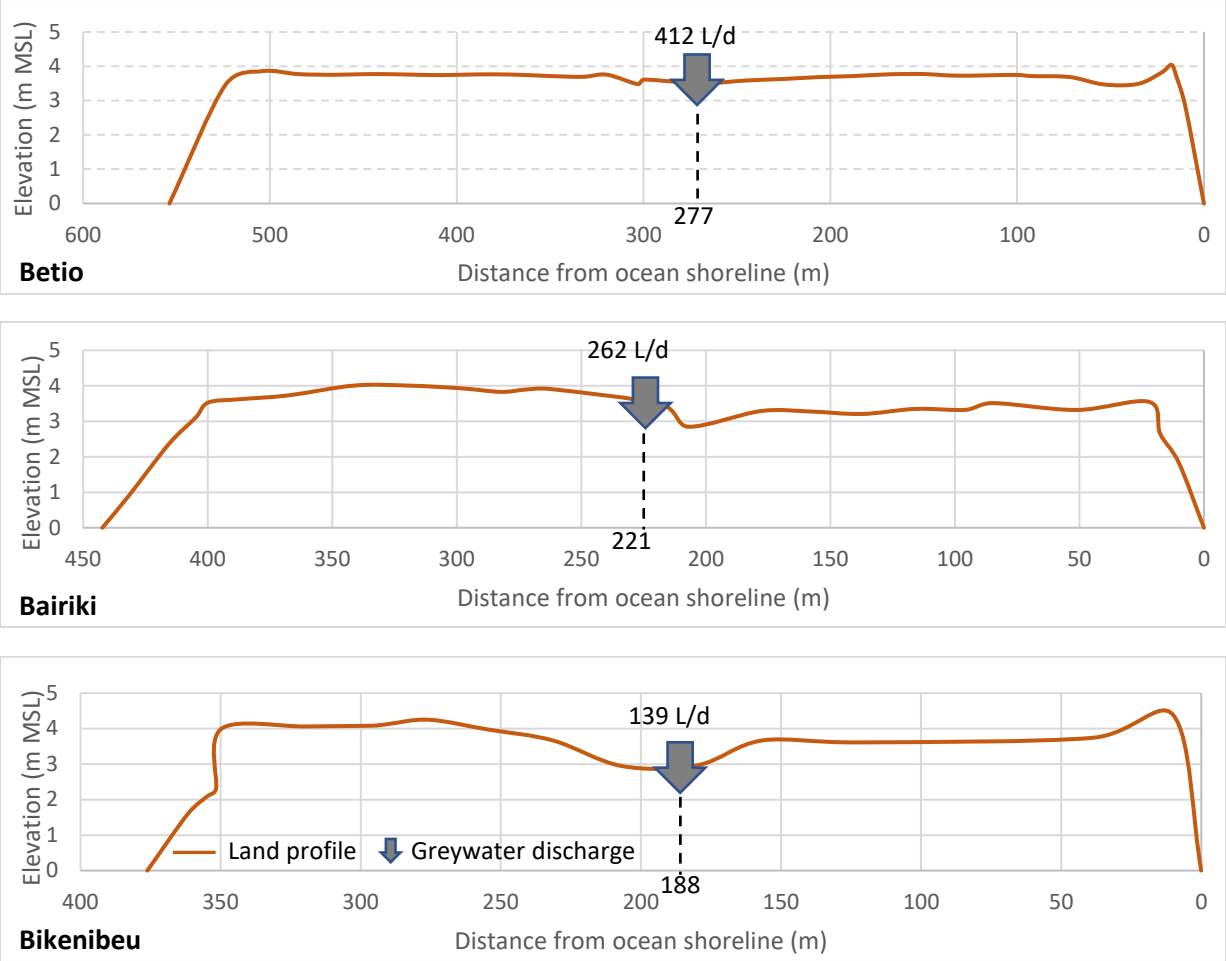

Figure 12. Greywater flux per unit area and their locations in future scenarios of centralised greywater disposal.

4.8 Hydrogeological conceptual model

An overview of the conceptual models used in this study is shown in Figure 13.

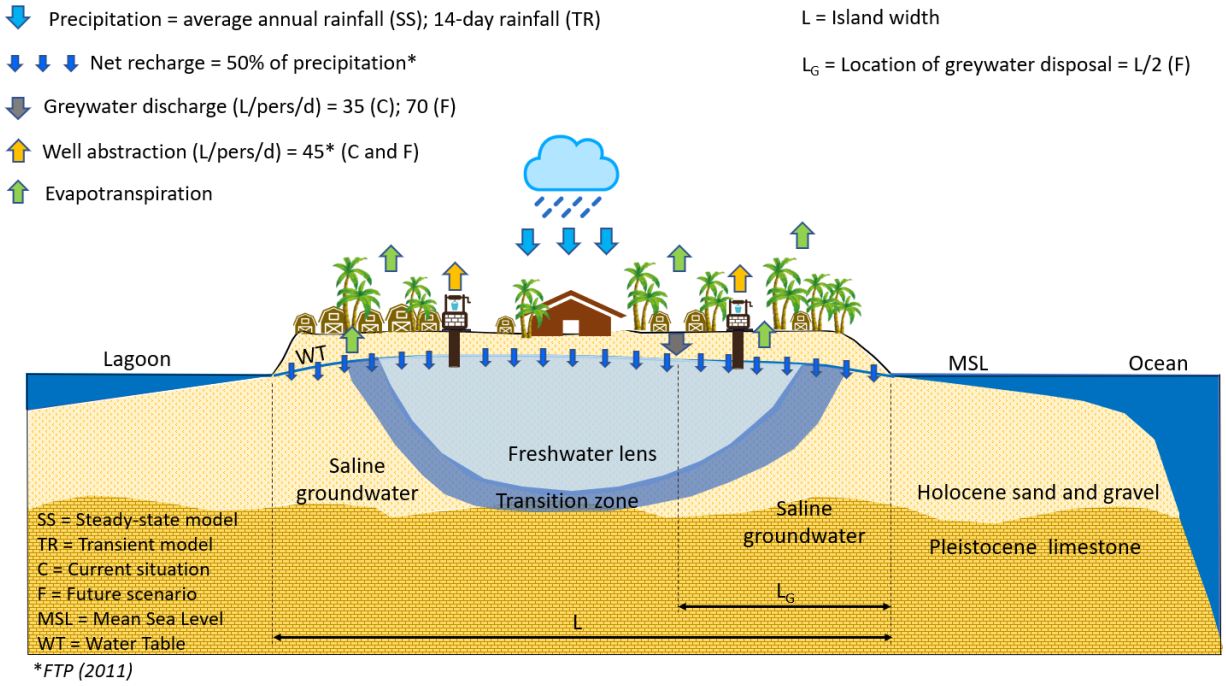

Figure 13. Conceptual model for numerical simulation.

Conceptual models for developing numerical models of the three island transects were created based on the information described above. The key attributes include:

- A dual-aquifer system (Holocene-Pleistocene) with zonation of aquifer properties is considered, commensurate with the general hydrogeology of atoll settings and previous studies that note sediment variation in the cross-island direction (e.g., Werner et al. 2017). The initial aquifer parameters are listed in Table 12 and the spatial distribution in K values is illustrated in Figure 6.
- Recharge was taken as 50% of rainfall and applied to the water table in the top layer of the model. In steady-state simulations, the average annual rainfall (from 1947 to 2018) was used in the estimation of recharge, and rainfall was summed to 14-day intervals (from 1947 to 2015) in transient simulations. Rainfall data were obtained from Betio meteorological station.
- Groundwater abstraction was treated as a distributed groundwater output and was subtracted from recharge, thereby assigning abstraction effects to the water table in the top layer of the model. Abstraction was estimated using 45 L/pers/day and considering the census population in 2015 and projected population in 2030, representing current and future conditions, respectively. This resulted in 'negative recharge' occurring during dry periods of transient simulations, i.e., when pumping exceeded recharge.

- Greywater discharge was estimated based on 35 L/pers/d greywater production and the 2015 population for the current situation. The modelling scenario of future conditions adopted 70 L/pers/d greywater production and used the projected 2030 population. Greywater discharge was applied to the model in closely spaced points for the current situation and using one centralised point of input for the future scenario. Two different future greywater disposal scenarios were tested: One where greywater discharged to the water table, and a second where greywater was injected into the mixing zone of the freshwater lens.

5. Model Construction

5.1 Overview of modelling strategy

The modelling strategy undertaken in this study is summarised in Figure 14.

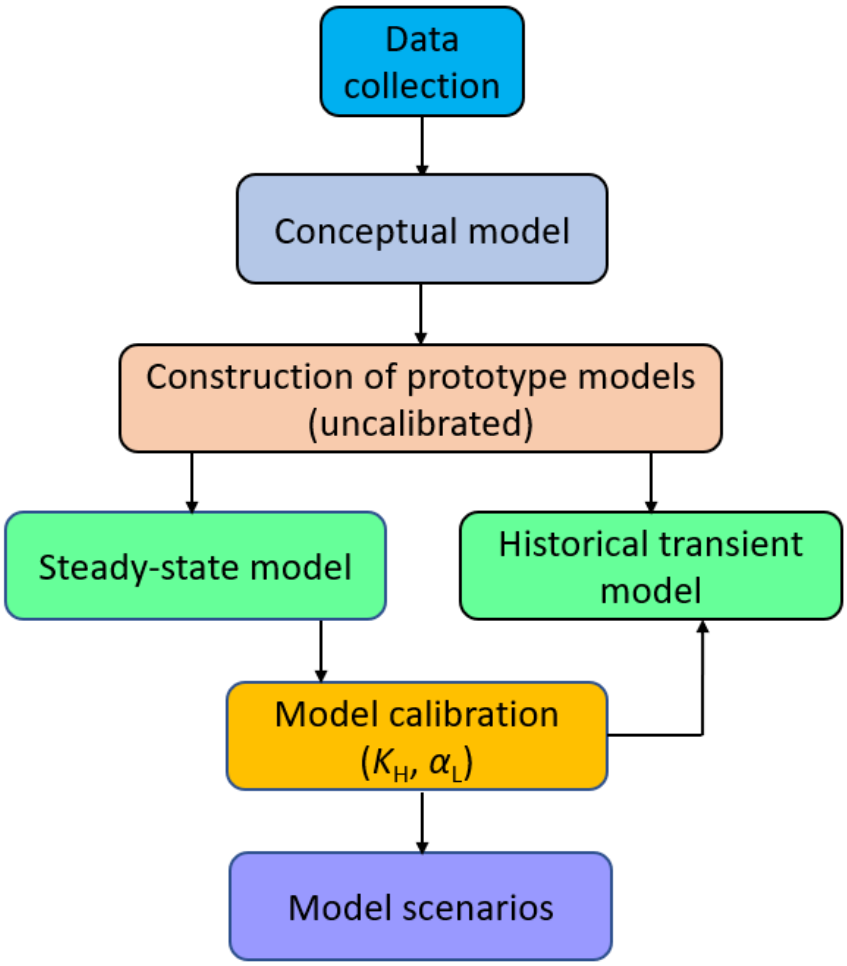

Figure 14. Model development sequence.

In the estimation of aquifer hydraulic properties for modelling island transects, steady-state models were used to calibrate K_H (K_H and K_V were related by a constant K_H:K_V ratio of 5, based on Bosserelle et al. 2015). This was achieved by matching simulated and measured salinities. The longitudinal dispersivity (α_L) was also modified during model calibration, with other components of dispersivity (α_T and α_V) linked to α_L through fixed ratios of α_L:α_T and α_L:α_V equal to 1 and 100, respectively. These ratios were informed through calibration and by the findings of previous studies, including analyses of tidal effects and the selection of surrogate dispersion

parameters (see Werner et al. 2017 for a review of relevant atoll island modelling studies). The transient historical models were used to verify the calibrated parameters obtained with the steady-state models, whereby the salinity distribution after transient simulation periods was checked against measured salinity profiles.

Salinity in the models was a scaled variable, whereby 0 represented freshwater and 1 the salt concentration of seawater. Salinity values from the monitoring wells are in EC measurements (µS/cm) and were converted to relative salinity concentrations by dividing by 50,000 µS/cm (e.g., average seawater EC; White and Falkland 2010). The freshwater lens thickness in the numerical results was assessed according to the depth below the water table of the 0.05 relative seawater concentration, which is equal to 2500 µS/cm as approximately the upper limit of palatable freshwater (White and Falkland 2010).

5.2 Modelling code

The numerical modelling code SEAWAT was used to study density-dependent flow and transport within the atoll islands of this investigation. SEAWAT is a density-coupled version of MODFLOW and MT3DMS designed to simulate 3D, variable density, saturated groundwater flow (Langevin et al. 2007). Fluid density is calculated as a function of one or more MT3DMS species. The code adopts a finite-difference approximation of the relevant variable-density groundwater flow and solute transport equations. SEAWAT has been used extensively in groundwater studies, including brine migration in continental aquifers, saltwater intrusion in coastal aquifers, and the behaviour of freshwater lenses in atoll islands (e.g., Langevin et al. 2007; Post et al. 2018; Werner et al. 2017).

5.3 Model layout

The geometry of the aquifer system is represented through the design of SEAWAT's finite-difference grid. Each of the three islands (Betio, Bairiki and Bikenibeu) was represented by a unique grid geometry, although all three models contain 61 layers. The number of columns was varied according to the horizontal extent of each cross-section, which was 1991.5 m, 1342 m and 1217.5 m for Betio, Bairiki and Bikenibeu, respectively. The grid discretisation was similar across the three models. That is, the horizontal discretisation (Δx) was modified so that the smallest cells occurred in areas where the largest salinity changes were expected to occur over short distances, leading to cells sizes that vary from 1 to 6 m in the horizontal plane. Similarly, the vertical discretisation (Δz) varies from 1 to 10 m. Other characteristics of the model grid are summarised in Table 17. Figure 15 shows the model discretisation for Betio.

Table 17. Model discretisation parameters.

		Betio	Bairiki	Bikenibeu
Number of layers (NLAY)		61	61	61
Number of columns (NCOL)		1120	762	678
Number of rows (NROW)		1	1	1
Total number of cells		68,320	46,482	41,358
Total number of active cells		66,273	44,813	39,669
Cell size (m×m)	Max	6×10	6×10	6×1 0
	Min	1×1	1×1	1×1

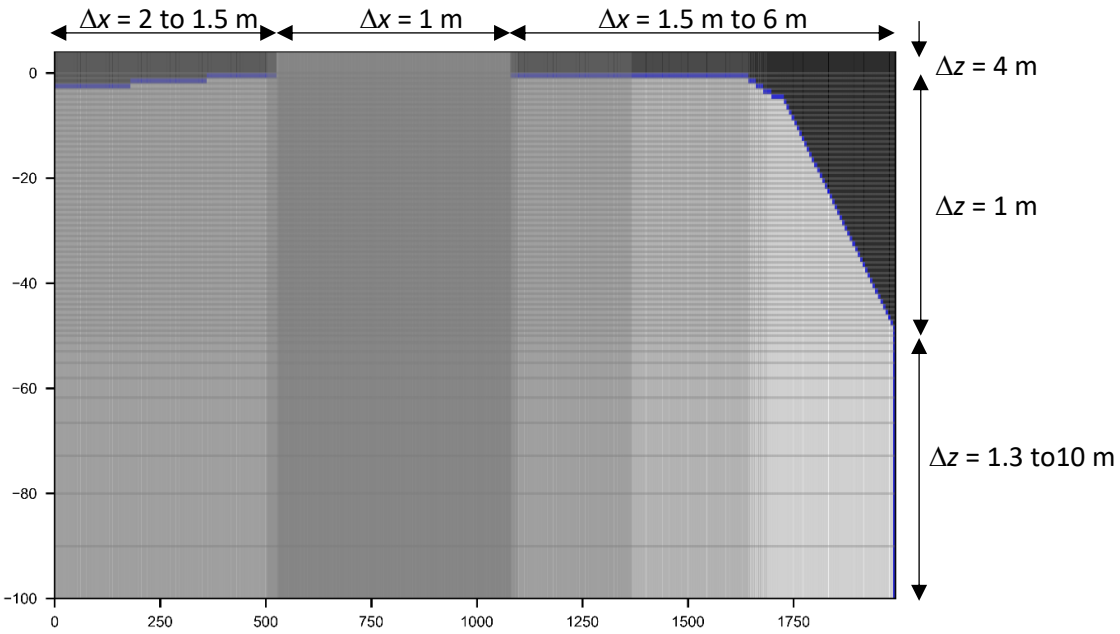

Figure 15. Discretisation of the model of the Betio transect. The black area identifies inactive cells, blue cells represent constant-head boundary conditions, and the grey area represents active cells.

5.4 Temporal discretisation

In addition to spatial discretisation (the subdivision of the study area), transient models required piecewise division of the simulation time. This is achieved by assigning stress periods, i.e., time intervals during which the input data for all external stresses such as recharge and abstraction are constant. Each stress period is further divided into time steps, which are the periods between calculations of the flow field and salinities within the model. Time steps are fundamental to the finite-difference method whereas stress periods have been incorporated in SEAWAT as a convenience for user input. Steady-state simulations utilise a single stress period and represent the equilibrium situation for the aquifer system that occurs after sufficient time has passed that the groundwater head and salinity patterns arrive at time-independent values.

The simulation period for the steady-state simulations used for calibration was 100 years, which was divided into 3650 time-steps. The initial condition in seeking steady-state conditions was one were the aquifer was freshwater-filled (except head-boundary cells, which contained seawater). The time-step lengths were variable, adopting a multiplier factor of 1.1, with an average period of 10 days. The use of a time-step multiplier affords the model higher computational effort during early-time periods in the steady-state simulation, when more rapid changes are expected, while also reducing the overall number of calculations. The period of simulation for transient models was 68 years and 8 months (1 May 1947 to 31 December 2015), equating to 1791 stress periods of 14 days duration, each comprising three time-steps.

Steady-state simulations used to test scenarios of greywater disposal adopted calibrated parameters and ran for 69 years, which was sufficient to ensure that the groundwater conditions had stabilised. The heads and solute concentrations of the calibration steady-state cases were used as initial conditions for scenario simulations (both steady-state and transient) of greywater disposal. The number of stress periods and time steps in transient greywater disposal scenarios were the same as those used for historical transient simulations. The details of scenario simulations used to explore various situations of greywater disposal are described in the 'Modelling Scenarios' section of this report.

5.5 Boundary conditions

Constant-head cells were used to represent the ocean and lagoon boundaries by imposing heads at the sea and lagoon floor equal to seawater depths below MSL. SEAWAT converts depths of seawater at constant-head boundaries to equivalent freshwater heads using the initial concentration (i.e., seawater) of the boundary cell. The equivalent freshwater heads remain constant throughout the simulation regardless of any changes in the concentration at the boundary, e.g., due to fresh groundwater discharge (Langevin et al. 2007). The salt concentration of constant-head cells can be changed during the simulation depending on the direction of flow into/out of the model, because seawater enters the model at locations of boundary inflow, whereas the ambient groundwater discharges at locations of boundary outflow causing boundary freshening. Constant-head boundary conditions are indicated by blue cells in Figure 15.

5.6 Initial conditions

Initial conditions represent the hydraulic head and concentration distribution at the start of each modelling simulation. In steady-state simulations, initial conditions only represent the starting point for SEAWAT calculations, and in theory do not influence the results. That is, as steady-state results were obtained by running transient models for extended durations, the initial conditions are theoretically inconsequential to the steady-state results; however, adopting initial conditions as close as possible to the steady-state solution reduces the computational load of SEAWAT calculations. In steady-state, calibration models, the initial head

was taken as 0 m MSL and the initial concentration set to the freshwater (relative concentration of 0) everywhere in the model domain except head-boundary cells, which were assigned seawater.

Steady-state models that explore greywater disposal adopted the steady-state calibration results as initial conditions. In transient simulations also, the simulated head and concentration from steady-state calibration simulations were used as the initial conditions.

6. Model Calibration and Validation

6.1 Approach

Model calibration was achieved using a steady-state model, in which time-averaged recharge and abstraction rates were adopted. A transient historical simulation that used calibrated parameters from the steady-state case was used to validate the calibration. The transient model used the steady-state results for initial heads.

The methodology adopted for the calibration process was a manual trial-and-error approach, similar to Post et al. (2018). This was considered reasonable given the limited nature of the field data (i.e., one salinity-monitoring bore for each island). Additionally, the use of automated calibration software would have invoked a considerable computational burden. Greywater inputs were neglected in calibration-validation models. The addition of greywater inputs did not cause models to depart excessively from the calibration match achieved in the absence of greywater inputs.

The period of simulation of the historical transient model was 1 May 1947 to 31 December 2015. Temporal discretisation was based on 14-day stress periods, which represented a balance between the need to limit the computational effort of transient simulations and capturing the temporal dynamics of the system (noting that both computation load and accuracy typically increase as time-steps are shortened). There are no historical data for abstraction rates from the study areas during the transient period, and therefore the average abstraction used in the steady-state calibration was adopted throughout the transient simulation. Transient model results were compared to field measurements at the end of the simulation (representing 31 December 2015) as a validation step. Ideally, the transient model would have been assessed against time-series of salinity or other temporal measurements; however, these data were not available.

Case 1: Steady-state calibration

Salinity measurements were available from five different times (i.e., during 2010, 2011 and 2019; see Table 13) for use as calibration targets. Average observed salinities (Table 13 and Figure 7) were repeatedly compared with computed salinities until a sufficient match was obtained by adjusting the model parameters (i.e., K_H, K_V and α_L; noting that changes to α_L modifies α_T and α_V through fixed ratios; see the 'Model Construction' section), while other model inputs were maintained constant (i.e., n, depth of unconformity, recharge, abstraction, etc.). The root-mean-square error was minimised in seeking the optimal match between computed and observed concentrations at the bore location. Computed freshwater lens thicknesses were also compared with the range of values obtained from field measurements (e.g., Table 14).

The final model parameters obtained from calibration are provided in Table 18. The freshwater lens and the comparison between simulated and measured concentration profiles for each island are shown in Figure 16.

Table 18. The calibrated hydraulic parameter values for Betio, Bairiki and Bikenibeu. The colours in this table match those of Figure 6 and values of α_L are for all zones.

		Betio		**Bairiki**		**Bikenibeu**	
		Elevation (m MSL)	**K_H (m/d)**	**Elevation (m MSL)**	**K_H (m/d)**	**Elevation (m MSL)**	**K_H (m/d)**
Zone 1	Top soil	0 to 3.46	5	0 to 1.82	5	0 to 4.38	5
Zone 2	Holocene sediment	-17.3 to 0	1.8	-14.3 to 0	5	-12.9 to 0	8
Zone 3	Holocene sediment	-17. 3 to 0	9	-14.3 to 0	25	-12.9 to 0	40
Zone 4	Holocene sediment	-17.3 to 0	14.4	-14.3 to 0	40	-12.9 to 0	64
Zone 5	Holocene sediment	-17. 3 to 0	21.6	-14.3 to 0	60	-12.9 to 0	96
Zone 6	Upper Pleistocene	-27.3 to -17.3	100	-24.3 to -14.3	60	-22.9 to -12.9	60
Zone 7	Upper Pleistocene	-27.3 to -17.3	160	-24.3 to -14.3	96	-22.9to -12.9	96
Zone 8	Lower Pleistocene	-100 to -27.3	500	-100 to -24.3	500	-100 to -22.9	500
α_L (m)		5		20		20	

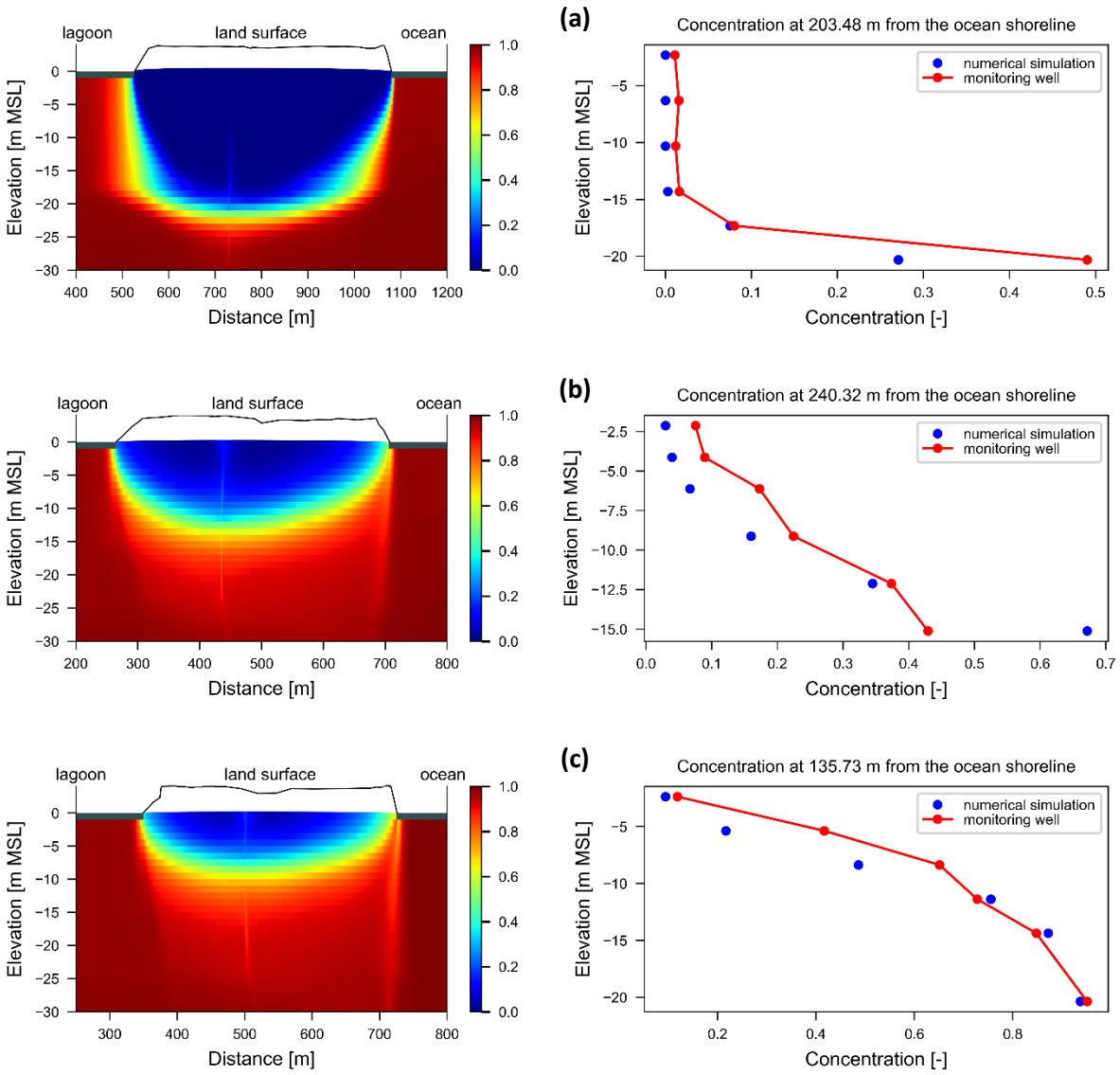

Figure 16. Simulated freshwater lenses and comparisons between measured and simulated concentration profiles for: (a) Betio, (b) Bairiki and (c) Bikenibeu.

Calibrated values of α_L (and α_T and α_V from α_L:α_T and α_L:α_V ratios of 1 and 100, respectively) are relatively large (i.e., α_L = 5 m for Betio and α_L = 20 m for Bairiki and Bikenibeu) compared to those obtained by Post et al. (2018) for their model of the Bonriki Island freshwater lens (i.e., α_L = 0.8 m, α_T = 0.04 m and α_V = 0.008 m). The higher dispersivities of the current study are nevertheless considered suitable for aquifers that are subjected to tidal forces, such as in atoll islands, where a wider mixing zone between freshwater and seawater is expected relative to non-tidal conditions (e.g., Ataie-Ashtiani et al. 1999; Werner et al. 2017). In this study, the effects of tides on the freshwater lens formation was not evaluated, although dispersivity values were expected to account at least partly for the widening of the mixing zone that arises from tidal mixing processes and other dynamic processes, enabling improved match to the measured salinity profiles shown in Figure 7.

While the relatively high α_L values produced optimal matches to measured salinity profiles, there was some evidence of artificial 'lifting' of salinity at the middle of the freshwater lens (e.g., see Figure 16). This is thought to have been produced by a numerical effect known as backward dispersion (e.g., Smith, 2004), which is the movement of salt mass in the opposite direction of flow caused by high dispersion from steep concentration gradients that increases with the value of dispersivity. Backward dispersion is an artefact of the advection-dispersion equation that we neglect in interpreting the modelling results and estimates of freshwater lens extent.

The comparison between observed and modelled freshwater lens thicknesses from calibrated models is summarised in Table 19. The calibration results show computed freshwater lens thicknesses for Betio and Bairiki that are within the range of field-based salinity measurements at the monitoring wells. In the case of Bikenibeu, the computed freshwater lens is thinner than the lens thickness based on monitoring well data; however, the modelled lens is similar to the results of the EM34 survey in 2011, from which no freshwater lens was detected.

Table 19. Comparison between observed and computed freshwater lens thicknesses from calibrated models.

Island	Freshwater lens thickness Jul 2010-Mar 2011 (m)	Freshwater lens thickness May 2019 (m)	Freshwater lens thickness from the EM34 survey in 2011 (m)	Computed freshwater lens – steady-state calibration (m)
Betio	17.1-19.7	19.8	15	19.0
Bairiki	0.7-5.0	8.4	2.5	4.9
Bikenibeu	2.1-3.8	4.2	0.0	1.0

Case 2: Transient validation

A transient model that captured historical recharge trends was developed to validate the calibration and evaluate the departure from steady-state conditions that arises when rainfall dynamics are considered. Figure 17 shows the salt concentration values at the end of the transient simulation, i.e., after 68 years and 8 months (31st December 2015) for Betio, Bairiki and Bikenibeu.

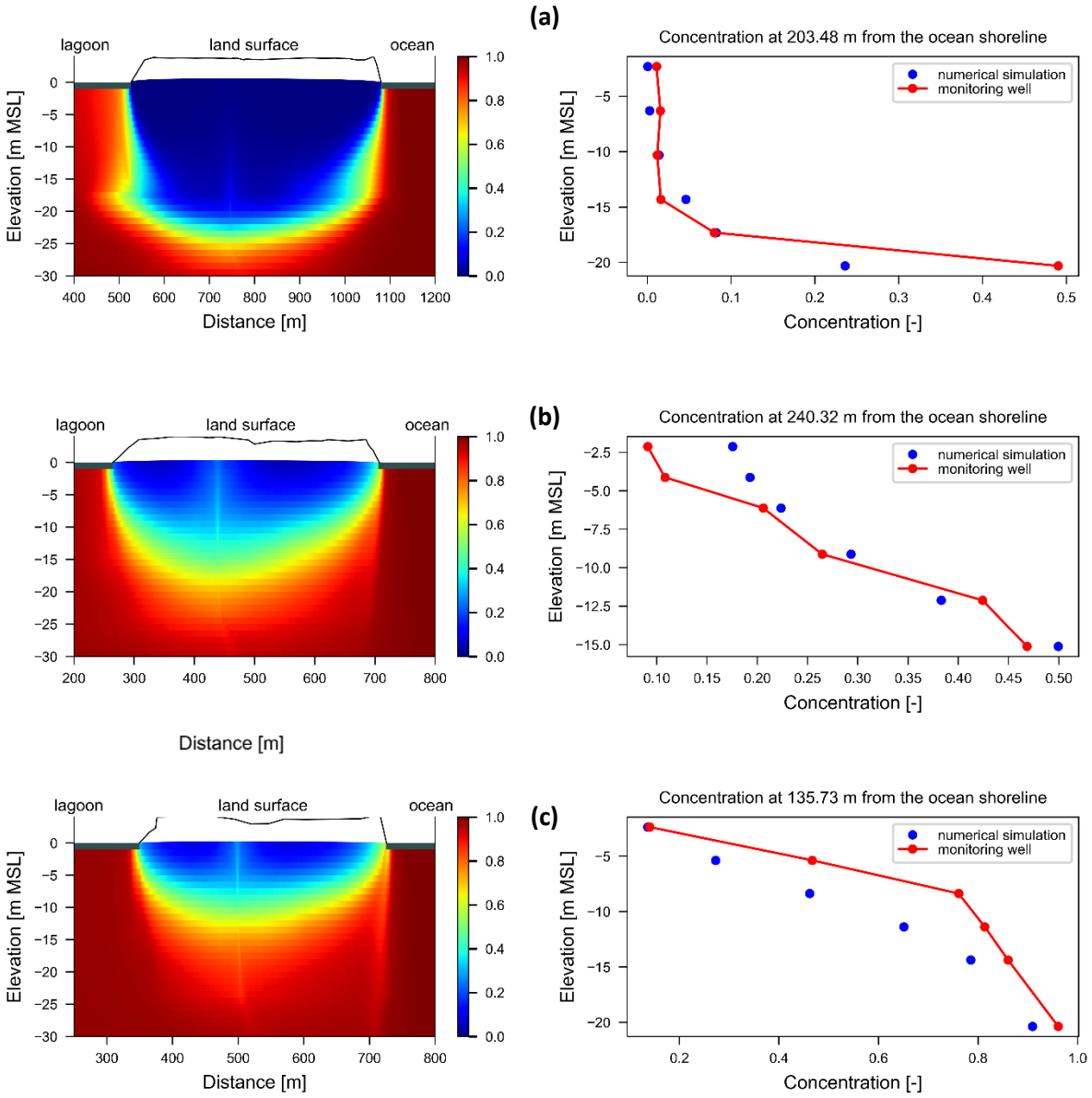

Figure 17. Simulated freshwater lens (left plots) and comparison between measured and simulated salinity profiles (right plots) at the end of the transient simulation: (a) Betio, (b) Bairiki and (c) Bikenibeu.

Comparison between Figures 15 and 16 shows that the calibration match between measured and observed salinities was only mildly changed at the end of the transient simulation compared to the steady-state results. Salinity profiles in the transient model appear more dispersed, especially in the Betio and Bairiki models. This is an expected outcome of the greater mixing that arises from the temporal variability in recharge, compared to the stable conditions in steady-state models. We anticipate that a better match between the transient model salinities and field-based values could be obtained by reducing α_L (and therefore α_T and α_V) in transient simulations, to account for the mixing effect of dynamic recharge, although this wasn't tested.

7. Modelling Scenarios

7.1 Overview of modelling scenarios

Eight simulations were used to assess greywater transport and its effects on freshwater lenses in current situation and future scenarios. A summary of all model cases in this study is provided in Table 20.

Table 20. Summary of all model cases in this study.

	Situation	Simulation type	Recharge	Abstraction (mm/y)			Greywater discharge
				Betio	Bairiki	Bikenibeu	
Case 1	Calibration	SS	956.5 (mm/y)	116	88.4	67.3	-
Case 2	Validation	TR	using 14-day rainfall	116	88.4	67.3	-
Case 3	C	SS	956.5 (mm/y)	116	88.4	67.3	L (Figure 10; Table 16)
Case 4	F	SS	956.5 (mm/y)	175	139	86.5	L (Figure 12)
Case 5	F	SS	956.5 (mm/y)	175	139	86.5	W (Figure 12)
Case 6	C	TR	using 14-day rainfall	116	88.4	67.3	L (Figure 10; Table 16)
Case 7	F	TR	using 14-day rainfall	175	139	86.5	L (Figure 12)
Case 8	F	TR	using 14-day rainfall	175	139	86.5	W (Figure 12)
Case 9	F	TR	using 14-day rainfall	-	-	-	L (Figure 12)
Case 10	F	TR	using 14-day rainfall	-	-	-	W (Figure 12)

C = Current situation; F = Future scenario; SS = Steady-state; TR = Transient; L= Land surface; W = Well

Case 3: Steady-state simulation of the current greywater disposal situation

Steady-state models were used to rapidly assess long-term and averaged effects of greywater disposal in various forms on the aquifers of the three islands being investigated. The first steady-state scenario aimed to explore the fate of greywater that is discharged to the land surface at intervals approximating the distance between dwellings, and at rates that reflect the current population (i.e., in 2015) and freshwater availability. The steady-state scenario simulation adopted the steady-state calibrated model's heads and salinities as initial conditions (merely to minimise the computational effort).

The multi-species capability of SEAWAT was necessary to simulate both greywater movement and the density-dependent mixing of freshwater and seawater. That is, two species were modelled: seawater and greywater. The simulation of greywater transport neglected the role of density in the estimation of the groundwater flow field. Greywater was represented by a relative concentration scale, where 0 represents uncontaminated groundwater and 1 denotes 100% greywater.

Figure 18 shows the results of steady-state runs for closely spaced inputs of greywater at the land surface (see Figure 10 for an illustration of greywater disposal points) in Betio, Bairiki and Bikenibeu. Here, we presume that contaminants applied to the land surface immediately reach the water table; on the basis of the shallow water table depth of the field sites.

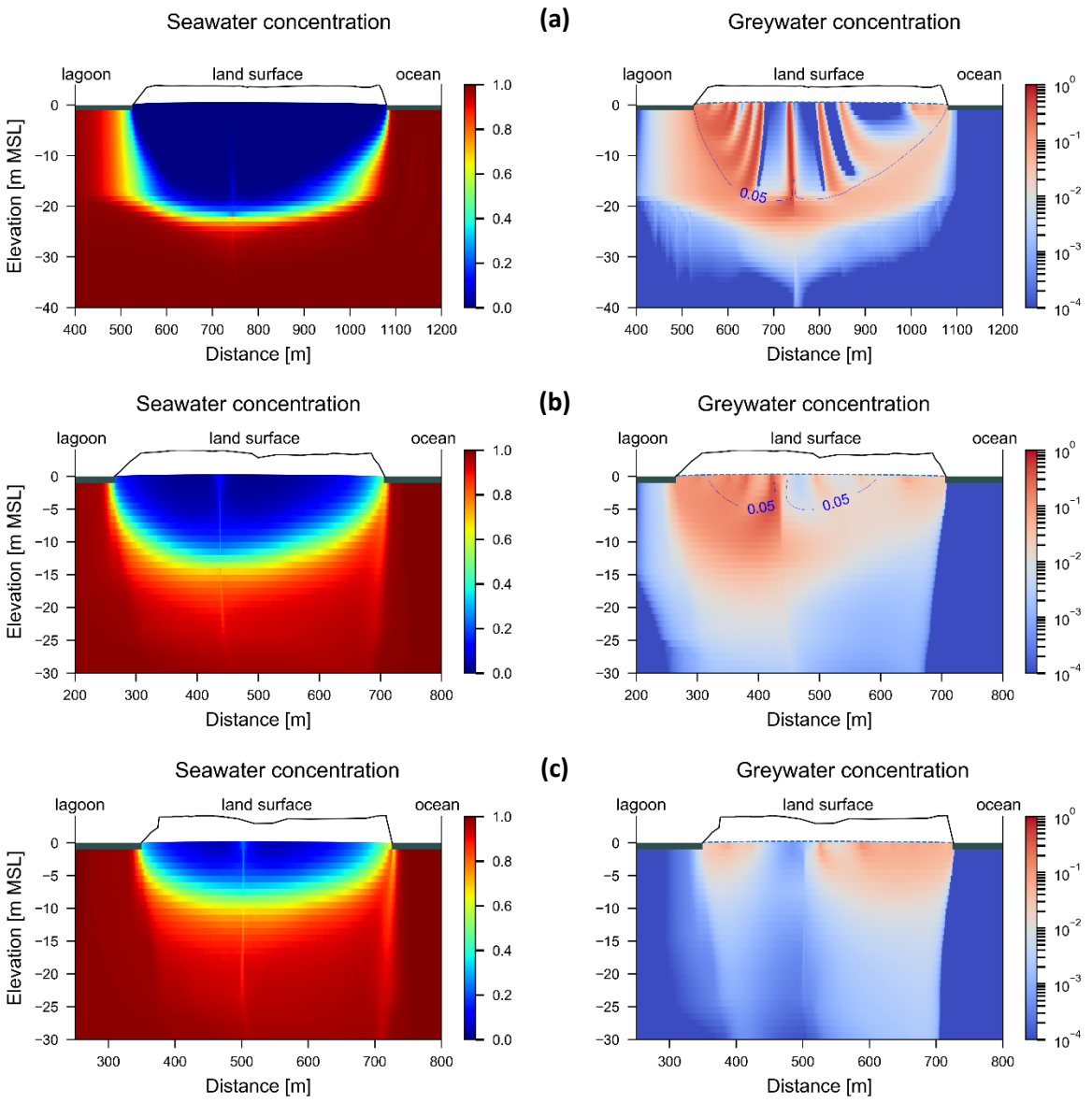

Figure 18. Concentrations of seawater (left plots) and greywater (right plots) from steady-state simulations of the current situation (i.e., population in 2015, average rainfall, etc.) in the islands of: (a) Betio, (b) Bairiki and (c) Bikenibeu. The 0.05 relative seawater contour is shown on the right column of figures (i.e., plots of greywater concentration) to overlay the depth of freshwater.

The effect of greywater input on the freshwater lens is assessed by calculating changes to the maximum freshwater lens thickness (i.e., as determined by the lowest point on the 0.05-

contour) due to the addition of greywater to the model. For example, the freshwater extents of Cases 1 (i.e., no greywater) and 3 were compared. Adding greywater disposal to the steady-state model led to an increase of 2% in the maximum freshwater lens thickness for Betio, and an increase of 12% in the maximum freshwater lens thickness for Bairiki. The 0.05-contour was not helpful in assessing the effect of greywater on the lens size in Bikenibeu because of its limited extent; however, the 0.5-contour was 1% deeper in the Bikenibeu model that included greywater disposal. The results indicate that adding greywater to the lens caused some increased mixing and widening of the lens, although in the case of Bikenibeu, enhanced mixing masked any increase in lens thickness arising from the addition of greywater.

Case 4: Steady-state simulation of future greywater disposal at the land surface

This model is an adaption of Case 3, where abstraction and greywater application rates correspond to expected values for a future population in 2030 (see Figure 12 and Table 15). Whereas the current situation presumes greywater disposal at several locations across the transect, the future scenarios involved greywater disposal in a central location (see Figures 10 and 11). The simulation results for Case 4 are shown in Figure 19.

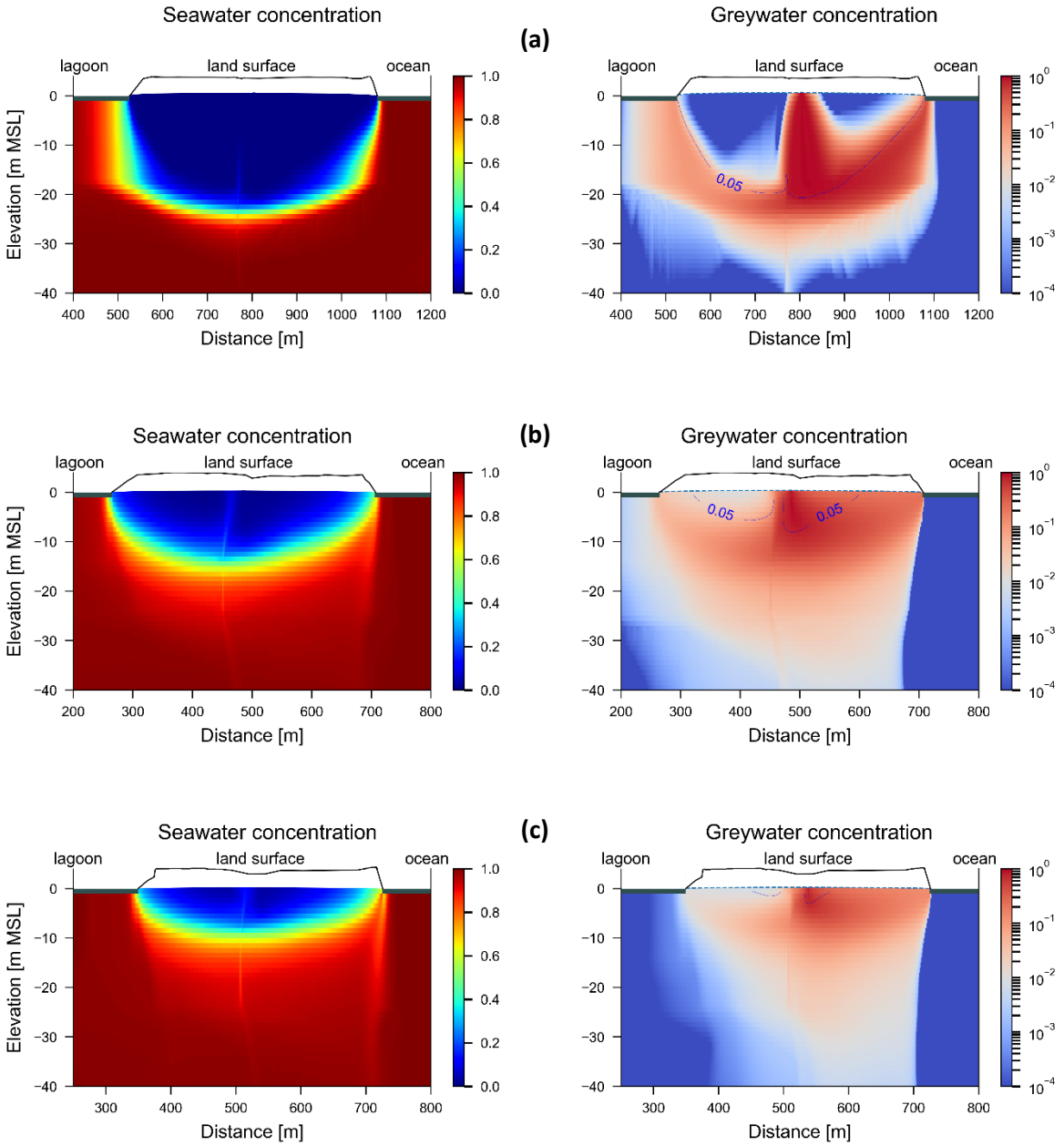

Figure 19. Concentrations of seawater (left plots) and greywater (right plots) from steady-state simulations of the future situation (i.e., population in 2030, average rainfall, etc.) in the islands of: (a) Betio, (b) Bairiki and (c) Bikenibeu. The 0.05 relative seawater contour is shown on the right column of figures (i.e., plots of greywater concentration) to overlay the depth of freshwater.

A comparison between the results in the right column of Figure 19 and the right column of Figure 18 shows that the concentrated greywater disposal enhances the extent of high greywater plume concentration (i.e., based on the spatial extent of relative greywater concentration higher than 0.1) in the freshwater lens. In addition to that, the greywater distribution in Figure 19 shows that in general, the concentration of greywater within the part

of the island closest to the ocean is larger due to higher values of hydraulic conductivity (*K*) towards the ocean boundary (see Table 18 and Figure 6).

The depth of freshwater (i.e., defined by the depth below the watertable of the 0.05 relative seawater concentration) was enhanced with the addition of greywater (Case 4; Figure 19) compared to the simulation without greywater (Case 3; Figure 18) for all three islands, as expected. That is, the largest freshwater lens thickness (i.e., within each transect) increased from 19 m to 21.4 m in Betio, from 4.9 m to 8.5 m in Bairiki, and from 1 m to 3.4 m in Bikenibeu.

Case 5: Steady-state simulation of future greywater disposal injected into a well

This modelling scenario simulates the injection of greywater at the projected future (2030) rate into a well that is open within the freshwater-seawater mixing zone. The well is located approximately in the middle of the island (i.e., same location as surface disposal of greywater occurred in Case 4). The adopted injection depths are 28 m BGL for Betio, 18 m BGL for Bairiki and 14 m BGL for Bikenibeu. The initial conditions of this case correspond to the steady-state calibrated model (i.e., Case 1), noting that the initial conditions do not affect the final steady-state results. The results of Case 5 are shown in Figure 20.

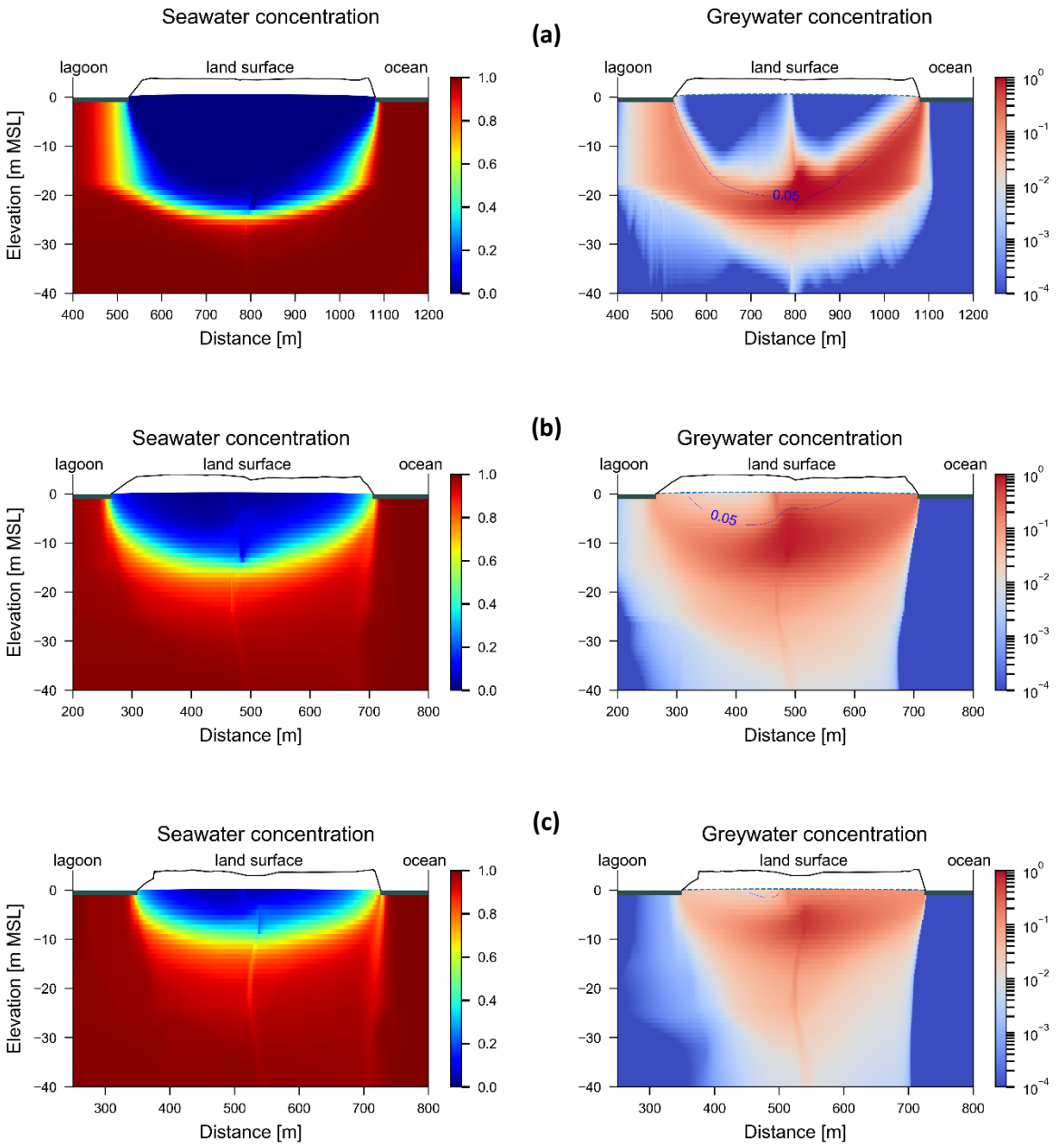

Figure 20. Concentrations of seawater (left plots) and greywater (right plots) from steady-state simulations of the future situation (i.e., population in 2030 and average rainfall) in the islands of: (a) Betio, (b) Bairiki and (c) Bikenibeu. The 0.05 relative seawater contour is shown on the right column of figures (i.e., plots of greywater concentration) to overlay the depth of freshwater.

The long-term effect of future greywater injection on the freshwater lens is assessed by comparing the freshwater thicknesses in Figure 20 to those of Case 4 (Figure 19), which simulates the same greywater rate input but through land surface infiltration also located centrally within each island. The comparison of freshwater depths (i.e., based on the depth below the watertable of the 0.05 relative seawater contour) between Case 4 and Case 5

indicates that when greywater is injected, the freshwater lens thickness increases from 21.4 m to 24.7 m in Betio. However, the thickness of freshwater decreases in Bairiki and Bikenibeu (from 8.5 m to 6.7 m in Bairiki, and from 3.4 m to 1.8 m in Bikenibeu) when greywater is injected (Case 5) rather than disposed of at the surface (Case 4). Larger dispersion parameters in Bairiki and Bikenbeu (i.e., α_L = 20 m, see Table 18) compared to that of Betio (α_L = 5 m, see Table 18) may be the reason for this outcome. That is, injection into a more dispersed mixing zone (due to higher dispersion) widens the mixing zone producing a shallower 0.05 relative seawater contour but a deeper 0.5 relative seawater contour. Evidence for this effect is apparent in the vertical separation of the 0.05 and 0.95 salinity contours (i.e., the *mixing zone thickness*) in Bairiki and Bikenibeu, whereby the mixing zone thickness widens with the addition of greywater injection by 8% in Bairiki, and by 10% in Bikenibeu.

Larger dispersion in Bairiki and Bikenibeu also causes greywater plumes to be more widespread. For example, in Case 5 the extent of higher greywater concentration (based on approximately relative greywater concentrations ≥ 0.1) in the freshwater lens is larger in comparison to that observed in Case 4.

Case 6: Transient simulation of the current greywater disposal situation

This modelling scenario is the transient version of Case 3 (i.e., steady-state fresh groundwater distribution) to explore the influence of the rainfall dynamics on the propagation of the greywater disposals in the freshwater lenses. Figures 20, 21 and 22 show the results of Case 6 for Betio, Bairiki, Bikenibeu, respectively. In all cases, seawater and greywater concentrations are presented for a dry year (2000, top row) and in a wet year (2004, bottom row).

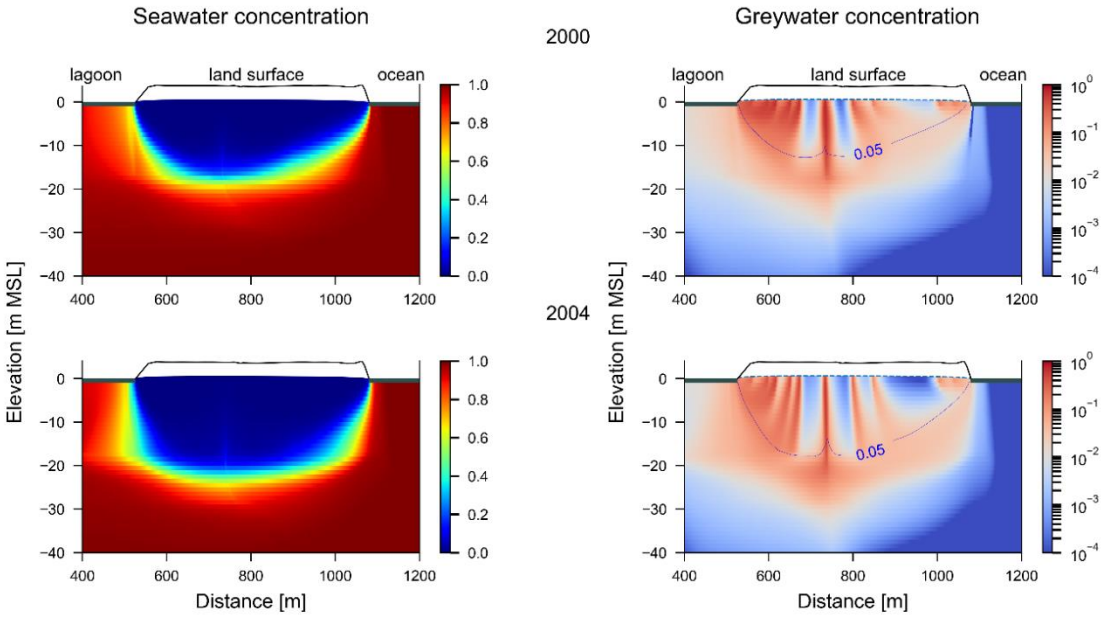

Figure 21. Concentrations of seawater (left plots) and greywater (right plots) from transient simulations of the current situation (i.e., population in 2015, average rainfall, etc.) in Betio for

dry and wet characteristic years, 2000 and 2004, respectively. The 0.05 relative seawater contour is shown on the right column of figures (i.e., plots of greywater concentration) to overlay the depth of freshwater.

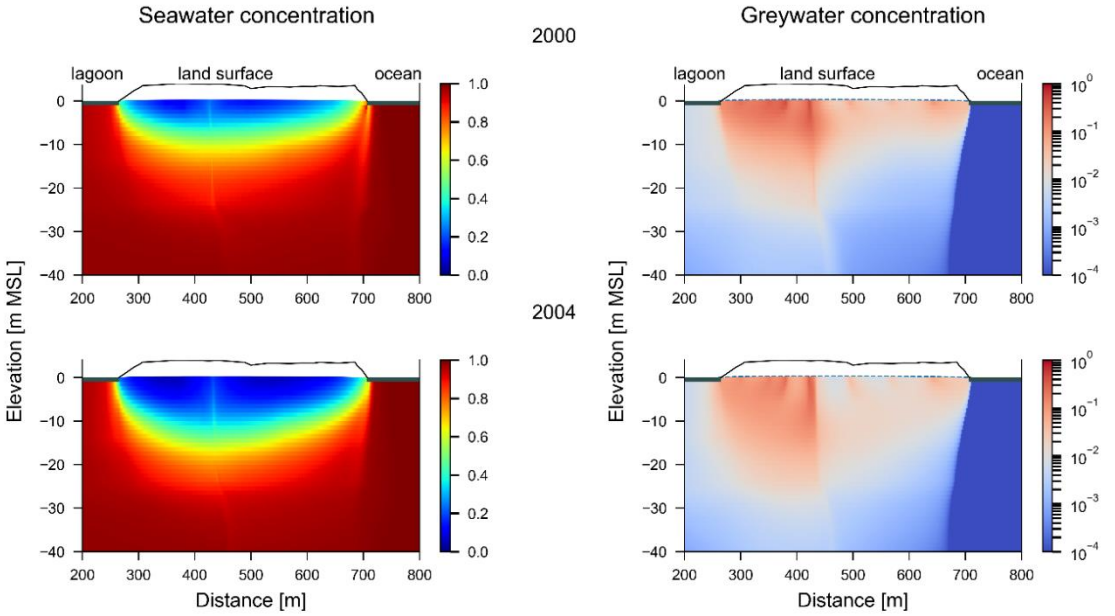

Figure 22. Concentrations of seawater (left plots) and greywater (right plots) from transient simulations of the current situation (i.e., population in 2015, average rainfall, etc.) in Bairiki for dry and wet characteristic years, 2000 and 2004, respectively.

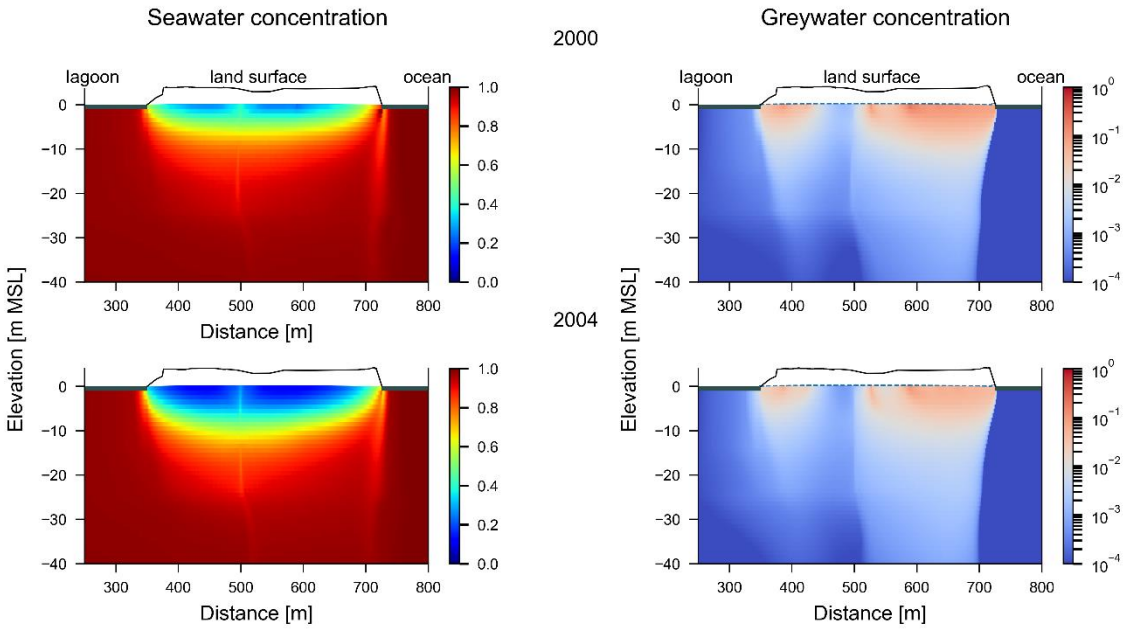

Figure 23. Concentrations of seawater (left plots) and greywater (right plots) from transient simulations of the current situation (i.e., population in 2015, average rainfall, etc.) in Bikenibeu for dry and wet characteristic years, 2000 and 2004, respectively.

As expected, the thickness of the freshwater lens differs substantially between 2000 (dry year) and 2004 (wet year). For example, the freshwater lens thickness (defined by the depth of the 0.05 relative seawater contour below the watertable) in Betio is 38% larger than in the dry season (Figure 21). In the cases of Bairiki (Figure 22) and Bikenibeu (Figure 23), the minimum relative seawater concentrations are higher than 0.05, mainly due to the joint influence of larger α_L and the flow dynamics caused by the transient rainfall recharge. Therefore, to compare the freshwater lenses between the dry and wet years in Bairiki and Bikenibeu, the freshwater depth below to the watertable to the 0.5 relative seawater contour is used. This comparison shows that the lens is increased by 69% in Bairiki (Figure 22) and 98% in Bikenibeu (Figure 23).

In addition, the greywater plume extent is larger in the wet season than in the dry season in the three islands (right column in Figures 20, 21 and 22).

Case 7: Transient simulation of future greywater disposal at the land surface

This scenario evaluates the rainfall dynamics on the freshwater lenses by using the historical rainfall data (adopted in Case 2) and the average future greywater and abstractions rates assuming the future population in 2030 (see Figure 12). The future greywater input is assumed to occur in a disposal located at the middle of the lens through land surface infiltration, same as in Case 4. Figures 23, 24 and 25 show the results of these simulations for Betio, Bairiki, Bikenibeu, respectively.

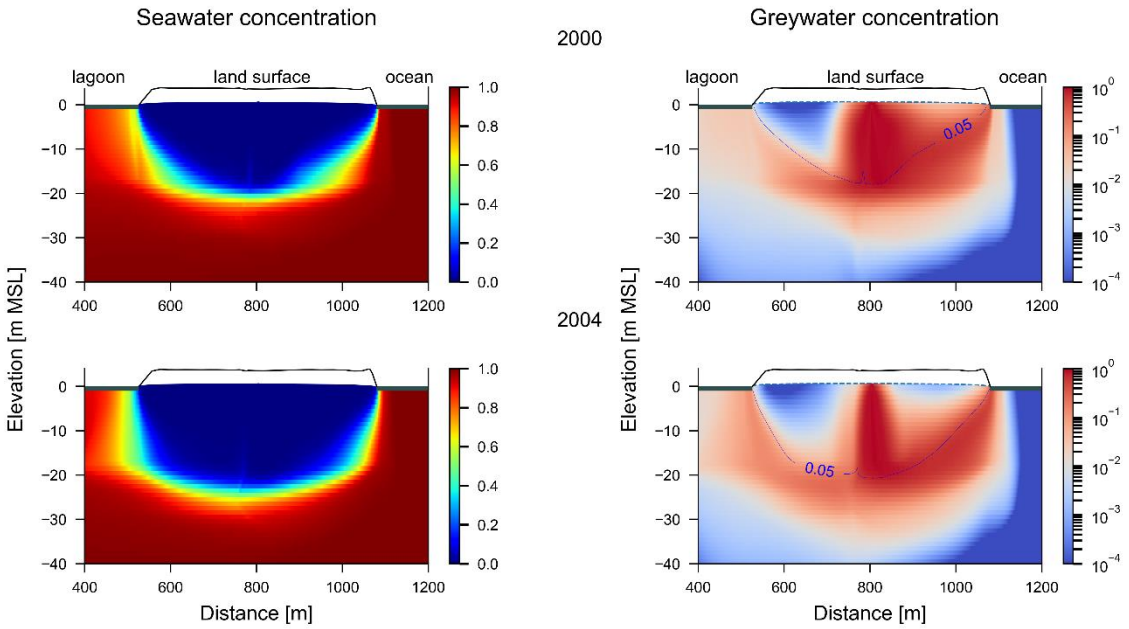

Figure 24. Concentrations of seawater (left plots) and greywater (right plots) from transient simulations of the future situation (i.e., population in 2030, average rainfall, etc.) with greywater disposal at the land surface in Betio for dry and wet characteristic years, 2000 and 2004, respectively. The 0.05 relative seawater contour is shown on the right column of figures (i.e., plots of greywater concentration) to overlay the depth of freshwater.

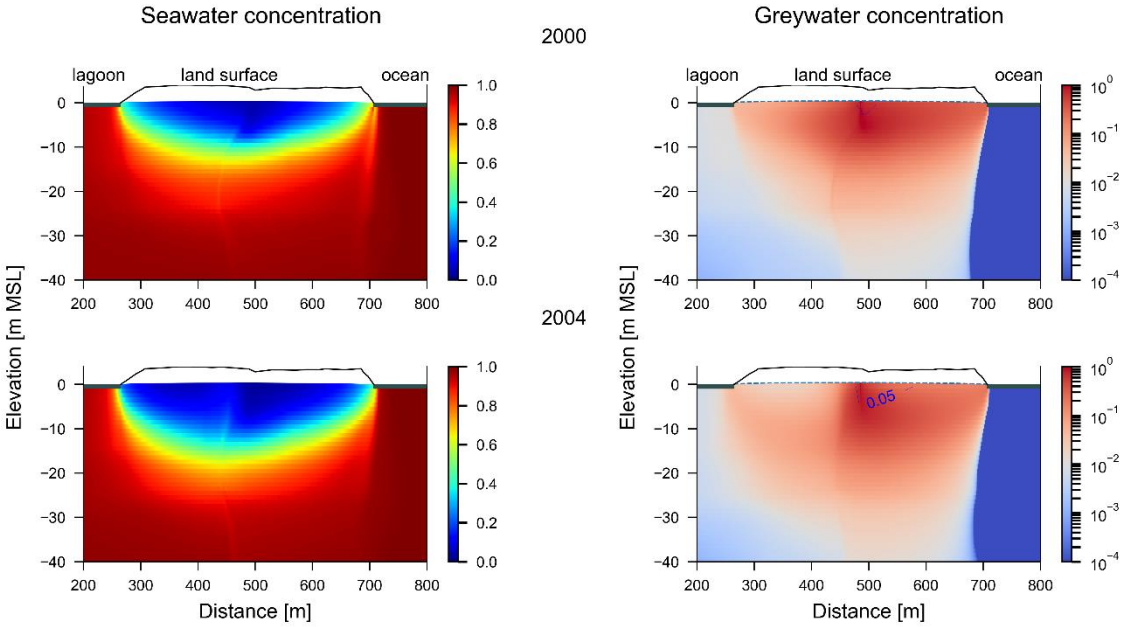

Figure 25. Concentrations of seawater (left plots) and greywater (right plots) from transient simulations of the future situation (i.e., population in 2030, average rainfall, etc.) with greywater disposal at the land surface in Bairiki for dry and wet characteristic years, 2000 and 2004, respectively. The 0.05 relative seawater contour is shown on the right column of figures (i.e., plots of greywater concentration) to overlay the depth of freshwater.

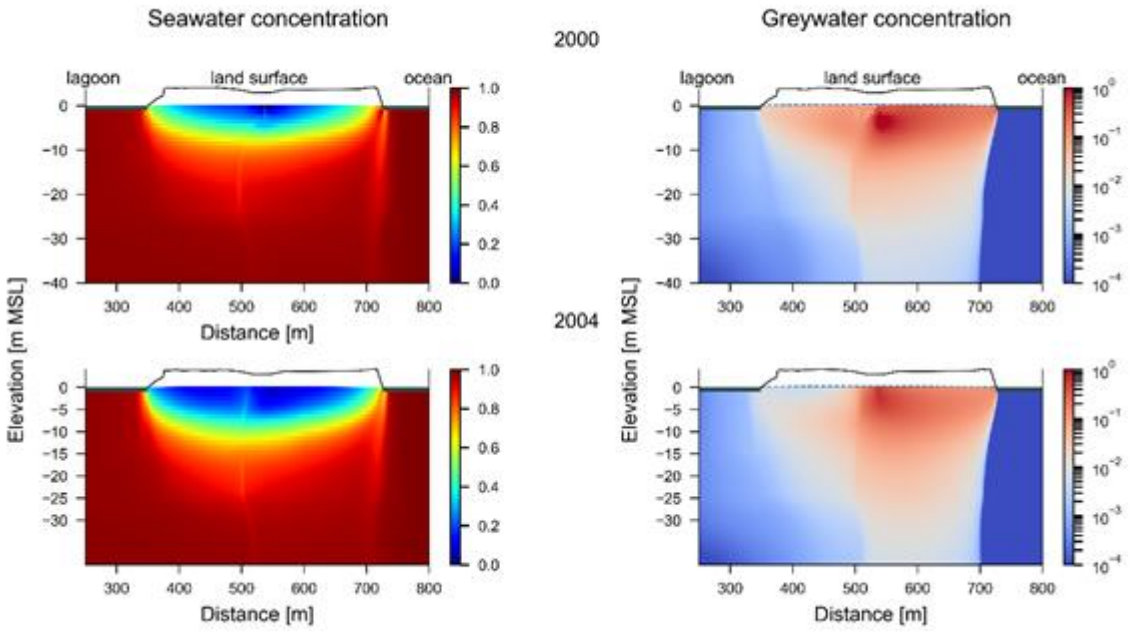

Figure 26. Concentrations of seawater (left plots) and greywater (right plots) from transient simulations of the future situation (i.e., population in 2030, average rainfall, etc.) with greywater disposal at the land surface in Bikenibeu for dry and wet characteristic years, 2000 and 2004, respectively.

The results of Case 7 suggest a general increase in the size of freshwater lenses during the wet years in comparison to the dry years. The increase of the freshwater lens between 2000 and 2004, estimated as the thickness between the water table and the 0.05 relative seawater contour, is 13% in Betio (Figure 24) and in Bairiki is 76%. In Bikenibeu, the depth of the freshwater lens was calculated based on the depth below the watertable of the 0.5 relative seawater contour due to a shallow freshwater depth with relative seawater concentrations higher than 0.05. A comparison between the dry and wet years indicates an increment in the freshwater depth of 49% (Figure 26). Larger extent of greywater relative concentration ≥ 0.1 in the freshwater lenses were observed in the dry years than in the wet years, as expected.

Case 8: Steady-state simulation of future greywater disposal injected into a well

Case 8 differs from Case 7 only in the location of the greywater disposal. Case 8 simulates a future greywater rates into a well that is open within the freshwater-seawater mixing zone (0.5-relative seawater concentration) at the centre of the lens, same as in Case 5. Figures 26, 27 and 28 shows the results of a typical dry and wet season (i.e., years 2000 and 2004, respectively).

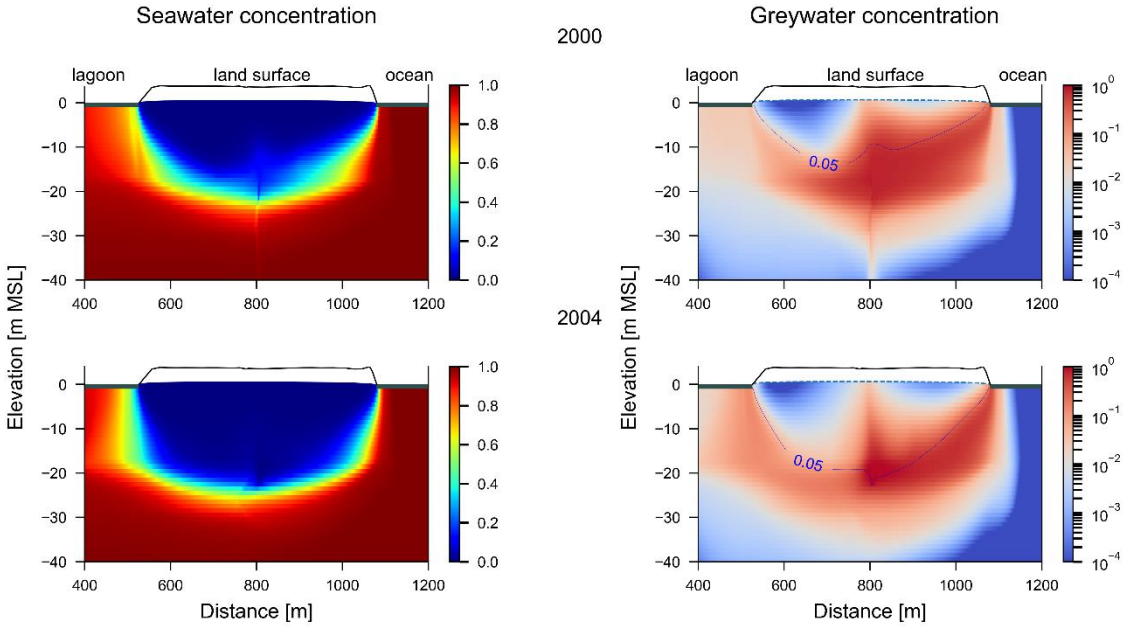

Figure 27. Concentrations of seawater (left plots) and greywater (right plots) from transient simulations of the future situation (i.e., population in 2030, average rainfall, etc.) with greywater disposal injected into a well in Betio for dry and wet characteristic years, 2000 and 2004, respectively. The 0.05 relative seawater contour is shown on the right column of figures (i.e., plots of greywater concentration) to overlay the depth of freshwater.

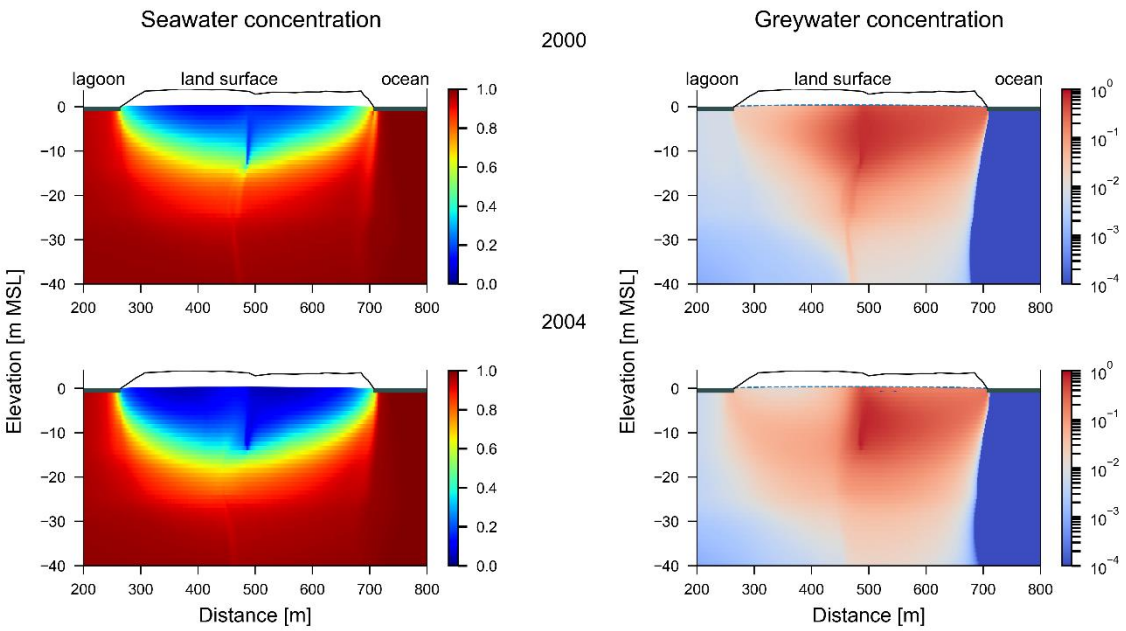

Figure 28. Concentrations of seawater (left plots) and greywater (right plots) from transient simulations of the future situation (i.e., population in 2030, average rainfall, etc.) with greywater disposal injected into a well in Bairiki for dry and wet characteristic years, 2000 and 2004, respectively. The 0.05 relative seawater contour is shown on the right column of figures (i.e., plots of greywater concentration) to overlay the depth of freshwater.

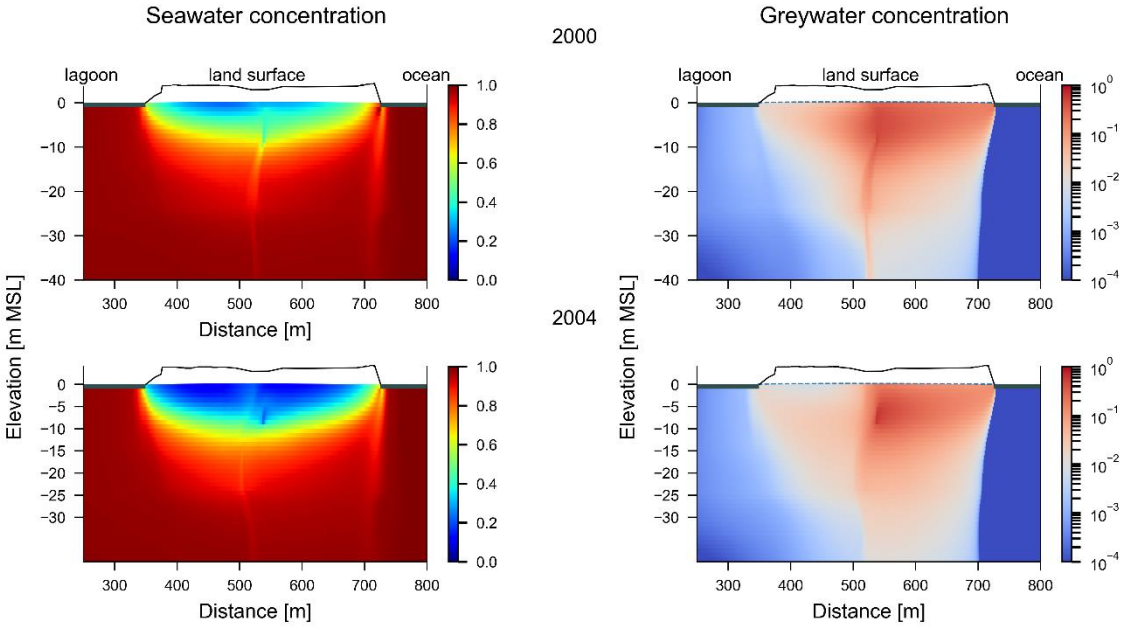

Figure 29. Concentrations of seawater (left plots) and greywater (right plots) from transient simulations of the future situation (i.e., population in 2030, average rainfall, etc.) with

greywater disposal injected into a well in Bikenibeu for dry and wet characteristic years, 2000 and 2004, respectively.

A comparison of Cases 7 and 8 suggests that in general, a larger extent of high relative greywater concentrations (between 0.01 and 1) is observed when the greywater injection occurs at the freshwater-seawater interface. The amount of rainfall recharge has also a large influence on the greywater distribution, that is, results for dry years (e.g., 2000) show a larger extent of higher greywater concentrations (i.e., relative greywater concentration ≥ 0.1) than in wet years (e.g., 2004), as it is observed in the right column of Figures 27, 28 and 29.

The results of Case 8 show that the freshwater depth in wet years is deeper than in dry years, as expected. For example, the freshwater depth in Betio (i.e., depth of the 0.05 relative seawater contour below the watertable) is 54% larger than in dry years. Based on the depth of the 0.5 relative contours, due to the shallow freshwater lenses in Bairiki and Bikenibeu, especially in the dry years, the increment in the freshwater depth is 13.5% and 9%, respectively. To assess the influence of the disposal approach (whether land surface infiltration or injection at the interface), a comparison of freshwater depths between Case 7 and Case 8 is shown in Table 21.

Table 21. Computed freshwater depths in Cases 7 and 8 for each representative season. The difference is estimated as [(Case 8−Case7)/Case 7]×100%. "Dry" and "Wet" times were 27th of December 2000 and 22nd of December 2004, respectively.

	Relative salinity contour used to calculate depth	**Dry**		**Wet**	
		Case 7	**Case 8**	**Case 7**	**Case 8**
Betio	0.05 relative seawater contour (m)	18.7	15.1	21.4	23.2
	Difference (%)	-19		8.0	
Bairiki	0. 5 relative seawater contour (m)	11.5	14.4	16.0	16.4
	Difference (%)	25		2.5	
Bikenibeu	0. 5 relative seawater contour (m)	6.70	9.50	10.0	10.3
	Difference (%)	42		3.0	

The negative value in the estimated difference for Betio in the dry season indicates that freshwater depth is reduced by 19% when the injection of greywater occurs at the interface. For the rest of conditions, the freshwater depth consistently increases in the simulated scenario of Case 8 in both seasons

Case 9: Transient simulation of future greywater disposal at the land surface-no abstraction

This model scenario is based on the assumption of no groundwater abstraction, combined with greywater disposal at the land surface and centrally within each island. Groundwater abstraction is removed to evaluate the future scenario (i.e., 2030) where low-salinity reticulated water substitutes for groundwater abstraction as a water source for domestic use. Case 9 is an adaptation of Case 7 (i.e., transient and future scenario), whereby groundwater abstraction is neglected in the estimation of net recharge.

Besides the differences in freshwater depths from dry to wet years already discussed in the previous cases (i.e., generally in the wet season the freshwater depth increases), the freshwater depth is expected to increase in Case 9 in comparison to the same years in Case 7 in which groundwater abstraction is included. Figures 29, 30 and 31 show the results of Case 9 for Betio, Bairiki and Bikinebeu, respectively.

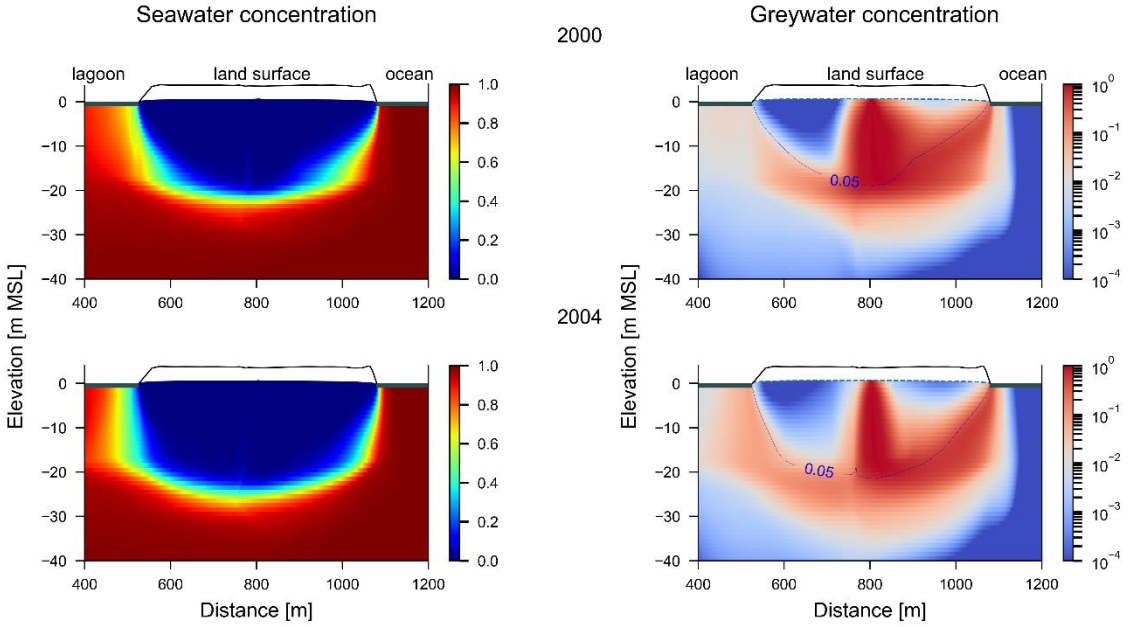

Figure 30. Concentrations of seawater (left plots) and greywater (right plots) from transient simulations of the future situation (i.e., population in 2030, average rainfall, etc.) with greywater disposal at the land surface and no abstraction in Betio for dry and wet characteristic years, 2000 and 2004, respectively. The 0.05 relative seawater contour is shown on the right column of figures (i.e., plots of greywater concentration) to overlay the depth of freshwater.

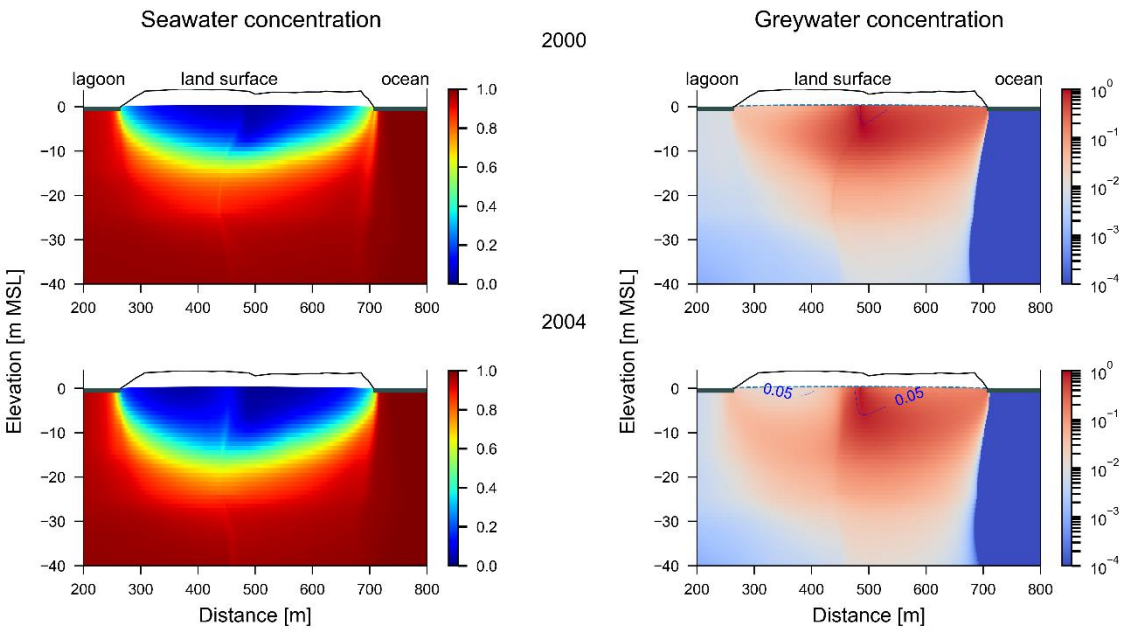

Figure 31. Concentrations of seawater (left plots) and greywater (right plots) from transient simulations of the future situation (i.e., population in 2030, average rainfall, etc.) with greywater disposal at the land surface and no abstraction in Bairiki for dry and wet characteristic years, 2000 and 2004, respectively. The 0.05 relative seawater contour is shown on the right column of figures (i.e., plots of greywater concentration) to overlay the depth of freshwater

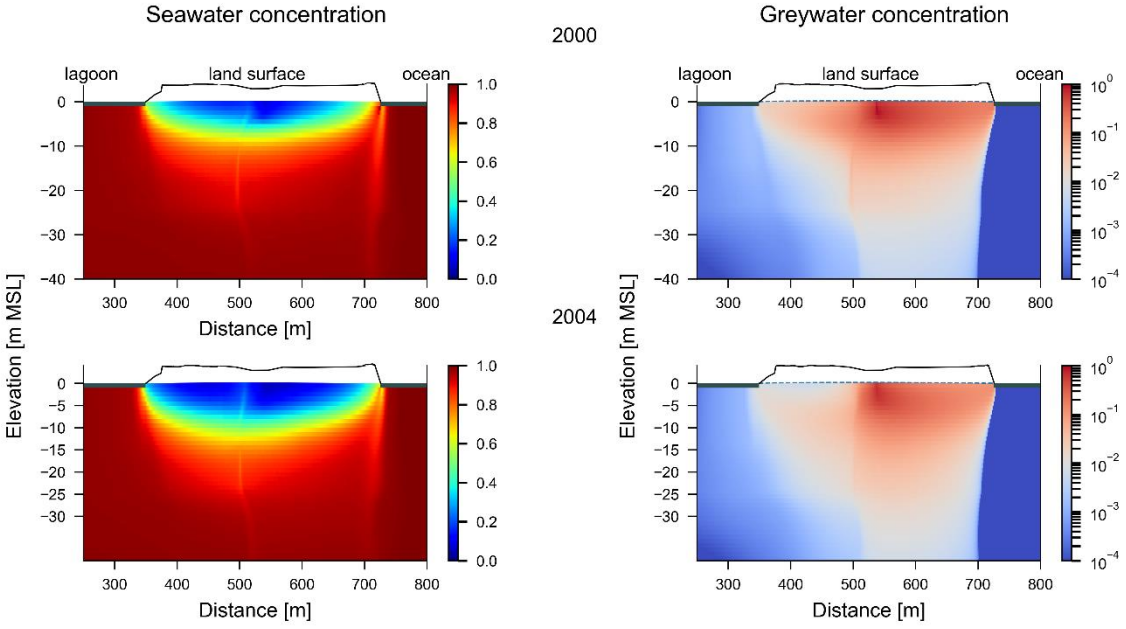

Figure 32. Concentrations of seawater (left plots) and greywater (right plots) from transient simulations of the future situation (i.e., population in 2030, average rainfall, etc.) with

greywater disposal at the land surface and no abstraction in Bikenibeu for dry and wet characteristic years, 2000 and 2004, respectively.

To evaluate the effects of no groundwater abstraction on the fresh groundwater and greywater distribution, the outputs of Case 9 (no groundwater abstraction) are compared to Case 7 (with groundwater abstraction). Results show that the freshwater lens is thicker in Case 9 compared to Case 7, as expected. The increase in freshwater depth is estimated by comparing the 0.05 relative seawater concentration in Betio and Bairiki, and the 0.5 relative seawater concentration in Bikenibeu where the freshwater lens is too thin to easily analyse changes in the 0.05 salinity. Table 22 shows the comparison between Case 7 and Case 9 for wet and dry times.

Table 22. Computed freshwater depths in Cases 7 and 9 for each representative season. The difference is estimated as [(Case 9−Case7)/Case 7]×100%. "Dry" and "Wet" times were 27th of December 2000 and 22nd of December 2004, respectively.

	Relative salinity contour used to calculate depth	**Dry**		**Wet**	
		Case 7	**Case 9**	**Case 7**	**Case 9**
Betio	0.05 relative seawater contour (m)	18.7	19.8	21.4	22.2
	Difference (%)	6.0		4.0	
Bairiki	0.05 relative seawater contour (m)	3.20	4.30	5.50	6.40
	Difference (%)	34		16	
Bikenibeu	0.5 relative seawater contour (m)	6.70	7.10	10.0	10.2
	Difference (%)	6.0		2.0	

Despite the deepening of the freshwater lens, the greywater concentration in the freshwater lens increases. In Case 7, the dynamics of a lower net rainfall recharge (i.e., net recharge is larger in Case 9 due to a neglected abstraction rate) cause higher greywater concentrations as a result of a constant greywater disposal for both cases. That is, the dilution of greywater is lower for a lower net recharge causing higher greywater concentrations in the freshwater lenses.

Case 10: Transient simulation of future greywater disposal injected into a well-no abstraction

Case 10 is a modified version of Case 9, whereby a greywater disposal injection well was inserted at the freshwater-seawater interface (i.e., 0.5 relative seawater contour) instead of land surface greywater disposal. Figures 32, 33 and 34 show the results of Case 10 for Betio, Bairiki and Bikenibeu, respectively.

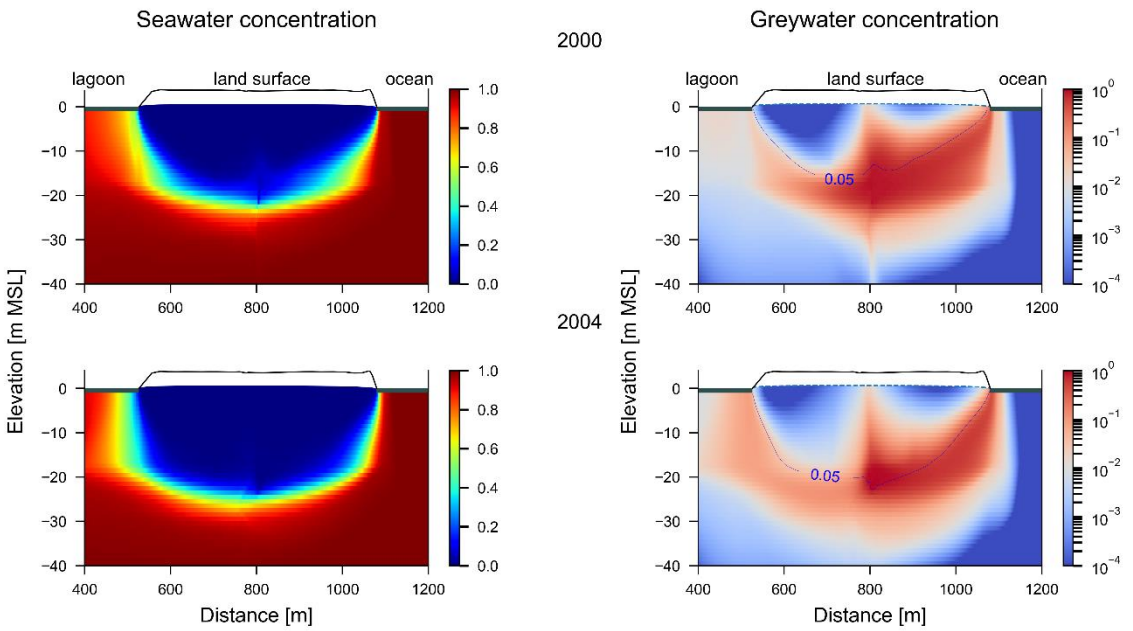

Figure 33. Concentrations of seawater (left plots) and greywater (right plots) from transient simulations of the future situation (i.e., population in 2030, average rainfall, etc.) with greywater disposal injected into a well and no abstraction in Betio for dry and wet characteristic years, 2000 and 2004, respectively. The 0.05 relative seawater contour is shown on the right column of figures (i.e., plots of greywater concentration) to overlay the depth of freshwater.

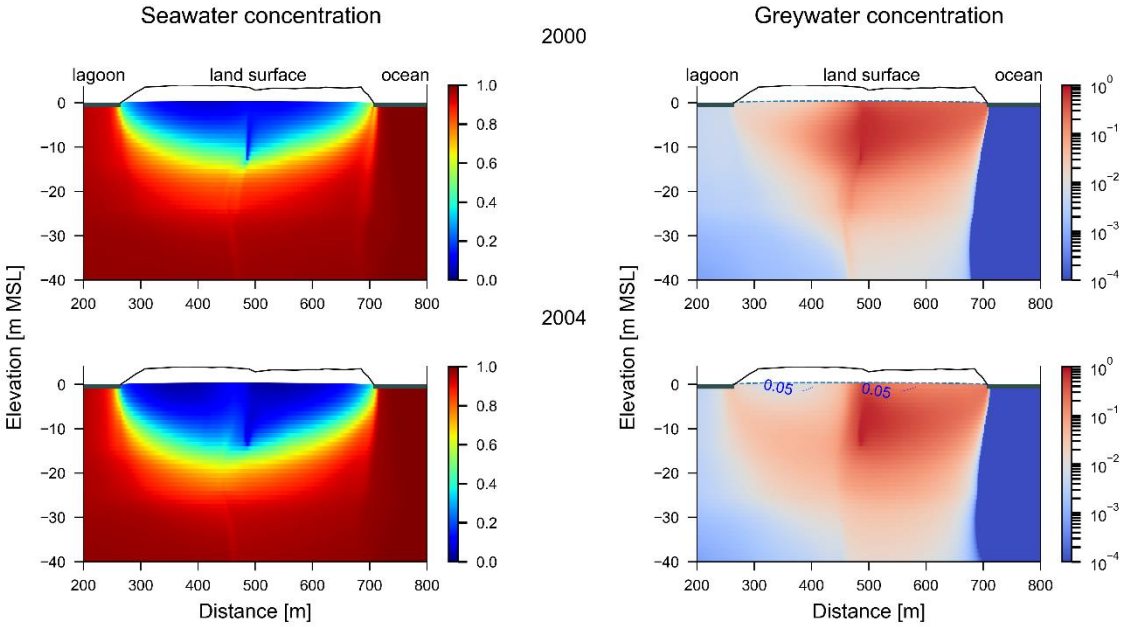

Figure 34. Concentrations of seawater (left plots) and greywater (right plots) from transient simulations of the future situation (i.e., population in 2030, average rainfall, etc.) with greywater disposal injected into a well and no abstraction in Bairiki for dry and wet

characteristic years, 2000 and 2004, respectively. The 0.05 relative seawater contour is shown on the right column of figures (i.e., plots of greywater concentration) to overlay the depth of freshwater.

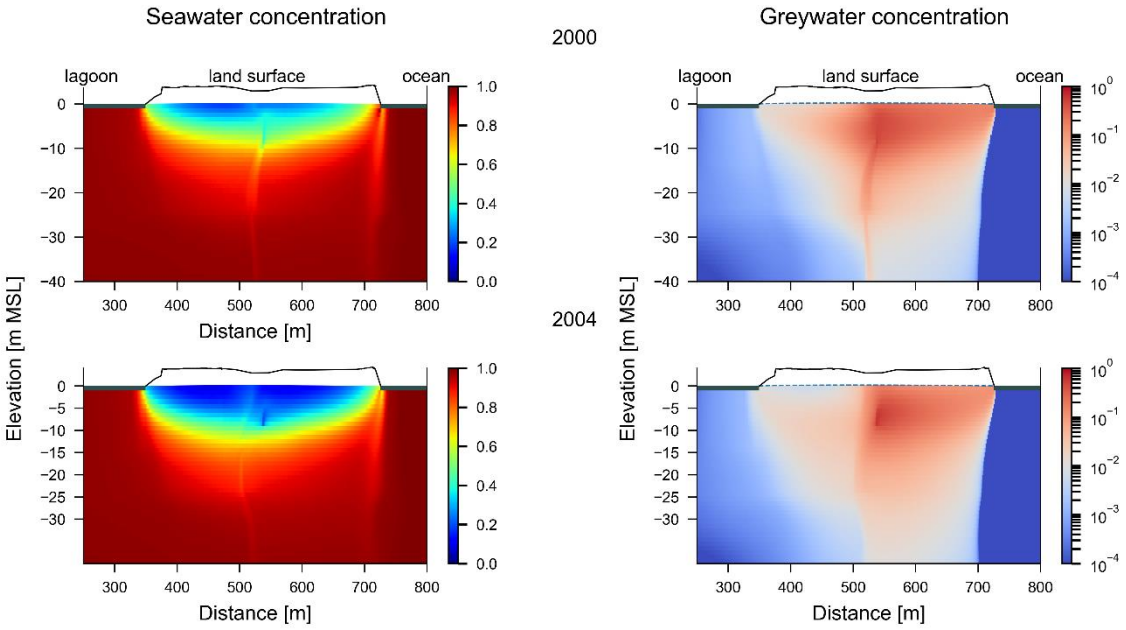

Figure 35. Concentrations of seawater (left plots) and greywater (right plots) from transient simulations of the future situation (i.e., population in 2030, average rainfall, etc.) with greywater disposal injected into a well and no abstraction in Bikenibeu for dry and wet characteristic years, 2000 and 2004, respectively.

The comparison between the results of Case 10 and the homologous Case 8 show similar results discussed in the previous scenario (the comparison between Case 9 and Case 7). The freshwater lens is increased in Case 10, using the 0.05 relative seawater contour in Betio and the 0.5 relative seawater contour in Bairiki and Bikenibeu. Here, different from the comparison discussed in the above Case 9, the comparison of the Bairiki's model results is based on the 0.5, since in the dry season the relative seawater concentrations are higher than 0.05. Table 23 shows the results of this comparison.

Lower relative greywater concentrations are also observed in Case 10 due to a higher net rainfall discharge that causes a higher dilution in the greywater distribution.

Table 23. Computed freshwater depths in Cases 8 and 10 for each representative season. The difference is estimated as [(Case 10−Case8)/Case 8]×100%. "Dry" and "Wet" times were 27th of December 2000 and 22nd of December 2004, respectively.

	Relative salinity contour used to calculate depth	Dry		Wet	
		Case 8	**Case 10**	**Case 8**	**Case 10**
Betio	0.05 relative seawater contour (m)	15.1	17.3	23.2	23.5
	Difference (%)	15		1.0	
Bairiki	0. 5 relative seawater contour (m)	14.4	14.6	16.4	17.0
	Difference (%)	1.0		4.0	
Bikenibeu	0. 5 relative seawater contour (m)	9.50	9.60	10.3	10.6
	Difference (%)	1.0		3.0	

A comparison between Case 9 and Case 10 shows that the freshwater depth during the dry season in the Case 10 of Betio (i.e, injection at the interface) decreases by 14%, whereas in the wet season the freshwater depth increases by approximately 3%. In Bikenibeu, the comparison of the 0.5 relative seawater contour depth demonstrates that in both seasons, dry and wet, the freshwater depth increases in Case 10 by 35% and 4%, respectively. Despite the freshwater depth in Bairiki for Case 9 was measured with 0.05 relative seawater contour, in Case 10 the relative seawater concentrations are higher than 0.05, especially in the dry season (top-right right panel of Figure 34)

8. Conclusions and Recommendations

This report focused on a numerical modelling assessment of the possible effects of greywater reuse on the freshwater lenses in South Tarawa. Available field data included topography, bathymetry, geological/stratigraphic data, aquifer hydraulic parameters, rainfall, groundwater abstraction, groundwater levels and salinity, and greywater discharge. These, along with parameters from previous studies, were used to develop conceptual models and 2D (cross-sectional) numerical models of selected transects of Betio, Bairiki and Bikenibeu Islands. Transects were located to intersect existing monitoring wells.

Numerical models were developed using the USGS software SEAWAT, which allows multi-species (i.e., greywater transport and freshwater-seawater mixing) simulation. SEAWAT's density-dependent capability is essential for proper representation of the buoyant freshwater lenses on these atolls islands.

Model calibration was achieved using a steady-state model (Case 1), which adopted time-averaged recharge and area-averaged abstraction rates. Model calibration involved manual trial-and-error adjustment of model parameters (i.e., K_H, K_V and α_L) to find optimal matches between SEAWAT outputs and available salinity measurements from monitoring wells. A transient model (Case 2) was subsequently produced for a period of 68 years and 8 months (from 1 May 1947 to 31 December 2015) to validate the calibration and to explore historical dynamics in response to recharge trends. Greywater input was not considered in both steady-state calibration and transient validation models; its effects on the selection of calibration parameters were found to be negligible.

Eight simulations then were used to assess greywater transport and its effects on freshwater lenses in current situation and future scenarios. In current situation, 2015 population was used to estimate the groundwater abstraction (based on 45 L/pers/d water abstraction from shallow wells; FTP 2011) and greywater discharge (based on 35 L/pers/d greywater production, i.e., 70% of the provided freshwater for each person), which was applied to the model in closely spaced points on the land surface. The models for future scenarios adopted the projected 2030 population to evaluate the groundwater abstraction (assumed a rate similar to the current situation i.e., 45 L/pers/d) and greywater discharge (considered 70 L/pers/d greywater production). The latter was added in the models in one centralised disposal point in the middle of each cross-section with two different greywater disposal forms, namely land surface injection or through injection well into the base of the freshwater lens (i.e., the freshwater-seawater mixing zone).

Of the eight simulations, three of them were steady-state models used for long-term assessment and averaged effects of greywater disposal in current situation (Case 3) and future scenarios in various forms (in land surface, Case 4; through injection well, Case 5). Changes in freshwater lens thickness, determined by the lowest point on the 5% of relative seawater

concentration contour, were used as an indicator to assess the effects of greywater discharge on the freshwater lenses. The modelling results show that adding the greywater discharge (i.e., Cases 3, 4 and 5) increases the freshwater thickness compared to Case 1 where greywater discharge was neglected. Although higher abstraction rates were applied in future scenarios, the greywater discharges were dominant and had greater effects on the freshwater lens thickness.

The injection of greywater in the well (Case 5) increased the freshwater lens thickness more than when greywater infiltrates on the land surface (Case 4) in Betio, while the opposite was observed for Bairiki and Bikenibeu. Comparing the greywater concentation for two different forms of greywater disposal in future scenarios reveals that in Betio the relative greywater concentration is lower in the freshwater lens when greywater is injected through the well (Case 5) than the land surface (Case 4). This is in contrast to the other islands (Bairiki and Bikenibeu), where lower relative greywater concentration was observed when greywater discharges in the land surface (Case 4). This is due to the fact that the larger dispersivity was applied in the models in Bairiki and Bikenibeu (i.e, α_L = 20 m) compared to Betio (i.e, α_L = 5 m). The simulation results of the future scenarios also indicate that in general, the concentration of greywater in the freshwater lenses in Betio, Bairiki and Bikenibeu is higher on the ocean side because of the effects of larger *K* towards the ocean.

The influence of the rainfall dynamics on the propagation of the greywater disposal on the freshwater lenses was then explored by running transient version of previous modelling cases. This is, Cases 6, 7 and 8 are corresponded transient versions of Cases 3, 4 and 5, respectively. The model results were evaluated at the end of years 2000 and 2004 as representatives for dry and wet years, respectively. As expected, the thickness of the freshwater lenses was highly affected by climate variations (i.e., consequently changes in the recharge) in dry (year 2000) and wet (year 2004) years, as thicker freshwater lenses were observed in the wet year compared to the dry year in all cases (i.e., Cases 6, 7 and 8). The changes in the freshwater lens thickness due to the effects of rainfall dynamics were more obvious in Bairiki and Bikenibeu, where the freshwater lenses are thinner, than in Betio. The changes in the rainfall amount had also a large influence on the greywater distribution. It was found that the greywater distribution in freshwater lens is more dispersive and its relative concentration is lower in the wet year than in the dry year. The influence of the form of disposal in future scenarios (i.e., land surface infiltration, Case 7 and injection well, Case 8) was assessed by comparing the freshwater lens thicknesses. The comparison showed that the thickness of the freshwater lenses in both dry and wet years is larger if the greywater discharges through well injection than on the land surface, except Betio where in dry year the thickness of freshwater lens was reduced.

The effects of groundwater abstraction in future scenarios was assessed by running two transient models (Cases 9 and 10 identical to Case 7 and 8, respectively) with the assumption of no well abstraction. The assumption relies on that by 2030, households will have access to other sources of high-quality water (e.g., reticulated water) rather than well water. An increase

was observed in the freshwater lenses thickness due to applying higher net recharge (i.e., neglecting groundwater abstraction) in both wet and dry years for Betio, Bairiki and Bikenibeu. Similar patterns to Cases 7 and 8 (i.e., with well abstraction) was observed in greywater distribution in Cases 9 and 10 (i.e., no well abstraction); however, the concentration of greywater in freshwater lenses were generally lower due to higher net recharge.

The following recommendations for future work are made to enhance the outcomes of future modelling efforts:

- Future field studies are required to provide more accurate details for stratigraphic information, aquifer hydraulic parameters and groundwater extent.
- A regular data collection program (e.g., salinity, water table level, etc.) from all existing monitoring wells would be extremely useful for model calibration.
- Sampling of greywater in the field to analyse its composition which has important role in groundwater quality.
- Obtain better estimation of groundwater abstraction and greywater production from a field survey.
- More sophisticated methods (e.g., water balance simulation) are needed to improve the recharge estimation.
- Including the tidal effects can improve the calibration of model.
- Re-calibrate the steady-state model using automated calibration software (e.g., PEST).
- Calibration the transient model to minimise the difference between simulated and observed concentration.
- Consider the effects of unsaturated flow for greywater discharge on land surface.
- Considering chemical reactions and degradation of greywater compositions in greywater movement simulation.

Acknowledgements

This investigation has benefited from technical contributions from Dr John Hutson (Flinders University). Adrian Werner is the recipient of an Australian Research Council Future Fellowship (project number FT150100403). Amir Jazayeri is funded by the Australian Research Council (project numbers FT150100403 and LP140100317).

References

Alam K. and Falkland A. 1997. Vulnerability to climate change of the Bonriki freshwater lens, Tarawa. Prepared for the Ministry of Environment and Social Development Republic of Kiribati.

Alam K., Falkland A. and Mueller N. 2002. Sustainable yield of Bonriki and Buota freshwater lenses, SAPHE Project, Hydrogeology Component, Tarawa, Kiribati.

Anthony S.S. 2004. Hydrogeology of selected islands of the Federated States of Micronesia. p. 693–706 In: Geology and Hydrogeology of Carbonate Islands. Vacher H.L. and Quinn T.M. (eds). Amsterdam: Elsevier.

Antoniou, E. A. Van Breukelen, B. M., Putters, B. and Stuyfzand, P. J. (2012). Hydrogeochemical patterns, processes and mass transfers during aquifer storage and recovery (ASR) in an anoxic sandy aquifer. Applied Geochemistry 27(12): 2435-2452.

Aonghusa, C. N., & Gray, N. F. (2002). Laundry detergents as a source of heavy metals in Irish domestic wastewater. Journal of Environmental Science and Health. Part A, Toxic/Hazardous Substances & Environmental Engineering, 37, 1–6.

Ataie-Ashtiani B., Volker R.E. and Lockington D.A. 1999. Tidal effects on sea water intrusion in unconfined aquifers. Journal of Hydrology 216(1-2): 17–31.

Ayers J.F. and Vacher H.L. 1986. Hydrogeology of an atoll island: a conceptual model from detailed study of a Micronesian example. Ground Water 24: 185–198. Doi: 10.1111/j.1745-6584.1986.tb00994.x.

Bosserelle A., Jakovovic D., Post V., Galvis Rodriguez S., Werner A.D. and Sinclair P. 2015. Assessment of sea-level rise and inundation effects on Bonriki freshwater lens, Tarawa Kiribati: groundwater modelling report. Report for Bonriki Inundation Vulnerability Assessment Project. Geoscience Division Technical Report. Secretariat of the Pacific Community.

Buddemeier R.W. and Oberdorfer J.A. 2004. Hydrogeology of Enewetak Atoll. p. 667–692 In: Geology and Hydrogeology of Carbonate Islands. Vacher H.L. and Quinn T.M. (eds). Amsterdam: Elsevier.

Burbery, L., Weaver, L., Humphries, B., and Gregor, J. (2015). Efficacy of coral sand for removal of escherichia coli and bacteriophage under saturated flow conditions. Journal of Environmental Quality, 44(5).

Crennan L. (2001). Integration of social and technical science in groundwater monitoring and management – Groundwater pollution study on Lifuka, Ha'apai, Tonga. IHP-V. Technical Documents in Hydrology 43. UNESCO. Paris.

Dolnicar, S., Schafer A.I. (2006). Public perception of desalinated versus recycled water in Australia. In: AWWA Desalination Symposium, Honolulu, Hawaii.

Дэя-Бøяg 2011. South Tarawa (map within Tarawa Atoll). https://commons.wikimedia.org/wiki/File:South_Tarawa_(map_within_Tarawa_Atoll).png#filelinks [Accessed July 25, 2019].

Eriksson E., Auffarth K., Henze M. and Ledin A. 2002. Characteristics of grey wastewater. Urban Water 4: 85–104. Doi:10.3390/w2020155.

Eriksson, E., Auffarth, K., Eilersen, A. M., Henze, M., &Ledin, A. (2003). Household chemicals and personal care products as sources for xenobiotic organic compounds in grey wastewater. Water SA, 29, 135–146.

Eriksson, E., Srigirisetty, S., & Eilersen, A. M. (2010). Organic matter and heavy metals in grey-water sludge. Water SA, 36, 139–142.

Falkland A. and Woodroffe C. 1997. Geology and hydrogeology of Tarawa and Christmas Island, Kiribati. p. 577–610. In: Geology and hydrogeology of carbonate islands. Vacher H.L. and Quinn T.M. (eds). Amsterdam: Elsevier.

Falkland A., White I. and Turner B. 2003. Report on Abatao-Tabiteuea groundwater investigations, Tarawa, Kiribati. Kiribati SAPHE Project. Prepared for Original Engineering Consultants, Osaka, Japan and SAPHE Project Management Unit, Bairiki, Tarawa.

Fatta-Kassinos, D., Kalavrouziotis, I. K., Koukoulakis, P. H., & Vasquez, M. I. (2011). The risks associated with wastewater reuse and xenobiotics in the agroecological environment. Sci Total Environ, 409, 3555–3563.

Firouzi, A., Homaee, M., Klumpp, E., Kasteel, R., and Tappe, W. (2015). Bacteria transport and retention in intact calcareous soil columns under saturated flow conditions. Journal of Hydrology and Hydromechanics, 63(2):102-109.

FTP (Fraser Thomas Partners). 2011. Groundwater resource assessment: Freshwater lens mapping and sustainable yield estimation at Betio, Bairiki and Bikenibeu, South Tarawa. South Tarawa Sanitation Improvement Project. Prepared for Government of Kiribati and Asian Development Bank.

GoK (Government of Kiribati). 2011. Kiribati government website. https://web.archive.org/web/20100626072239/http://www.kiribatitourism.gov.ki/index.php/aboutkiribati/aboutkiribatioverview [Accessed July 25, 2019].

GWPC (GWP Consultants). 2011. Drilling report: Nabeina, Tabiang, Tabuki (North Tarawa), Bikenibeu, Bairiki and Betio (South Tarawa) for Kiribati Adaptation Project-Phase II. Kiribati improving the sustainability and supply of freshwater KAPII: FSS0943 FS-07/2009. Prepared by GWP Consultants LLP.

Humphries B. L. (2018). Examining the use of coral sand for the treatment of domestic effluent in Kiribati. Master Thesis. University of Canterbury, Christchurch, New Zealand.

Jacobson G. and Taylor F.J. 1981. Hydrogeology of Tarawa Atoll, Kiribati. Bureau of Mineral Resources Record No. 1981/31. Government of Australia.

KNSO (Kiribati National Statistics Office) and SPC (Secretariat of the Pacific Community) 2016. 2015 Population and Housing Census. Volume 1: Management report and basic tables.

Kumar S., Kruger J., Begg Z. and Baleilevuka A. 2015. Single Beam Survey. Report for Bonriki Inundation Vulnerability Assessment Project. Geoscience Division Technical Report. Secretariat of the Pacific Community.

Langevin C.D., Thorne D.T., Dausman A.M., Sukop M.C. and Gou W. 2007. SEAWAT Version 4: A computer program for simulation of multi-species solute and heat transport. p. 39. In: US Geological Survey Techniques and Methods, Book 6. USGS, Reston, Virginia.

Maliva, R. G. and Missimer, T. M. (2010). Aquifer storage and recovery and managed aquifer recharge using wells: planning, hydrogeology, design and operation. Schlumberger.

National Statistics Office (2012). Report on the Kiribati 2010 Census of Population and Housing. Ministry of Finance. Republic of Kiribati. Bairiki, Tarawa.

National Statistics Office (2016). 2015 Population and Housing Census. Ministry of Finance. Republic of Kiribati. Bairiki, Tarawa.

O'Toole, J., Sinclair, M., Malawaraarachchi, M., Hamilton, A., Barker, S. F., & Leder, K. (2012). Microbial quality assessment of household greywater. Water Research, 46, 4301– 4313.

Oberdorfer J.A., Buddemeier R.W. 1983. Hydrogeology of a Great Barrier Reef: implications for groundwater in reef and atoll islands. EOS. Transactions American Geophysical Union 64(45): 703–704.

Oteng-Peprah M., Acheampong M.A. and de Vries N.K. 2018. Greywater characteristics, treatment systems, reuse strategies and user perception—a review. Water, Air, & Soil Pollution: 229–255. Doi: 10.1007/s11270-018-3909-8.

Overacre, R., Clinton, T., Pyne, D., Snyder, S. and Dillon, P. J. (2006). Reclaimed water aquifer storage and recovery: Potential changes in water quality. WEFTEC. Dallas, Water Environment Foundation: 1339-1360.

Pang, L. (2009). Microbial removal rates in subsurface media estimated from published studies of field experiments and large intact soil cores. Journal of Environmental Quality, 38:1531-1559.

Pavelic, P., Nicholson, B. C., Dillon, P. J. and Barry, K. E. (2005). "Fate of disinfection by-products in groundwater during aquifer storage and recovery with reclaimed water." Journal of Contaminant Hydrology 77(1–2): 119-141.

Peterson, F.L. 2004. Hydrogeology of the Marshall Islands. p. 611–636 In: Geology and Hydrogeology of Carbonate Islands, Vacher H.L. and Quinn T.M. (eds). Amsterdam: Elsevier.

Post V.E.A., Bosserelle A.L., Galvis S.C., Sinclair P.J. and Werner A.D. 2018. On the resilience of small-island freshwater lenses: Evidence of the long-term impacts of groundwater abstraction on Bonriki Island, Kiribati. Journal of Hydrology, 564 pp. 133-148.

Schijven, J., Pang, L., and Ying, G. (2017). Evaluation of subsurface microbial transport using microbial indicators, surrogates and tracers, chapter Part two: indicators and microbial source tracking markers. Michigan State University, E. Lansing, MI, UNESCO.

Smith A.J. 2004. Mixed convection and density-dependent seawater circulation in coastal aquifers. Water Resources Research 40(8): W08309. Doi: 10.1029/2003WR002977.

Vacher H.L., Quinn T.M. (Eds). 2004. Geology and Hydrogeology of Carbonate Islands, Developments in Sedimentology 54, Elsevier, Amsterdam.

Vanderzalm, J. L., Le Gal La Salle, C., L., H. J. and Dillon, P. J. (2002). Water quality changes during aquifer storage and recovery at Bolivar, South Australia. Management of Aquifer Recharge for Sustainability. P. J. Dillon, A. A. Balkema: 83-88.

Werner A.D., Sharp H.K., Galvis S.C., Post V.E.A. and Sinclair P. 2017. Hydrogeology and management of freshwater lenses on atoll islands: Review of current knowledge and research needs. Journal of Hydrology 551: 819-844. Doi: 10.1016/j.jhydrol.2017.02.047.

White I. 2010. Tarawa Water Master Plan: 2010–2030. Coordinated by the National Adaptation Steering Committee under Office Te Beretitenti and the National Water and Sanitation Coordination Committee through the Ministry of Public Works and Utilities.

White I., Falkland A., Etuati B., Metai E. and Metutera T. 2002. Recharge of fresh groundwater lenses: Field study, Tarawa Atoll, Kiribati. 302–323. In: Proceedings of the Second International Colloquium on Hydrology and Water Resources Management in the Humid Tropics, Panama, 22–25 March 1999. Gladwell J.S. (ed). UNESCO-IHP, CATHALA.

White I., Falkland T., Perez P., Dray A., Metutera T., Metai E. and Overmars M. 2005. Challenges in freshwater management in low coral atolls. Journal of Cleaner Production. Special Edition Water Management in Coastal Zones.

White I. and Falkland A. 2008. Report on the protection and management of water reserves, South Tarawa. Preparation of Water Master Plan for Tarawa.

White I. and Falkland T. 2010. Management of freshwater lenses on small Pacific islands. Hydrogeology Journal 18(1): 227–246. Doi: 10.1007/s10040-009-0525-0.

Xu, S., Gao, B., and J.E, S. (2006). Straining of colloidal particles in saturated porous media. Water Resources Research, 42.

Appendices

Appendix 1. Measured EC profiles in monitoring wells in 2010, 2011 and 2019.

Betio (18-Jul-2010); GWPC (2011)					
Elevation (m MSL)	Depth (m BGL)	EC (µS/cm)			
		1	2	3	Mean
-2.31	6	568	562	548	559
-6.31	10	2049	1633	1346	1676
-10.31	14	392	399	411	401
-14.31	18	660	677	669	669
-17.31	21	1682	1605	1581	1623
-20.31	24	>20000	>20000	>20000	>20000
2.31	1.38	Water table in PVC pipe			
3.69	Elevation of monitoring well interpolated from survey				

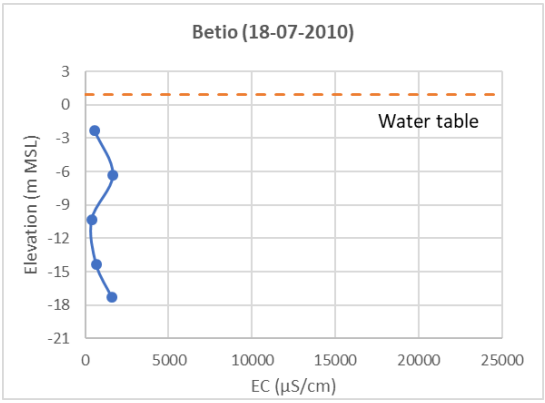

Bairiki (21-Jul-2010); GWPC (2011)					
Elevation (m msl)	Depth (m BGL)	EC (µS/cm)			
		1	2	3	Mean
-2.12	5	2403	2369	2254	2342
-4.12	7	2790	2370	2720	2627
-6.12	9	8120	8220	8210	8183
-9.12	12	10920	10900	10660	10827
-12.12	15	17640	17980	17730	17783
-15.12	18	19720	19780	19830	19777
0.90	1.98	Water table in PVC pipe			
2.88	Elevation of monitoring well interpolated from survey				

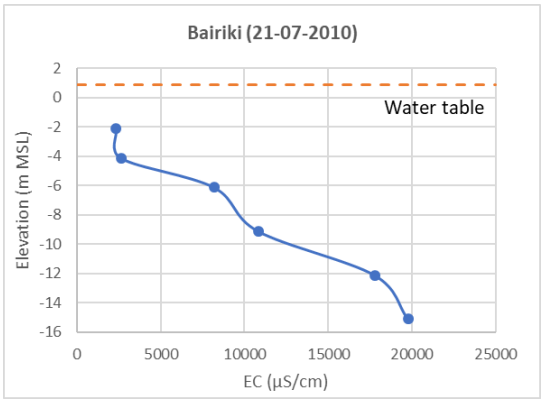

Bikenibeu (21-Jul-2010); GWPC (2011)					
Elevation (m MSL)	Depth (m BGL)	EC (µS/cm)			
		1	2	3	Mean
-2.37	6	3590	3620	3630	3613
-5.37	9	15400	15620	15790	15603
-8.37	12	>20000	>20000	>20000	>20000
1.46	2.17	Water table in PVC pipe			
3.63	Elevation of monitoring well interpolated from survey				

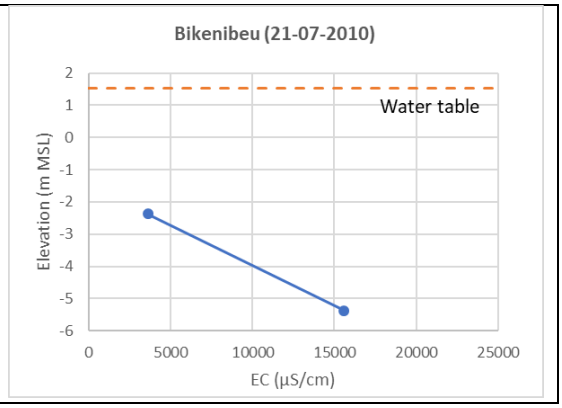

Betio (19-Oct-2010); GWPC (2011)	

Elevation (m MSL)	Depth (m BGL)	EC (µS/cm)			
		1	2	3	Mean
-2.31	6	567	559	553	560
-6.31	10	517	518	536	524
-10.31	14	619	630	643	631
-14.31	18	836	842	841	840
-17.31	21	3700	3570	3410	3560
-20.31	24	>25000	>25000	>25000	>25000
1.96	1.73	water table in PVC pipe			
3.69	Elevation of monitoring well interpolated from survey				

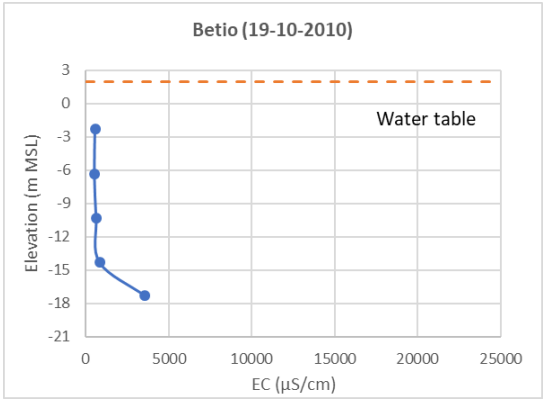

Bairiki (19-Oct-2010); GWPC (2011)					
Elevation (m MSL)	Depth (m BGL)	EC (µS/cm)			
		1	2	3	Mean
-2.12	5	4490	4520	4480	4497
-4.12	7	5780	5470	5230	5493
-6.12	9	10090	10190	10130	10137
-9.12	12	13080	13340	13200	13207
-12.12	15	21200	21320	21360	21293
-15.12	18	22900	23020	22820	22913
0.90	1.98	Water table in PVC pipe			
2.88	Elevation of monitoring well interpolated from survey				

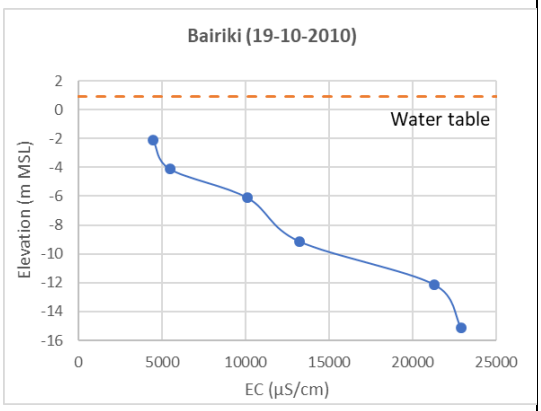

Bikenibeu (20-Oct-2010); GWPC (2011)					
Elevation (m MSl)	Depth (m BGL)	EC (µS/cm)			
		1	2	3	Mean
-2.37	6	5110	5310	5390	5270
-5.37	9	21240	21440	21610	21430
1.38	2.25	Water table in PVC pipe			
3.63	Elevation of monitoring well interpolated from survey				

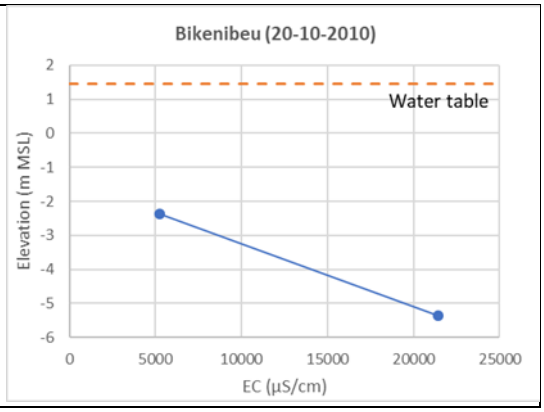

Betio (28-Jan-2011); GWPC (2011)						
Elevation (m MSL)	Depth (m BGL)	EC (µS/cm)				
		1	2	3	4	Mean
1.92	1.77	-	-	623	-	623
-0.31	4	-	-	1411	-	1411
-2.31	6	552	552	553	-	552
-6.31	10	559	572	573	-	568
-10.31	14	705	682	674	-	687
-14.31	18	923	1088	946	921	970
-17.31	21	7010	6590	6380	6190	6543
-20.31	24	30800	31300	31800	-	31300
1.92	1.77	Water table in PVC pipe				
3.69	Elevation of monitoring well interpolated from survey					

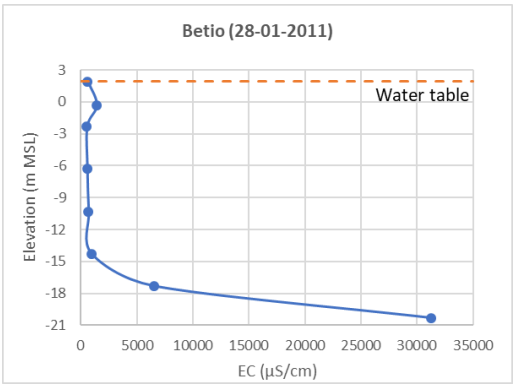

Bairiki (28-Jan-2011); GWPC (2011)					
Elevation (m MSL)	Depth (m BGL)	EC (µS/cm)			
		1	2	3	Mean
0.90	1.98	-	-	1249	1249
-1.12	4	-	-	4960	4960
-2.12	5	6850	6370	6220	6480
-4.12	7	7330	7310	7240	7293
-6.12	9	12060	11590	11450	11700
-9.12	12	14740	14740	14800	14760
-12.12	15	22000	23190	22600	22597
-15.12	18	25200	25200	25200	25200
0.90	1.98	Water table in PVC pipe			
2.88	Elevation of monitoring well interpolated from survey				

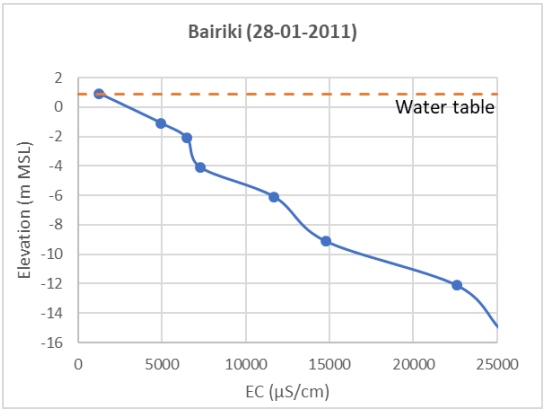

Bikenibeu (28-Jan-2011); GWPC (2011)					
Elevation (m MSL)	Depth (m BGL)	EC (µS/cm)			
		1	2	3	Mean
1.52	2.11	-	-	1270	1270
-0.37	4	-	-	1475	1475
-2.37	6	9610	9330	9180	9373
-5.37	9	26800	26800	26800	26800
-8.37	12	37700	37800	37800	37767
-11.37	15	40200	40200	40300	40233
-14.37	18	42700	42600	42600	42633
-20.37	24	47500	47700	47800	47667
1.52	2.11	Water table in PVC pipe			
3.63	Elevation of monitoring well interpolated from survey				

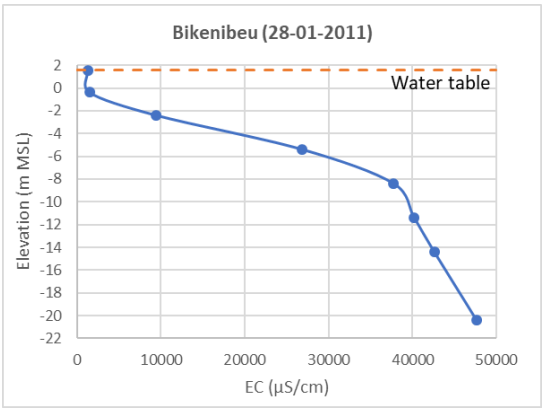

Betio (04-Mar-2011); GWPC (2011)					
Elevation (m MSL)	Depth (m BGL)	EC (µS/cm)			
		1	2	3	Mean
-2.31	6	591	581	586	586
-6.31	10	628	592	595	605
-10.31	14	683	686	686	685
-14.31	18	992	994	995	994
-17.31	21	7690	7410	7220	7440
-20.31	24	30500	30900	30900	30767
???	Water table in PVC pipe				
3.69	Elevation of monitoring well interpolated from survey				

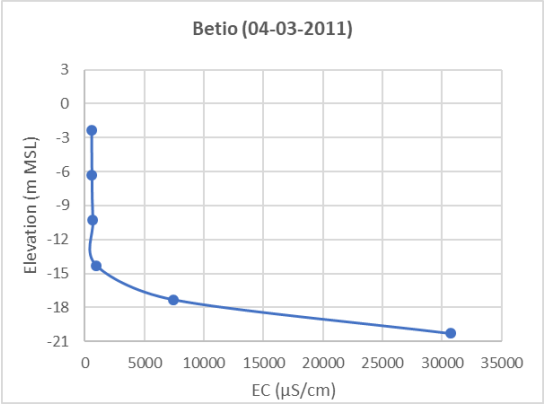

Bairiki (04-Mar-2011); GWPC (2011)					
Elevation (m MSL)	Depth (m BGL)	EC (µS/cm)			
		1	2	3	Mean
-2.12	5	4850	4880	4880	4870
-4.12	7	6190	6200	6230	6207
-6.12	9	11030	11220	11240	11163
-9.12	12	14120	14120	14130	14123
-12.12	15	23300	23000	23100	23133
-15.12	18	25800	25800	25800	25800
???	Water table in PVC pipe				
2.88	Elevation of monitoring well interpolated from survey				

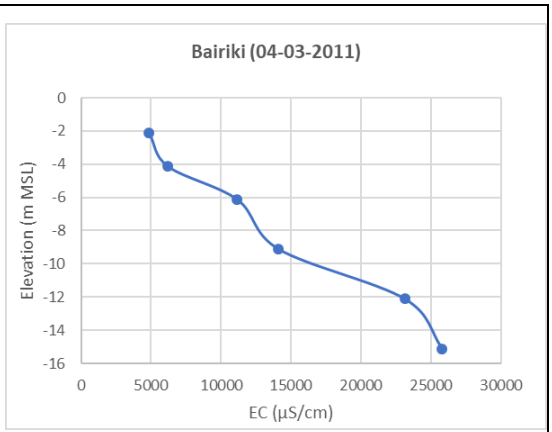

Bikenibeu (04-Mar-2011); GWPC (2011)					
Elevation (m MSL)	Depth (m BGL)	EC (µS/cm)			
		1	2	3	Mean
-2.37	6	10110	9650	9660	9807
-5.37	9	29600	29500	29500	29533
-8.37	12	38300	38300	38400	38333
-11.37	15	41200	41100	41000	41100
-14.37	18	43500	43400	43300	43400
-20.37	24	48300	48500	48500	48433
???	Water table in PVC pipe				
3.63	Elevation of monitoring well interpolated from survey				

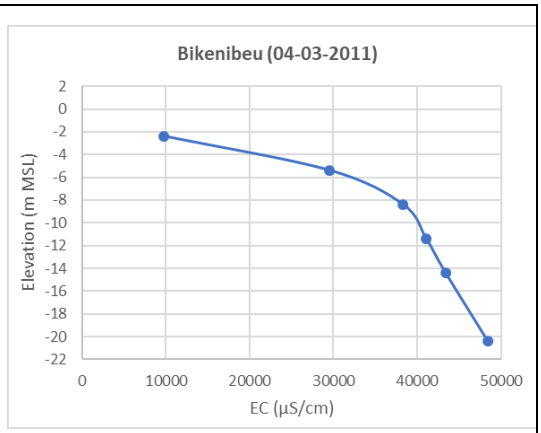

Betio (03-May-2019); SPC					
Elevation (m MSL)	Depth (m)	EC (µS/cm)			
		1	2	3	Mean
-2.31	6	480	485	483	483
-6.31	10	535	534	536	535
-10.31	14	581	578	562	574
-14.31	18	582	585	577	581
-17.31	21	838	850	848	845
-20.31	24	11460	11530	11430	11473
2.04	1.65	Water table in PVC pipe			
3.69	Elevation of monitoring well interpolated from survey				

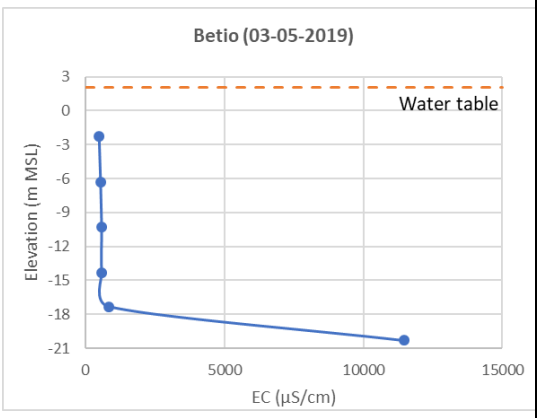

Bairiki (06-May-2019); SPC					
Elevation (m MSL)	Depth (m)	EC (µS/cm)			
		1	2	3	Mean
-2.12	5	620	620	622	621
-4.12	7	674	670	663	669
-6.12	9	1982	2000	2010	1997
-9.12	12	3080	3220	3200	3167
-12.12	15	8500	8580	8640	8573
-15.12	18	13610	13590	13650	13617
1.00	1.88	Water table in PVC pipe			
2.88	Elevation of monitoring well interpolated from survey				

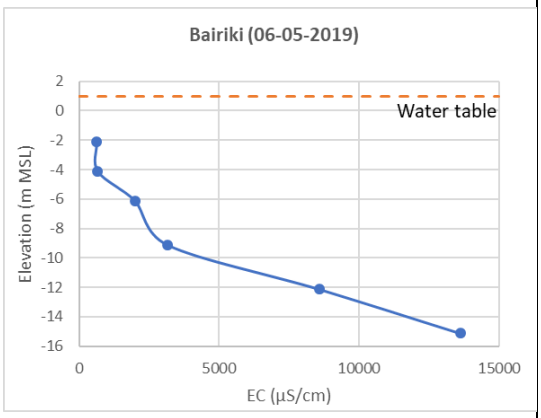

Bikenibeu (07-May-2019); SPC					
Elevation (m MSL)	Depth (m)	EC (µS/cm)			
		1	2	3	Mean
-2.37	6	1490	1486	1475	1484
-5.37	9	10950	10810	10710	10823
-8.37	12	21680	21530	21530	21580
-11.37	15	27900	27900	27600	27800
-14.37	18	41400	40700	41300	41133
-20.37	24	46500	46700	46600	46600
1.54	2.09	Water table in PVC pipe			
3.63	Elevation of monitoring well interpolated from survey				

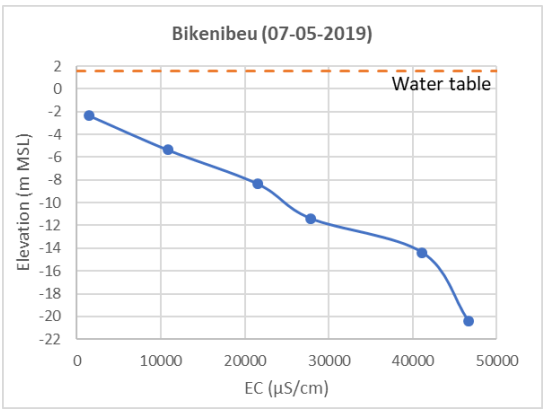

Appendix 2. Equivalent greywater discharges and their locations in current and future scenario for Betio, Bairiki and Bikenibeu

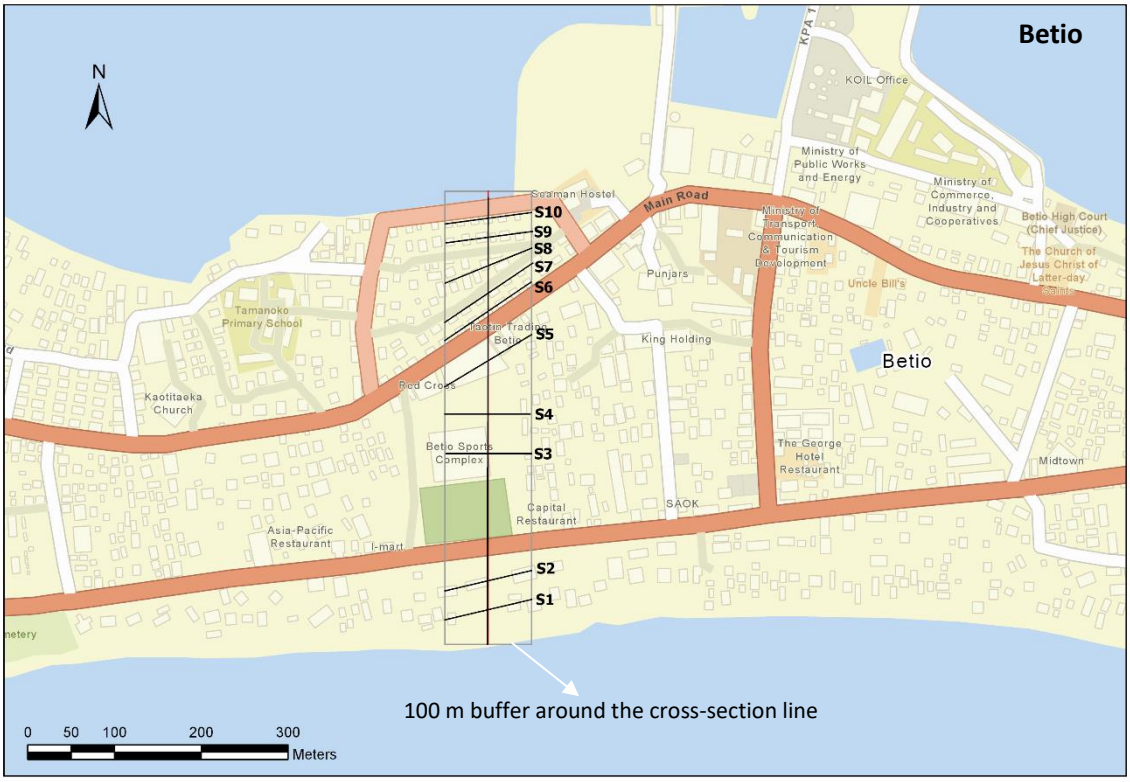

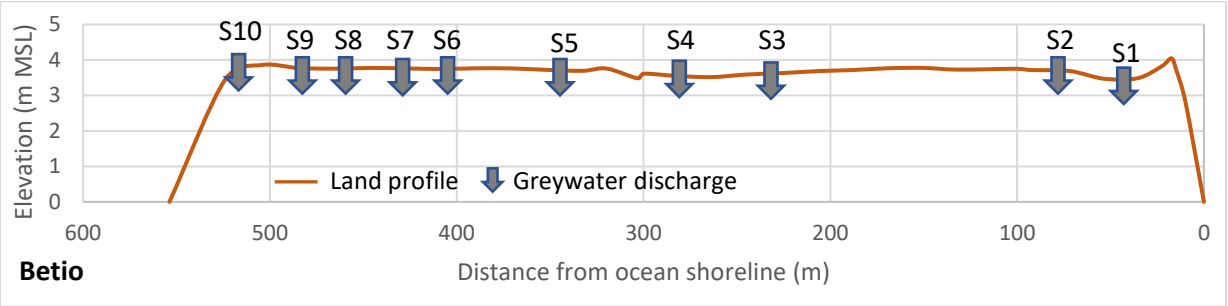


Bairiki
N
Ferry to North Tarawa
Slim Price
Beach Road
S7
S6
S5
S4
S3
S2
S1
Bairiki Police Station
Taotin Bairiki Mall
TSKL (Telekom) Kiribati
DBK Warehouse
MISA (Ministry of Internal and Social Affairs)
Handicraft Shop
Australian High Commissioner's Residence
Public Library
Bairiki Super Mall
Catholic Church
Nanotasi
Bairiki Market
Stadium Road
Runubao School
Taken Bairiki Primary School
0 50 100 200 300
Meters

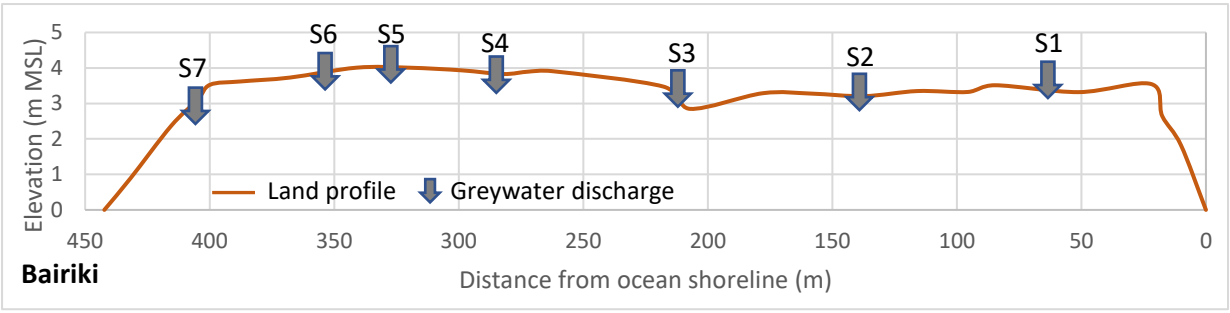
Elevation (m MSL)
5
4
3
2
1
0
S7
S6
S5
S4
S3
S2
S1
Land profile
Greywater discharge
450
400
350
300
250
200
150
100
50
0
Distance from ocean shoreline (m)
Bairiki


Bikenibeu
N
S7
S6
S5
S4
S3
S2
S1
Otintaai Hotel
Jecs Chinese
Toboroi
Kakari kava bar
Main Road
Kaana Catholic Community
Main Road
National Bahai Centre
Taiwan Agriculture
Medical Cuban Cooperation
Ministry of Education-Curriculum Unit
0 50 100 200
Meters

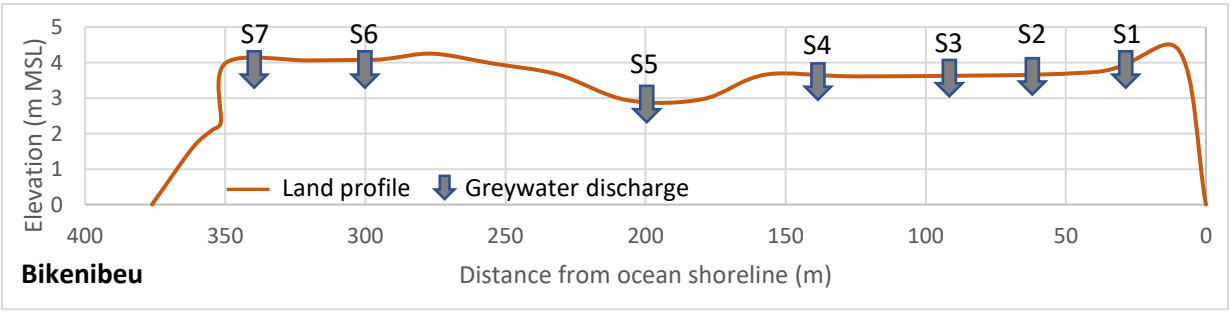
S7
S6
S5
S4
S3
S2
S1
Elevation (m MSL)
5
4
3
2
1
0
Land profile
Greywater discharge
400
350
300
250
200
150
100
50
0
Bikenibeu
Distance from ocean shoreline (m)

Equivalent greywater discharges and their locations in current situation

	Section	Length (m) [1]	Number of people in each house [2]	Number of houses in each section [3]	Greywater flux per houses (L/d) [4] =35×[2]	Total greywater flux (L/d) [5] = [3]×[4]	Greywater flux applied to model (m^3/d) [6] = [5]/1000/[1]	Distance from ocean shoreline (m)
Betio	S1	102.7	8	3	280	840	0.00818	42.1
	S2	102.7	8	3	280	840	0.00818	77.3
	S3	100	8	1	280	280	0.00280	233.0
	S4	100	8	2	280	560	0.00560	281.7
	S5	116.7	8	7	280	1960	0.01680	346.1
	S6	120.4	8	6	280	1680	0.01395	407.4
	S7	120.9	8	6	280	1680	0.01390	429.0
	S8	107.7	8	9	280	2520	0.02340	463.4
	S9	100.9	8	6	280	1680	0.01665	482.6
	S10	100.9	8	6	280	1680	0.01665	520.7
Bairiki	S1	100	7	6	245	1470	0.01470	64.4
	S2	100	7	1	245	245	0.00245	139.3
	S3	100	7	1	245	245	0.00245	212.8
	S4	100	7	8	245	1960	0.01960	285.2
	S5	100.9	7	7	245	1715	0.01700	326.4
	S6	100.5	7	5	245	1225	0.01219	354.0
	S7	100.5	7	6	245	1470	0.01463	405.4
Bikenibeu	S1	100	7	3	245	735	0.00735	31.1
	S2	100	7	4	245	980	0.00980	61.8
	S3	100	7	3	245	735	0.00735	90.5
	S4	100	7	6	245	1470	0.01470	137.3
	S5	100	7	1	245	245	0.00245	199.9
	S6	100	7	1	245	245	0.00245	302.2
	S7	101.9	7	4	245	980	0.00962	338.8

[4] based on 35 L/pers/d greywater production

[6] based on 1 m width for greywater disposal area

Equivalent greywater discharges and their locations in future scenario

	Number of people in each house [1]	Total number of houses in a 100 m buffer [2]	Greywater flux per house (L/d) [3] = 70×[1]	Greywater flux applied to model (m^3/d) [4] = [2]×[3]/1000/100	Distance from ocean shoreline (m) [5]
Betio	12	49	840	0.412	276.9
Bairiki	11	34	770	0.262	221.2
Bikenibeu	9	22	630	0.139	188.1

[3] based on 70 L/pers/d greywater production

[4] based on 1 × 1 m greywater disposal area

[5] in the middle of cross-section

Appendix 3. Geophysical survey results (Ground Penetrating Radar)


Bairiki 5
W6
TCol/ECol (1 ml): TNTC/5
TCol/ECol (100 ml): TNTC/180
Bairiki 3 + 4
Bairiki 2
W4
TCol/ECol (1 ml): TNTC/TNTC
TCol/ECol (100 ml): TNTC/TNTC
Bairiki 1
W3
TCol/ECol (1 ml): TNTC/26
TCol/ECol (100 ml): TNTC/TNTC
0
25
50
75
Bairiki
GPR
monitoring_bores
Saltwater lines
Fire hydrants
Seawater 150 valve
Seawater 150 pipe
Sewer lines
Sewer_branch
Sewer_branch
Sewer_manhole
Sewer_pumpstation
Sewer_trunk_mains
Well
< 1500 µS/cm
1500 - 2500 µS/cm
> 2500 µS/cm

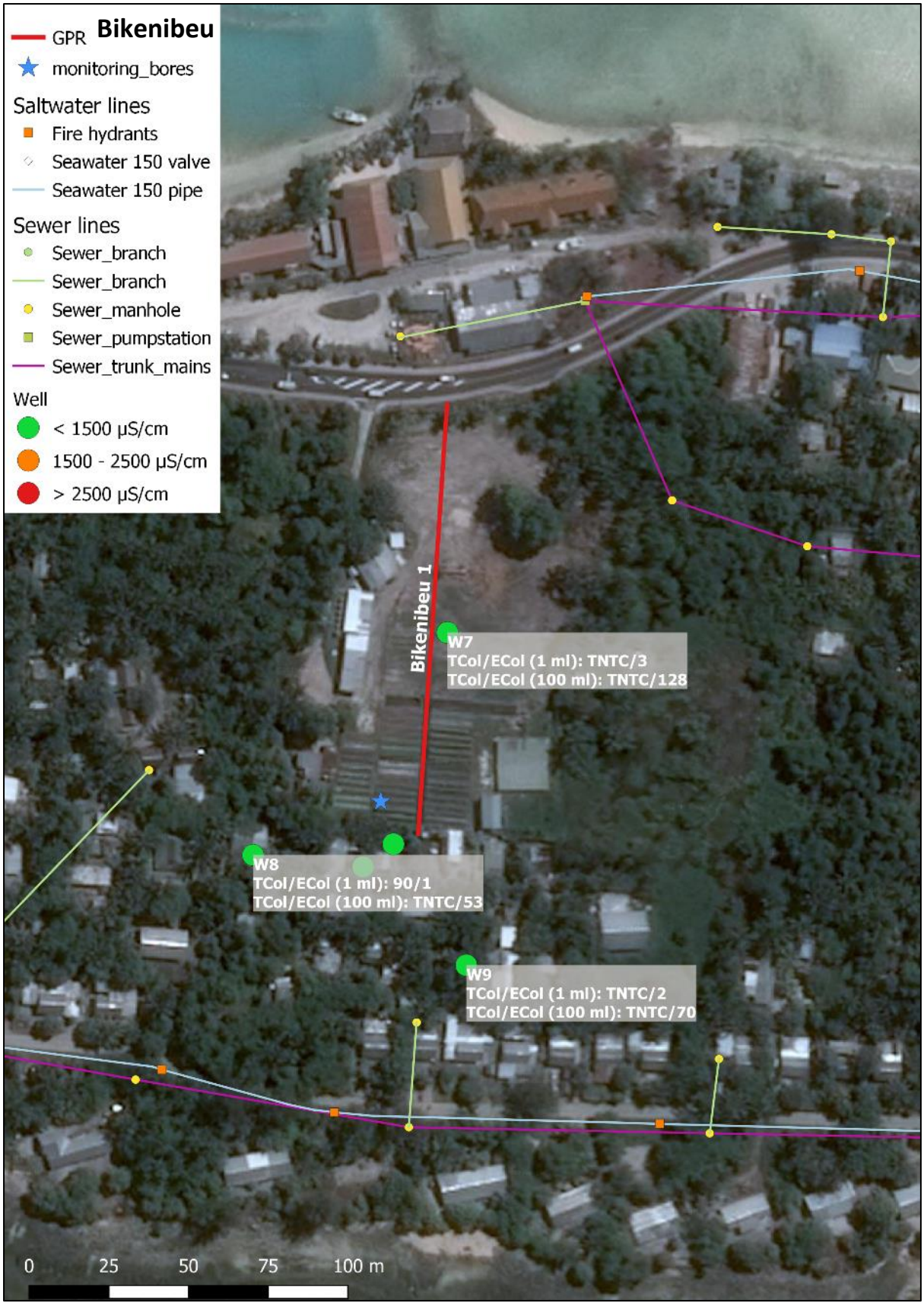
Bikenibeu
GPR
monitoring_bores
Saltwater lines
Fire hydrants
Seawater 150 valve
Seawater 150 pipe
Sewer lines
Sewer_branch
Sewer_branch
Sewer_manhole
Sewer_pumpstation
Sewer_trunk_mains
Well
< 1500 µS/cm
1500 - 2500 µS/cm
> 2500 µS/cm
Bikenibeu 1
W7
TCol/ECol (1 ml): TNTC/3
TCol/ECol (100 ml): TNTC/128
W8
TCol/ECol (1 ml): 90/1
TCol/ECol (100 ml): TNTC/53
W9
TCol/ECol (1 ml): TNTC/2
TCol/ECol (100 ml): TNTC/70
0
25
50
75
100 m

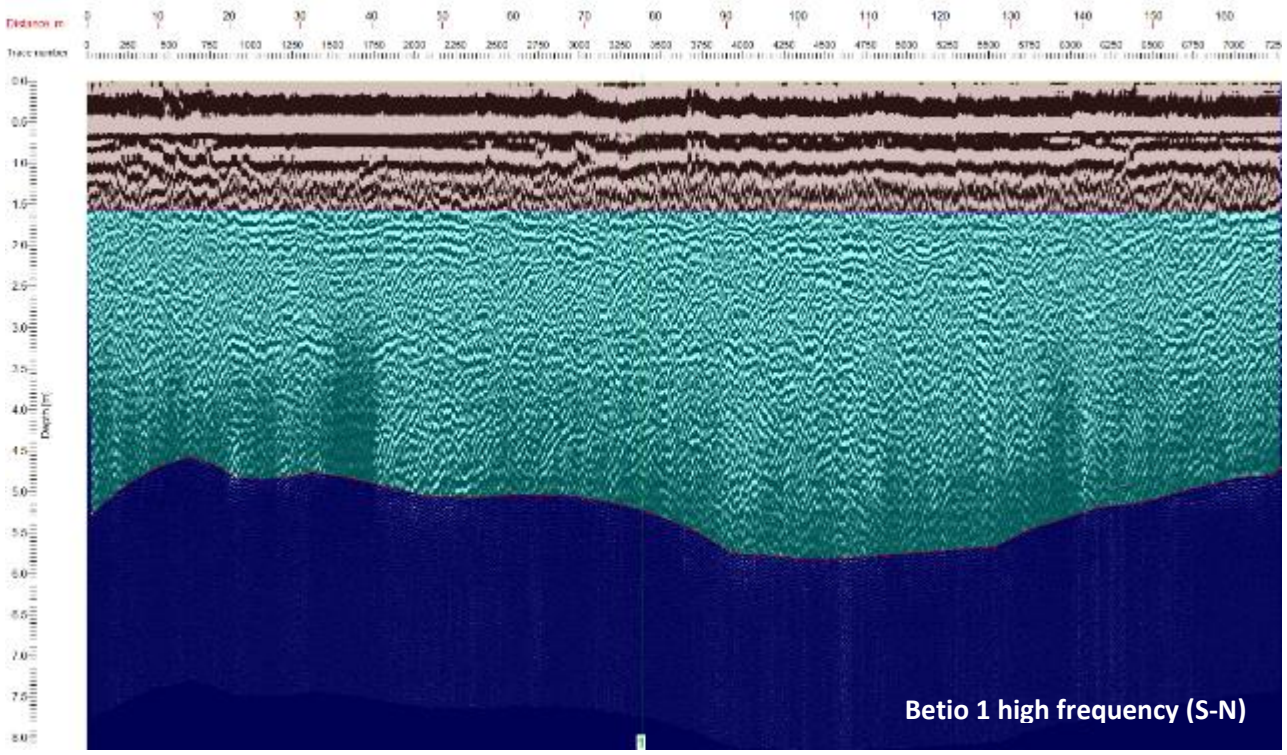
Betio 1 high frequency (S-N)

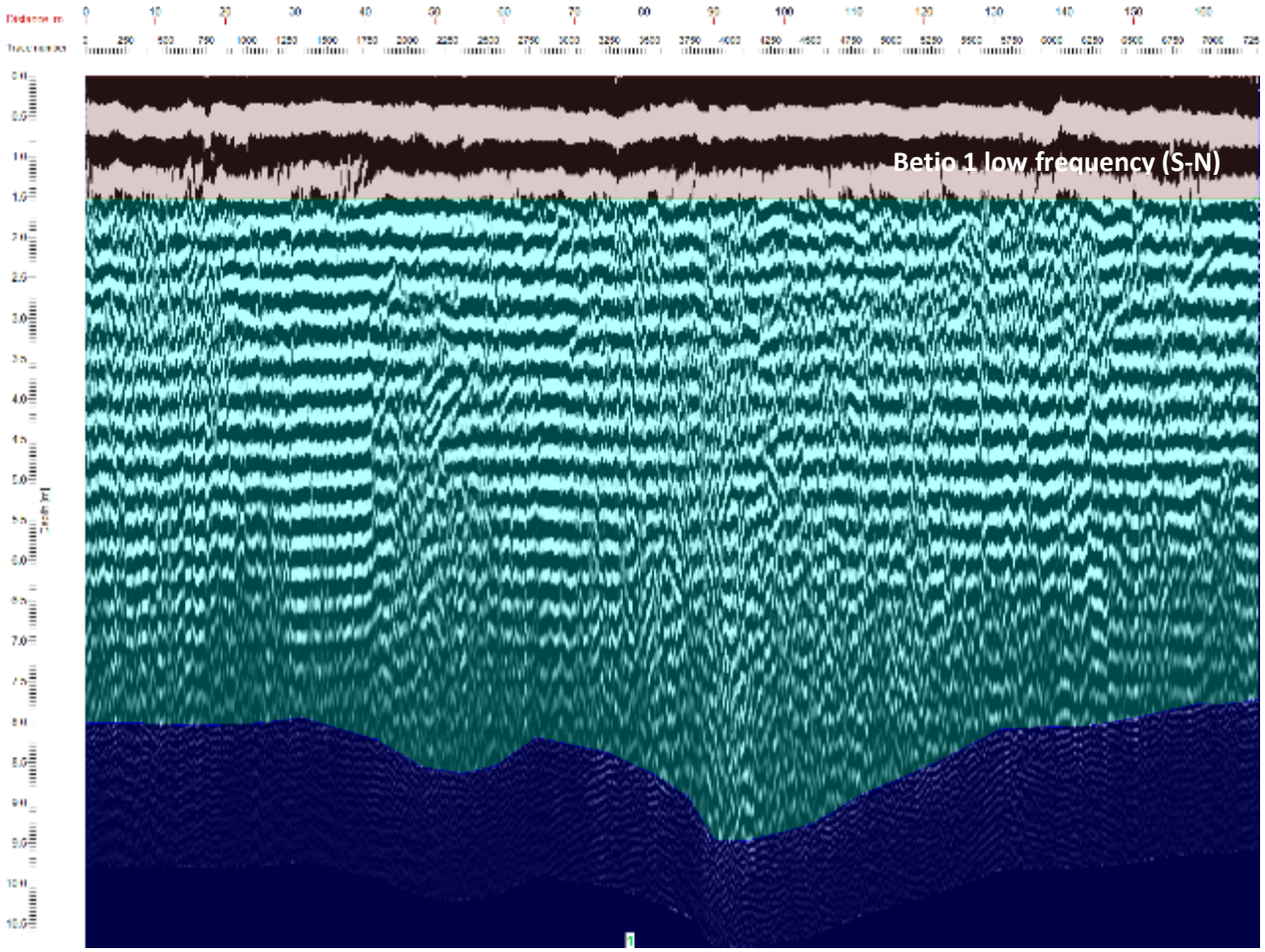
Betio 1 low frequency (S-N)

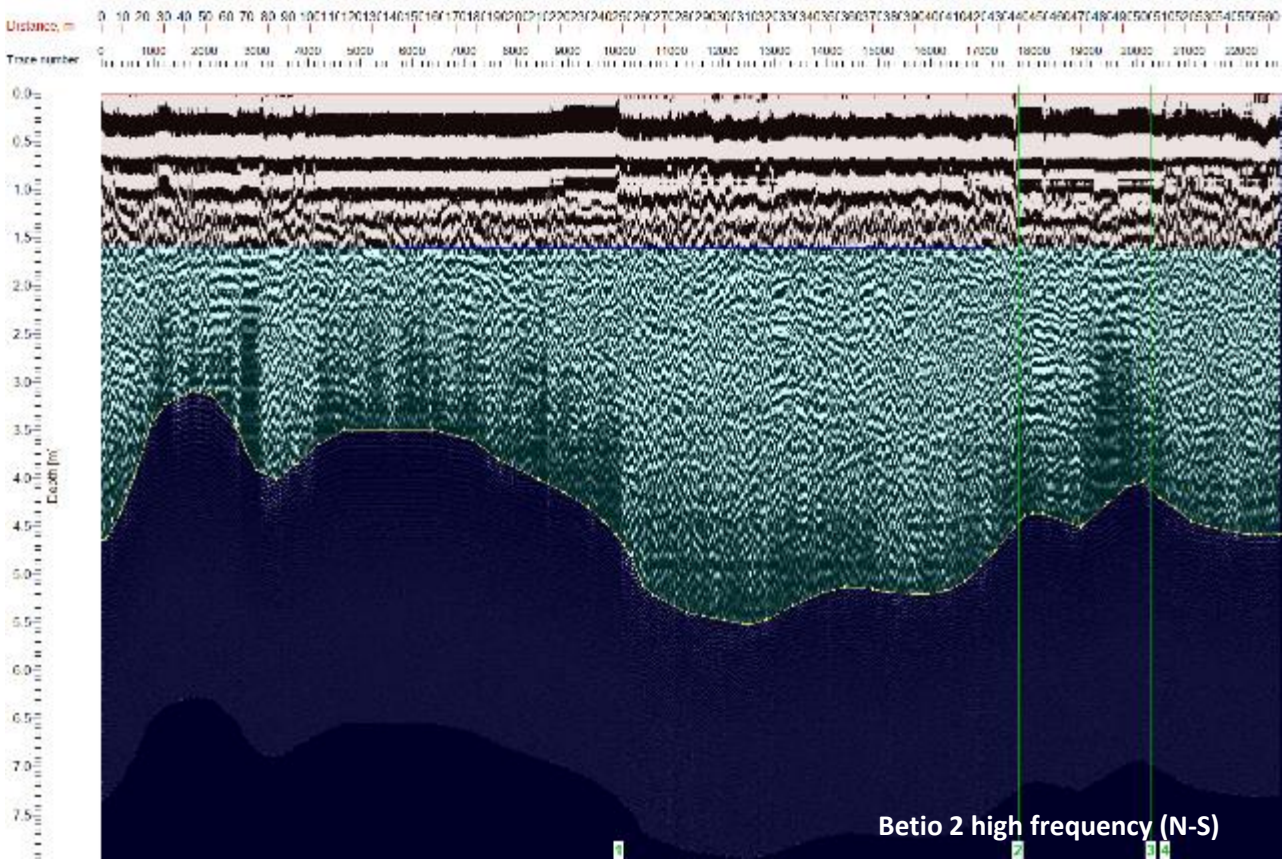
Betio 2 high frequency (N-S)

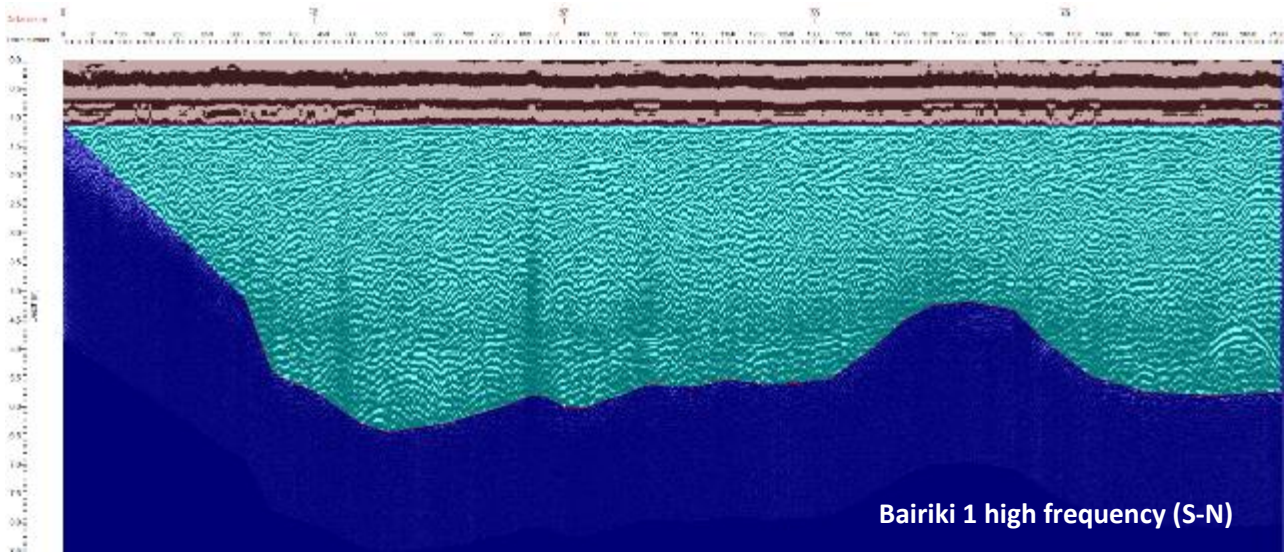
Bairiki 1 high frequency (S-N)

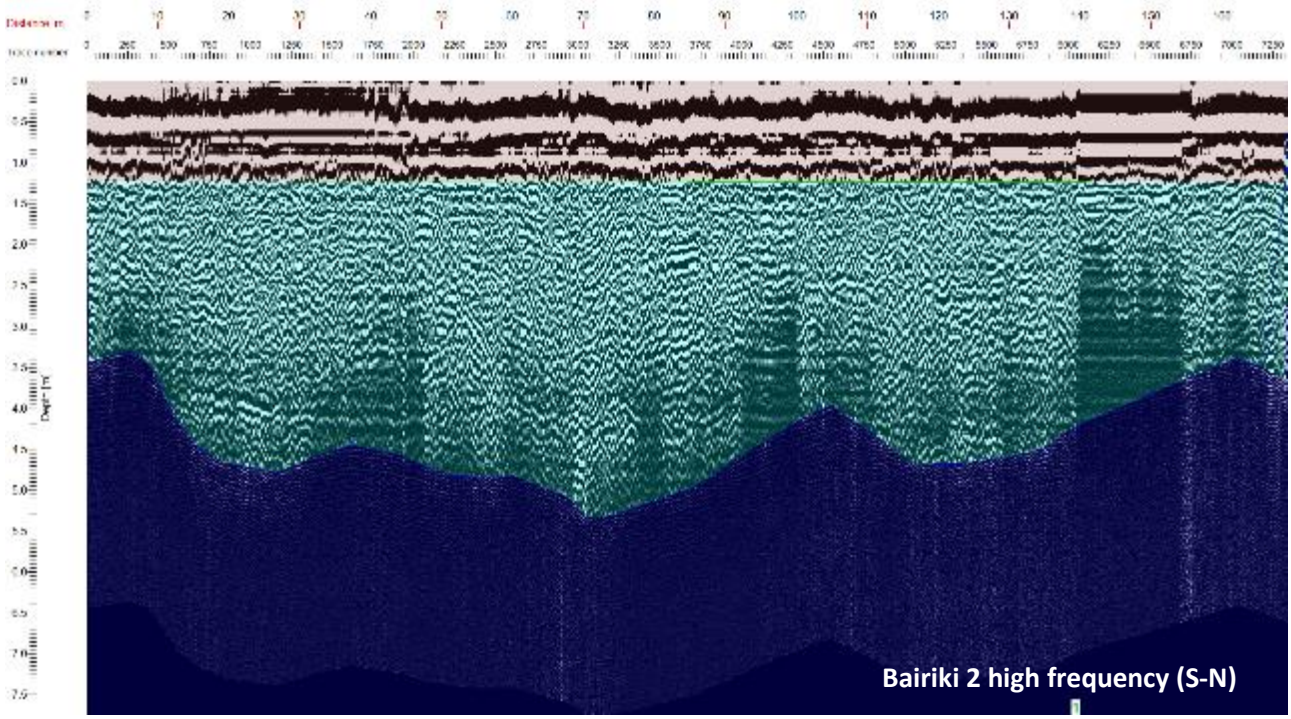
Bairiki 2 high frequency (S-N)

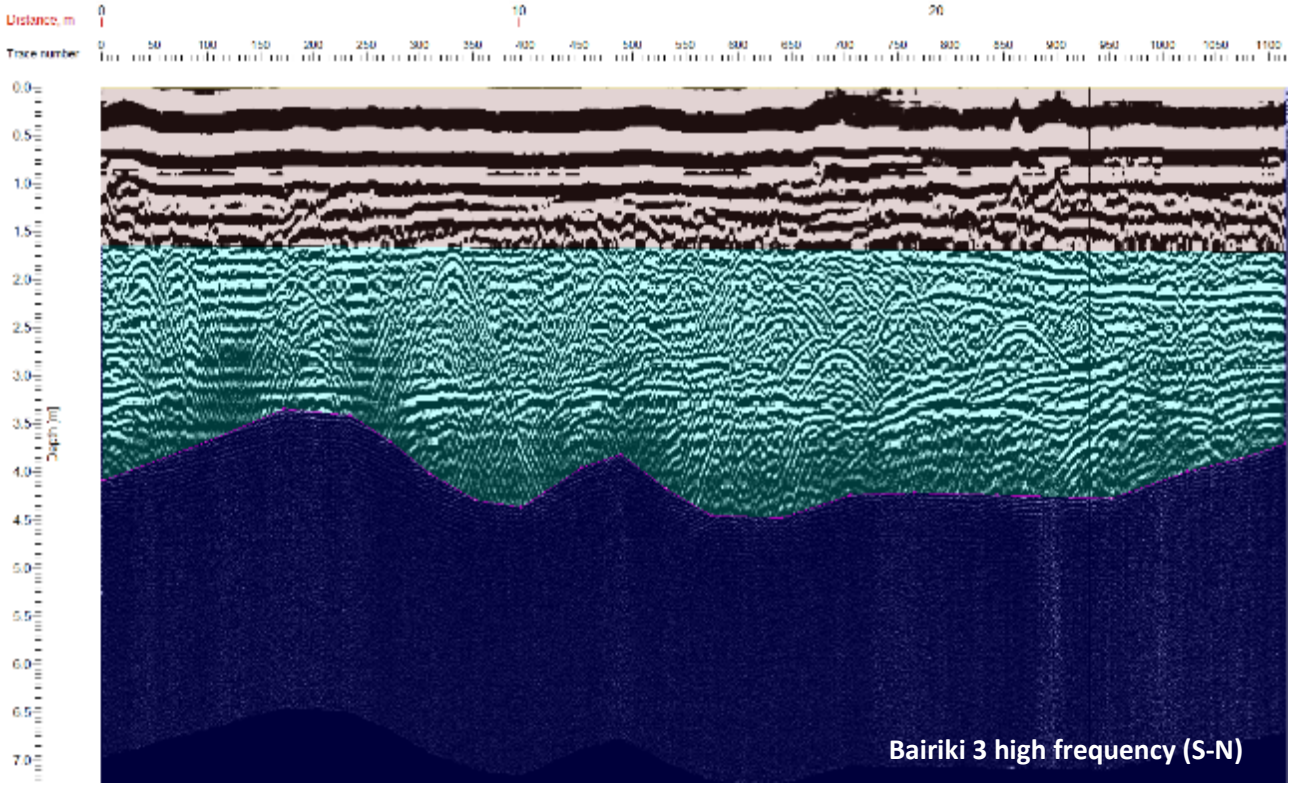
Bairiki 3 high frequency (S-N)

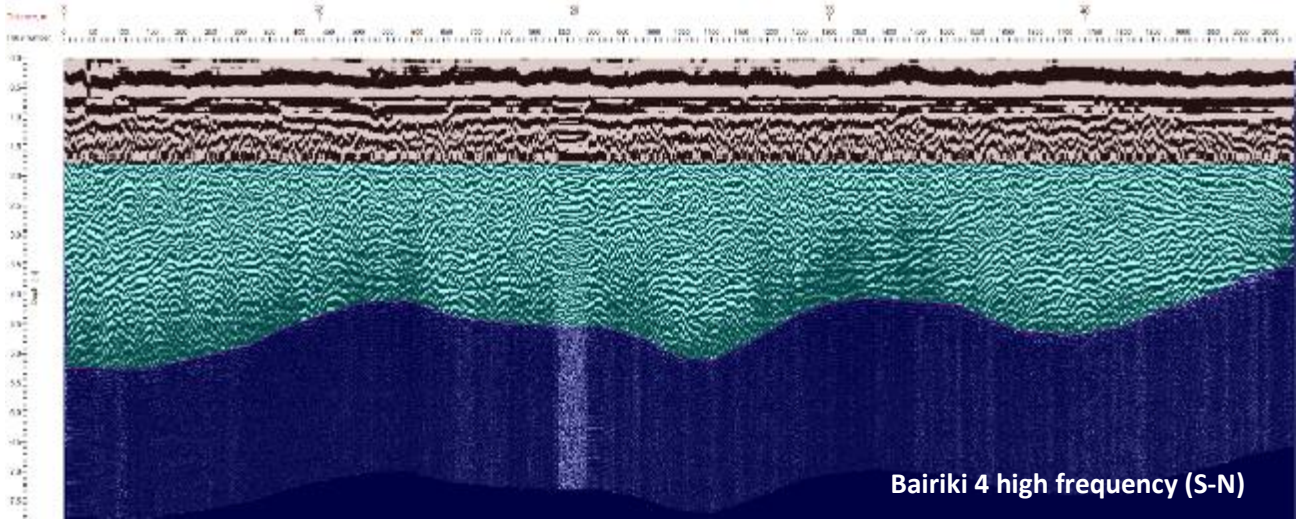
Bairiki 4 high frequency (S-N)

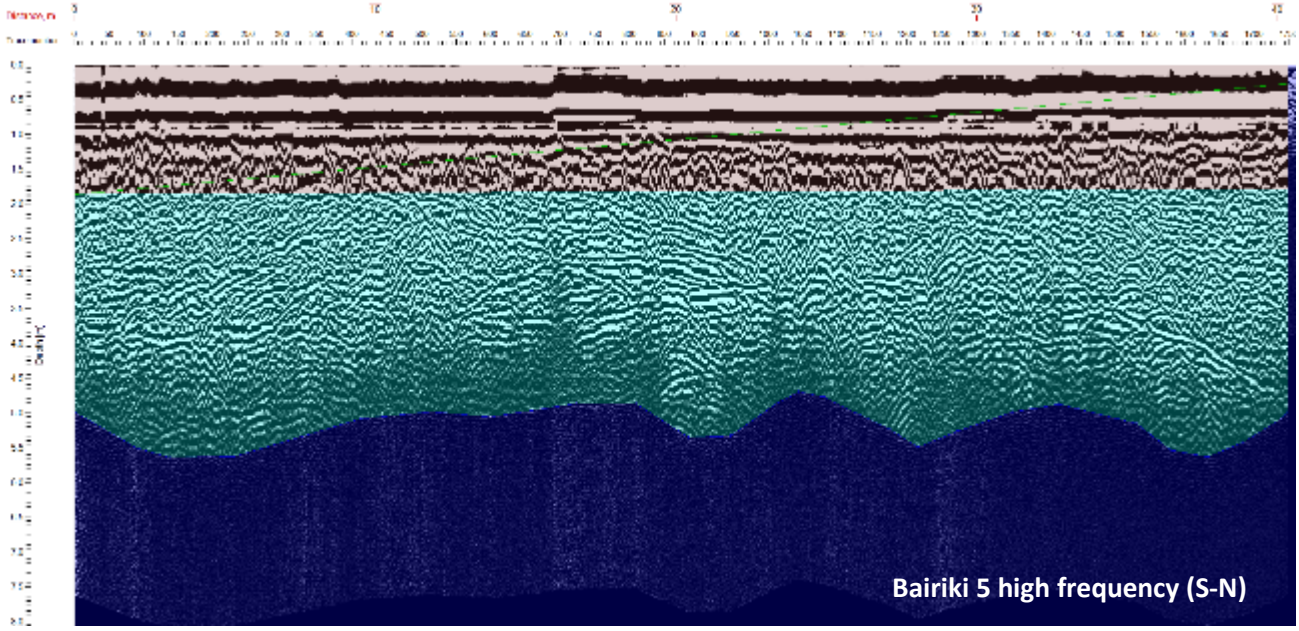
Bairiki 5 high frequency (S-N)

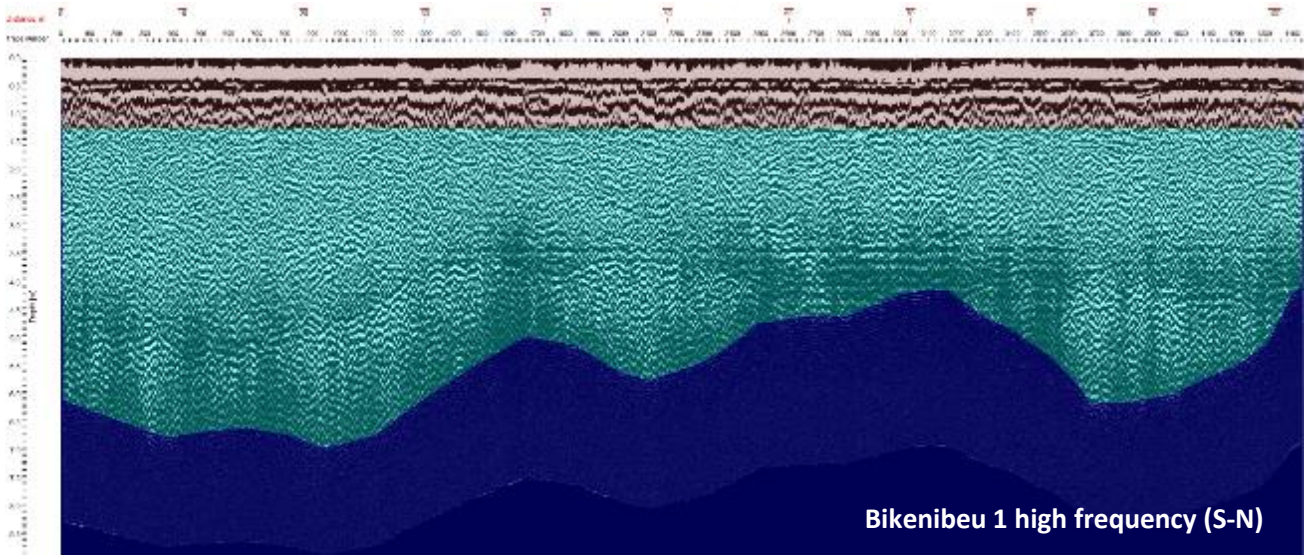
Bikenibeu 1 high frequency (S-N)


WORLD BANK GROUP